CR- 72457
PWA-3516

QUIET ENGINE DEFINITION PROGRAM
FINAL REPORT

BY
JOHN H. LEWIS, III, PROGRAM MANAGER

VOLUME III
TASK II

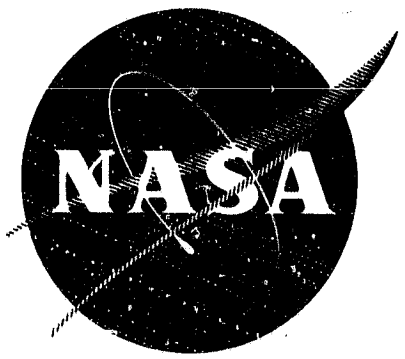

PREPARED FOR
NASA-LEWIS RESEARCH CENTER CLEVELAND, OHIO 44135
UNDER CONTRACT NAS3-10497

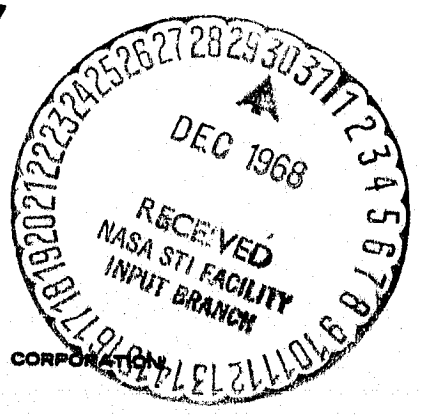

Pratt & Whitney Aircraft
DIVISION OF UNITED AIRCRAFT CORPORATION

FINAL REPORT
ON THE
QUIET ENGINE DEFINITION PROGRAM
PWA-3516

by

John H. Lewis, III, Program Manager

VOLUME III
TASK II

prepared for

NATIONAL AERONAUTICS AND SPACE ADMINISTRATION

October 4, 1968

CONTRACT NAS3-10497

Technical Management

NASA Lewis Research Center
Cleveland, Ohio
Propulsion Systems Acoustics Branch
J. J. Kramer
J. F. McBride

Pratt & Whitney Aircraft
DIVISION OF UNITED AIRCRAFT CORPORATION

EAST HARTFORD, CONNECTICUT

COPY NO.

Preface

The Final Report for the Quiet Engine Definition Program has been prepared in five volumes. This volume describes the work carried out under Task II, which was a preliminary design study of three candidate Quiet Engine cycles. A summary of the over-all program and discussions of Tasks I and III are given in the other four volumes, which are listed below:

Volume I	Summary
Volume II	Task I
Volume IV	Task III
Volume V	QE-3 Performance

TABLE OF CONTENTS

LIST OF ILLUSTRATIONS

LIST OF ILLUSTRATIONS (Cont'd)

LIST OF TABLES

SECTION I

SUMMARY

This volume presents the results of Task II of the Quiet Engine Definition Program. The effort under Task II was initially devoted to preliminary design evaluations of three selected configurations. At the request of NASA, however, the contract was revised during the task to include an additional configuration.

The completed Task II results consist of mechanical design layouts and performance for four candidate engines. The three configurations initially selected for Task II studies are chiefly distinguished by their design bypass ratios. The design bypass ratios were 3.0, 5.0, and 8.0, and the associated engine designs have been designated QA, QB, and QC, respectively. Each engine had an over-all design pressure ratio of 24.5, and the fan pressure ratios were selected to be best suited to each individual bypass ratio. Turbine inlet temperatures were chosen to be consistent with state-of-the-art technology representative of the next generation of commercial transports. These design characteristics were chosen by the NASA Project Manager to take the best advantage of the low-noise features of the cycles.

In the selection of the original configurations, the NASA Project Manager further stipulated that the QA and QB configurations (with design bypass ratios of 3.0 and 5.0 respectively) were to be designed with two-stage low-tip-speed fans, while the QC (with an 8.0 design bypass ratio) would have a low-tip-speed single-stage fan. In each case, the low fan tip speed was dictated by the predominant influence of fan noise revealed in the Task I results. The two-stage fans were specified to ensure feasible fan designs with low tip speed and relatively high fan pressure ratios.

The low fan speed also increases the difficulty in realizing the designated 24.5 over-all cycle pressure ratio (to which the inner portion of the fan contributes directly) and shifts an added burden to the compressor section. To ensure that this burden could be met with minimum development risk, the NASA Project Manager added a fourth candidate configuration which employs the three-spool concept. This configuration, designated QD, has a cycle that is identical to the QB engine, but rather than a single compressor spool with a high pressure ratio, it has the compressor split into two separately rotating spools with moderate pressure ratio.

Originally scheduled to last three months, Task II was extended to five months total duration to allow for adding the QD configuration to the effort. During this period, work on the QA, QB, QC, and QD configurations started with the selec-

tion of the components, preliminary design layouts, and concluded with predictions of uninstalled performance and noise.

In choosing the general arrangement for each engine early in the task, a series of possible component arrangements was worked out on the basis of preliminary flowpaths and the most suitable arrangement was selected in each case.

When the general arrangement had been selected, analytical design for each of the major components was undertaken. This phase of the effort was conducted in sufficient detail to define the performance and physical dimensions of the engine components: compressor, turbine, and burner. For the turbine components, such key design variables as blade aspect ratio, passage Mach numbers, and blade loadings were chosen.

Mechanical design layouts based on the completed analytical designs of components involved establishing the mechanical configuration in sufficient detail to define key dimensions, predict weights, and ascertain mechanical integrity. To this end, certain static structures were checked under critical loading conditions and rotor dynamics were checked for adequate critical-speed margins.

Performance tabulations were compiled to define thrust, specific fuel consumption, and other key variables over a range of operating conditions from sea level to 45,000 feet (13,700 meters) and from Mach 0 to Mach 0.9.

Noise presentations consist of airport neighborhood contours representing take-off and landing conditions for each candidate engine. Calculations were based on the latest refined techniques of noise prediction developed from full-scale testing of the JT3D (two-stage fan) and the JT9D (single-stage fan) engines.

Noise calculations and engine thrust sizing have also been predicated on applications of the candidate engines to the Boeing 707 and the Douglas DC-8 class of commercial aircraft. Compared with the JT3D-3B engine currently powering these aircraft, all the Quiet Engines offer appreciable reductions in over-all uninstalled noise at the expense of additional weight and larger physical dimensions, but with lower fuel consumption.

Table I summarizes the over-all configuration, physical characteristics, and performance results for the Task II engines selected for preliminary design.

TABLE I

SUMMARY OF TASK II ENGINE DESIGNS

Engine Designation	QA-1	QB-3	QC-1	QD-1A
Configuration:				
Fan	2 Stages	2 Stages	1 Stage	2 Stages
Low-Pressure Compressor	3 Stages Axial	None	3 Stages Axial	6 Stages Axial
High-Pressure Compressor	11 Stages Axial	14 Stages Axial	14 Stages Axial	7 Stages Axial
Combustor	Annular Burner with Integral Diffuser			
High-Pressure Turbine	2 Stages	2 Stages	2 Stages	2 Stages
Intermediate-and Low-Pressure Turbines	4 Stages	5 Stages	5 Stages	6 Stages
Physical Characteristics:				
Weight (lbs)	5,080	5,420	5,610	5,570
Weight (kg)	2,310	2,460	2,550	2,530
Maximum Diameter (in)	63.2	70.0	84.5	70.6
Maximum Diameter (cm)	161	178	215	180
Length (in)	131.2	125.8	125.5	146.8
Length (cm)	333	320	319	373
Performance:				
Take-Off Thrust (lbs)	20,670	22,750	25,550	23,300
Take-Off Thrust (N)	92,100	101,000	113,500	103,700
Cruise* Thrust (lbs)	4,900	4,900	4,900	4,900
Cruise* Thrust (N)	21,800	21,800	21,800	21,800
Cruise * TSFC ($lb_m/hr\text{-}lb_f$)	0.64	0.61	0.60	0.62
Cruise * TSFC (kg/sec-N)	1.81×10^{-5}	1.73×10^{-5}	1.70×10^{-5}	1.75×10^{-5}

*Cruise conditions are Mach 0.82, 35,000 feet (10,800 meters) altitude

SECTION II

INTRODUCTION

A. BACKGROUND

The Quiet Engine Definition Program was divided into four separate tasks. Task I was devoted to parametric studies of 242 discrete cycle combinations. These studies were used as a basis for the NASA Project Manager's selection of three cycle combinations for further study under Task II. The Task II work served as a basis for the NASA Project Manager's selection of the final engine (QE) for more thorough evaluation under Task III. Task IV was concerned with a recommended test program for the quiet engine.

The cycle characteristics specified for the Task II engines are tabulated in Table II. For these characteristics, the aim of Task II has been to define performance, noise, weight, and physical dimensions in sufficient detail to select a final candidate engine for more refined design in Task III. To this end, the work was divided into four reporting categories:

1. Analytical design of the components
2. Preliminary design layouts
3. Uninstalled performance data tabulations
4. Uninstalled noise predictions

These categories are numbered according to the applicable work statement paragraph.

TABLE II

SPECIFIED CYCLE CHARACTERISTICS

	QA	QB	QC	QD
Bypass Ratio	3	5	8	
Fan Pressure Ratio *	1.8 (1.7)	1.55 (1.60)	1.35	Same as
Cycle Pressure Ratio	24	24	24	QB
Turbine Inlet Temperature at Mach 0.8, 35,000 feet (°F)*	1700 (1650)	1800 (1750)	1750	except three-spool
Turbine Inlet Temperatures at Mach 0.8, 10,700 m (°K)*	1200 (1170)	1255 (1230)	1230	configuration
Cruise Thrust (lb)	4900	4900	4900	
Cruise Thrust (N)	21,800	21,800	21,800	
Turbine Inlet Temperature at Sea Level Standard-Day Take-Off (°F)	1800	1950	1950	
Turbine Inlet Temperature at Sea-Level Standard-Day Take-Off (°K)	1235	1340	1340	
Minimum Take-Off Thrust (lb)	20,000	20,000	20,000	
Minimum Take-Off Thrust (N)	80,900	80,900	80,900	
Number of Fan Stages	2	2	1	
Fan Tip Speed at Maximum Take-Off Power (ft/sec)	1000 preferred, 1100 maximum			
Fan Tip Speed at Maximum Take-Off Power (m/sec)	305 preferred, 336 maximum			

B. WORK ACCOMPLISHED

Analytical components design was concerned with selecting combustor configurations; numbers of fan, compressor, and turbine stages; fan blades and vanes; turbine cooling requirements; and nozzle areas. Aspect ratios, hub-to-tip ratios, tip speeds, and appropriate component maps were determined for the fan and compressors; while for the fan, pressure ratio and blade loadings at primary and bypass sections were established.

*To be optimized as part of Task II studies (numbers in parenthesis denote final selected values).

For the preliminary design layouts the work accomplished included preliminary dynamic analysis, structural arrangement concepts, approximate case and disk sizes, over-all dimensions, and estimated weights.

Performance data tabulations were assembled for each of the four cycles. Thrust, specific fuel consumption, and other pertinent performance data were included in the tabulations, which cover flight operating conditions from sea level to 45,000 feet (13,700 meters) and speeds from 0 to Mach 0.9.

Noise data were prepared in the form of 90, 95, and 100 PNdb contours in the airport vicinity for both take-off and landing conditions. Noise values are provided for both total engine noise and jet exhaust noise under the cases of mixed and unmixed fan and engine exhaust streams.

The initial effort in Task II was devoted to establishing a suitable configuration arrangement within the confines of the specified characteristics shown in Table I. Since selection of the over-all configuration is such a key step in the early preliminary design process, it is covered by a separate section in this volume. In addition, certain supplementary studies were undertaken during the latter portion of the task to evaluate possible variations in configuration, particularly in the fan section.

SECTION III

CONFIGURATION SELECTION

The first step in the design process is to establish a well integrated combination of components - fans, compressors, burner, and turbines. The engine configuration must represent compromises of the conflicting needs of each component in satisfying the imposed over-all cycle. This section describes the methods and assumptions that were used in the beginning of Task II in the preliminary selection of configuration arrangements for each of the three cycles. The selection process involved a cycle-refinement study, the development of gas paths for several promising configurations, and final selection of configurations based on evaluations of the gas paths as indicators of ultimate designs.

As a result of this process, three configurations were selected to start the task effort. These three configurations were designated QA-1, QB-3, and QC-3. Later in the program, the NASA Project Manager requested that an alternate, three-spool configuration be included in the study, so additional preliminary gas paths were created. From these additional three-spool gas paths, a fourth configuration, the QD-1A, was selected.

A. CYCLE REFINEMENTS

1. Method

It was recognized at the start of Task II that the cycle initially specified might require some refinement in order to achieve better levels of predicted weight, performance, and airport-vicinity noise. The initial cycles selected for Task II are shown in Table II. For each of these cycles, the cruise design-point turbine inlet temperature and fan pressure-ratio were varied within narrow limits to determine their effects on cruise thrust-specific fuel consumption, total engine airflow (indicative of engine weight), and total noise at take-off.

Using the computer programs which had been prepared for the Task I parametric cycle studies, performance calculations for the 27 cycle combinations listed in Table III were made at cruise (Mach 0.82 and 35,000 feet or 12,200 meters altitude) and take-off. With the engines sized for 4900 pounds (21,800 newtons) thrust at cruise, equilibruim matching calculations obtained thrust, fan rotor speed, and jet velocities during take-off. With the assumption of a fully loaded aircraft similar to a Boeing 707 or a Douglas DC-8, the calculated thrust characteristics of the engine were used to determine the aircraft's altitude at a distance of 3 miles (4.83 kilometers) from the start of the take-off roll. Finally, the engine noise level at the 3-mile (4.83-kilometer) point was estimated from the predicted fan rotor speed and jet velocities, densities, and areas.

TABLE III

CYCLE REFINEMENT COMBINATIONS

Bypass Ratio	3	5	8
Cycle Pressure Ratio	24	24	24
Take-Off Turbine Inlet Temperature (°F)	1800	1950	1950
Take-Off Turbine Inlet Temperature (°K)	1255	1285	1285
Fan Pressure Ratio	1.6, 1.7, 1.8	1.45, 1.55, 1.65	1.2, 1.3, 1.4
Cruise Turbine Inlet Temperature (°F)	1550, 1650, 1750	1750, 1850, 1950	1650, 1750, 1850
Cruise Turbine Inlet Temperature (°K)	1115, 1170, 1230	1230, 1285, 2310	1170, 1230, 1285

The cycle refinement calculations were predicated on the same assumptions used in the Task I parametric studies. Design-point efficiencies for all components of the engine except the fan are given in Table IV. Off-design efficiencies were held constant at the design-point adiabatic value. Off-design fan rotor speeds were calculated using the generalized fan performance map used in Task I.

TABLE IV

COMPONENT EFFICIENCY ASSUMPTIONS

Polytropic Compressor Efficiency	0.89
Polytropic Turbine Efficiency	0.90
Burner Pressure Loss	0.047
Engine Exhaust Pressure Loss	0.016
Fan Duct Pressure Loss	0.010
Nozzle Velocity Coefficient	0.99
Effective Turbine Cooling Air Flow (Percent of Compressor Air Flow)	3.2 - 4.9

2. Results

The results of the cycle refinement studies are summarized in Figures 1 through 3. Each curve represents the change in value of design air flow, cruise thrust-specific fuel consumption, and take-off noise level from their base levels. Design air flow is the amount required to produce 4900 pounds (21,800 newtons) of cruise thrust at Mach 0.82 and 35,000 feet (12,200 meters). The base combina-

tions of pressure ratio and temperature were chosen to represent the center of the range in which the optimum combination was likely to occur.

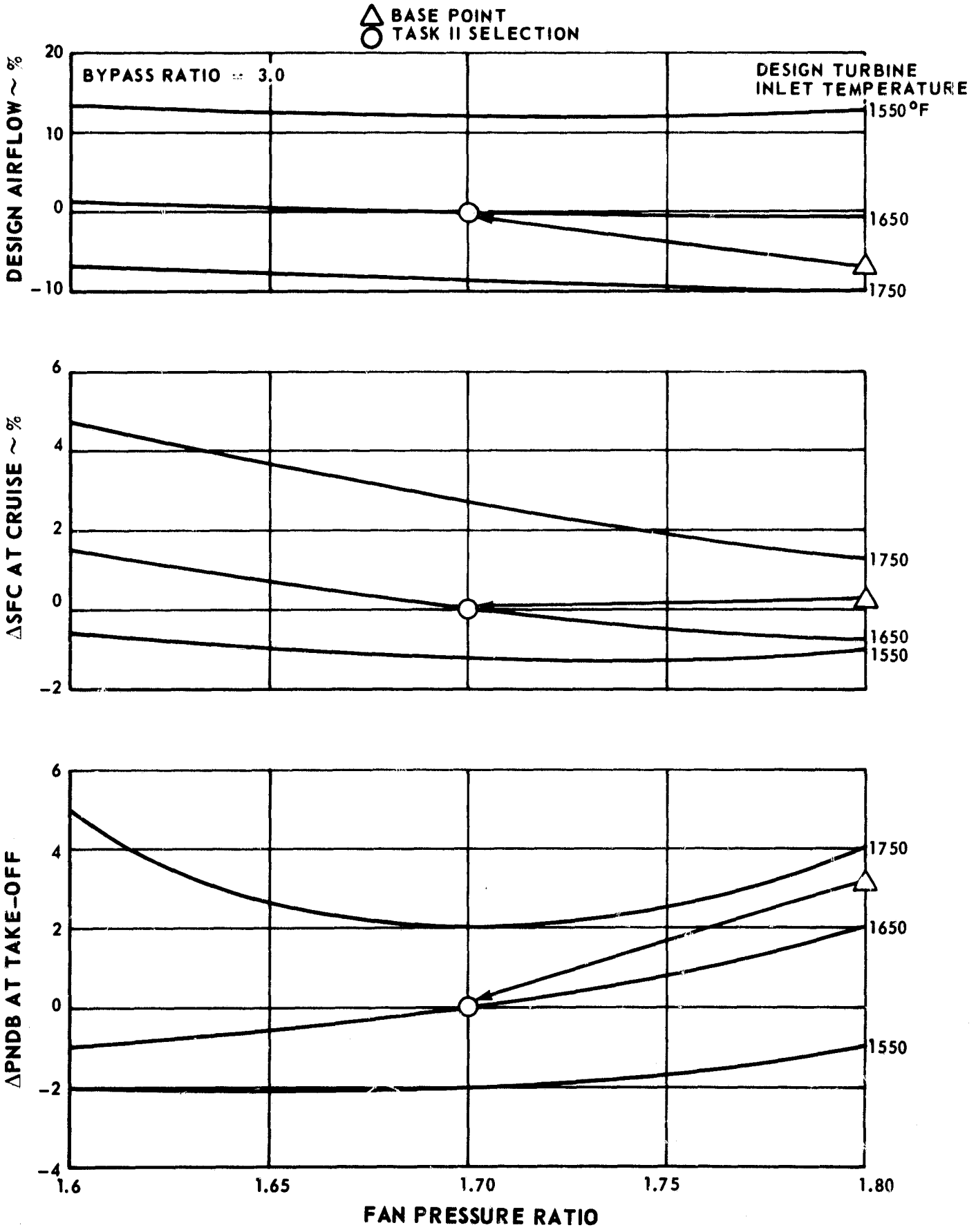

Figure 1 Results of the Fine-Tuning Study on the QA Engine Cycle

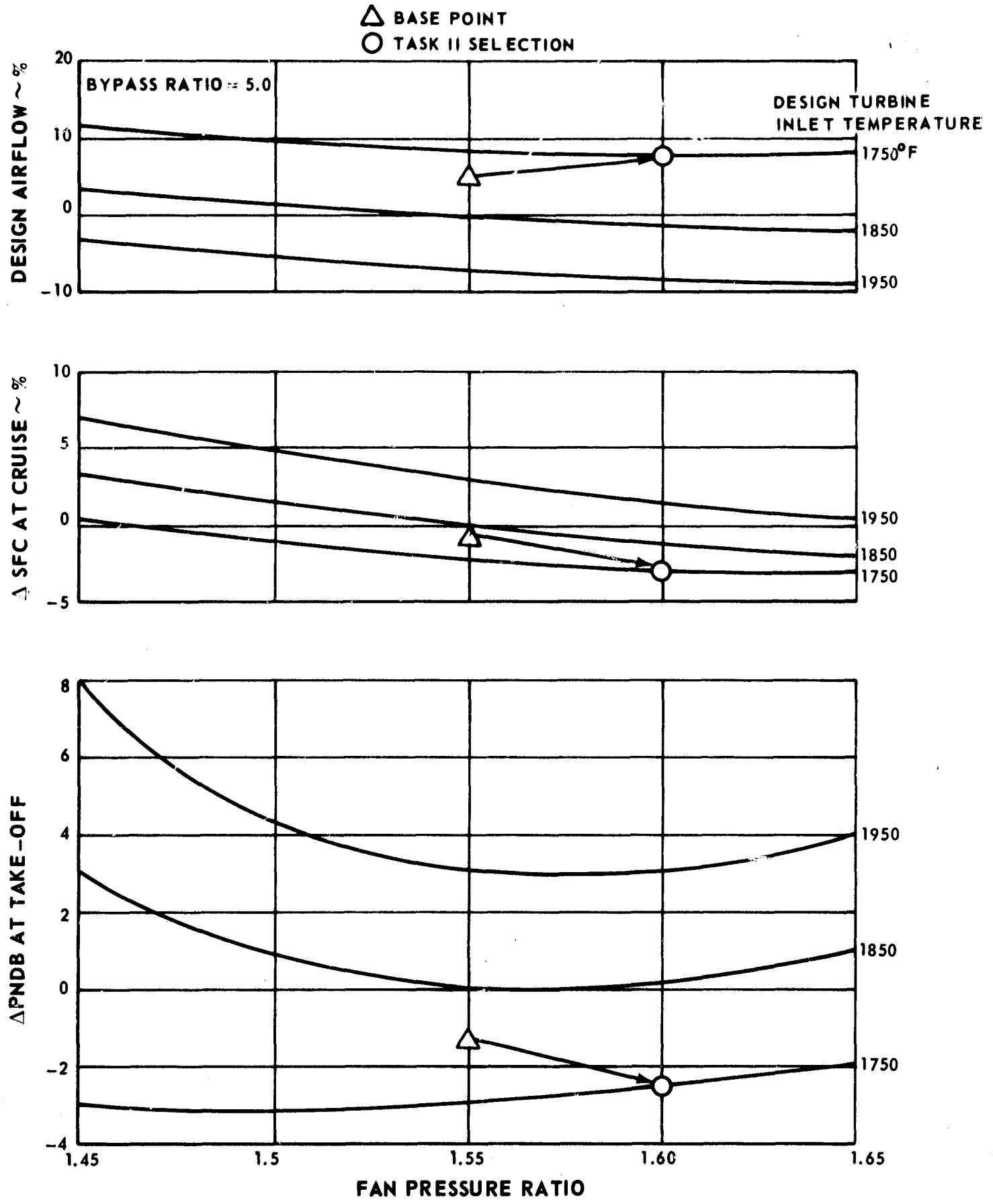

Figure 2 Results of the Fine-Tuning Study on the QB and QD Engine Cycles

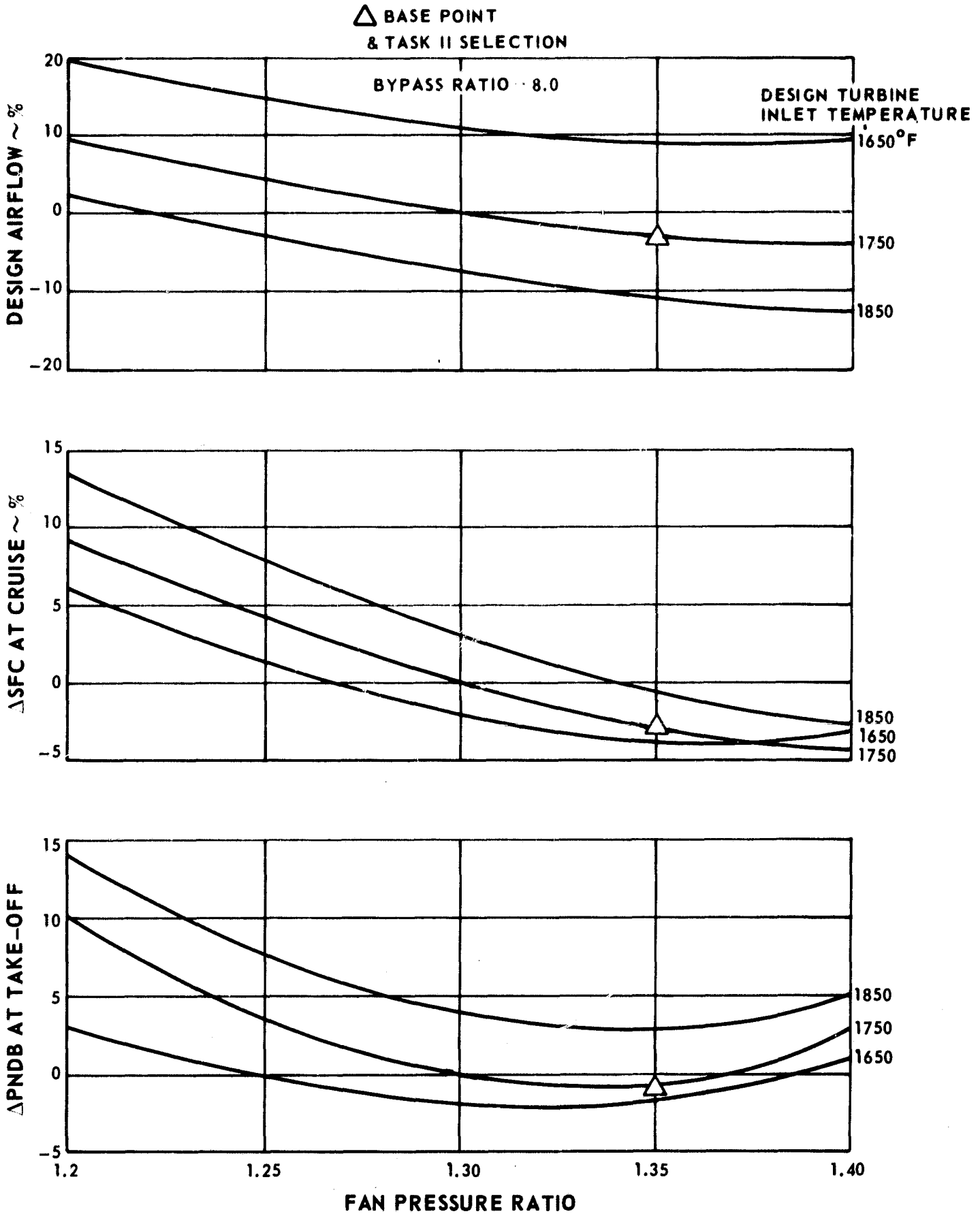

Figure 3 Results of the Fine-Tuning Study on the QC Engine Cycle

As shown in Figure 1, the original selection for the QA cycle was modified by reducing the fan pressure ratio in order to gain three PNdb at take-off. This modification left specific fuel consumption essentially unchanged, but increased design airflow (and hence weight) by five percent. A further reduction in design turbine inlet temperature would have resulted in a smaller noise reduction for a larger weight penalty.

The refinement for the QB and QD engine cycle (with a bypass ratio of 5.0) from 1.55 to 1.60 and decreased turbine inlet temperature at cruise design from 1800°F (1258°K) to 1750°F (1229°K). These changes, illustrated in Figure 2, were made in order to reduce thrust-specific fuel consumption by 2.0 percent and take-off noise by 1.0 PNdb. As a consequence of the shift, weight was increased by 4.0 percent, but this increase was more than offset by the improvement in fuel consumption.

For the QC cycle, with a bypass ratio of 8.0, the refinement results illustrated in Figure 3 show that the initial cycle selection could not be improved within the narrow range of variables studied. A reduction in cruise turbine inlet temperature below the selected value of 1750°F (1229°K) would penalize the design airflow with only a slight improvement in fuel consumption and take-off noise level. Increasing the cruise turbine inlet temperature would penalize fuel consumption and noise levels without a sufficiently compensating reduction in design airflow. Increasing the fan pressure ratio would have increased noise, while decreasing it would have increased thrust-specific fuel consumption and design airflow with no improvement in noise level.

B. CONFIGURATION ARRANGEMENT SELECTIONS

1. Method

Preliminary configuration studies were started at the same time as the cycle refinement studies. Gas paths were drawn for several work splits and numbers of compressor and turbine stages. Three of the gas paths represent possible arrangements for the 3.0-bypass-ratio cycle, and are designated QA-1, QA-2, and QA-3 (see Figures 4, 5, and 6). Three gas paths represent the 5.0-bypass-ratio cycle and are labelled QB-1, QB-2, and QB-3. They are shown in Figures 7, 8, and 9. Two gas paths represent the 8.0-bypass-ratio cycle and are designated the QC-1 and QC-2 (see Figures 10 and 11). Later in the program, five additional three-spool arrangements were drawn at the request of the NASA Program Manager. These configurations were designated the QD-1, QD-2, QD-3, QD-4, and QD-5 (see Figures 12 through 16).

The purpose of this initial work was to define the dimensions of the gas paths and to illustrate the spatial relationships of the engine components. The several candidate configurations chiefly represent various combinations of the following arrangements:

- Different numbers of low-pressure compressor stages on the same spool as the fan.
- In-line compressor compared with offset compressors linked by a transition duct.
- In-line turbines compared with offset turbines linked by a transition duct.
- Two spools compared with three spools.

The five QD configurations illustrate the effect on the total number of compressor stages of altering the work splits between the high-pressure and the intermediate-pressure spool as well as the compromises between in-line and offset turbine flow path locations. A list of flow path assumptions is given in Table V.

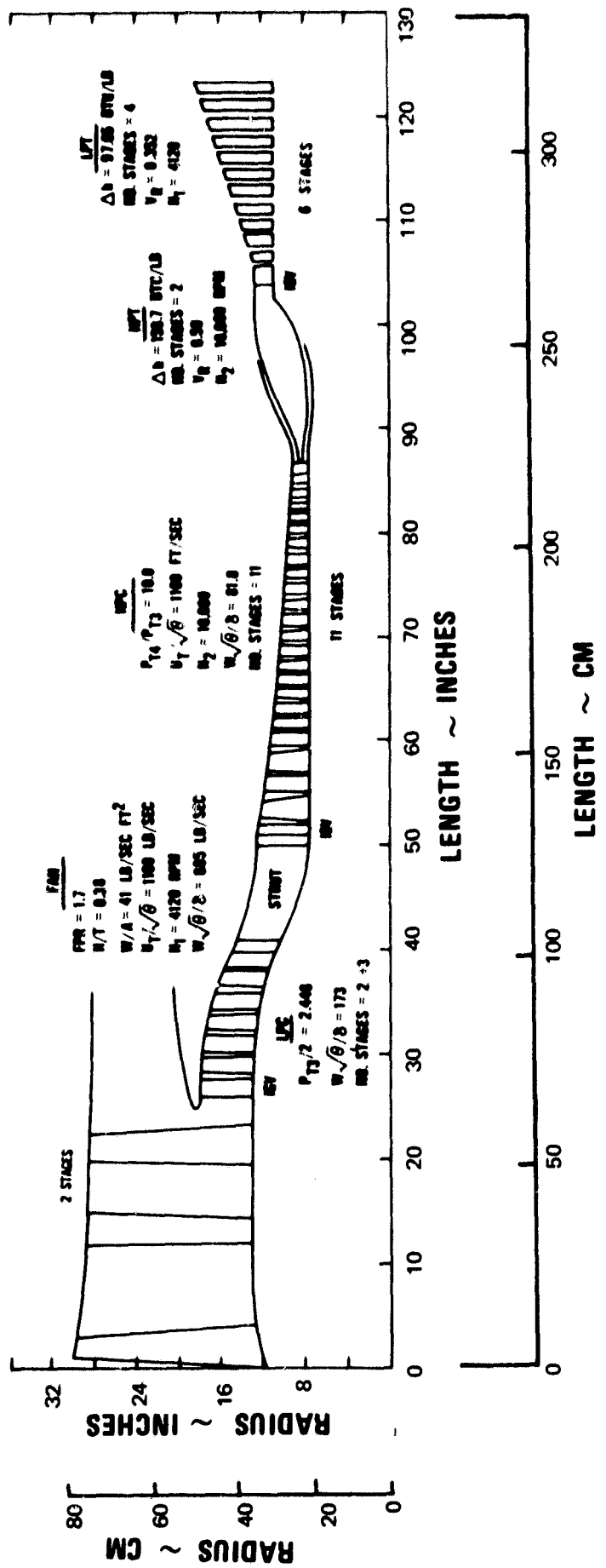

Figure 4 QA-1 Preliminary Working Flowpath

M-51017

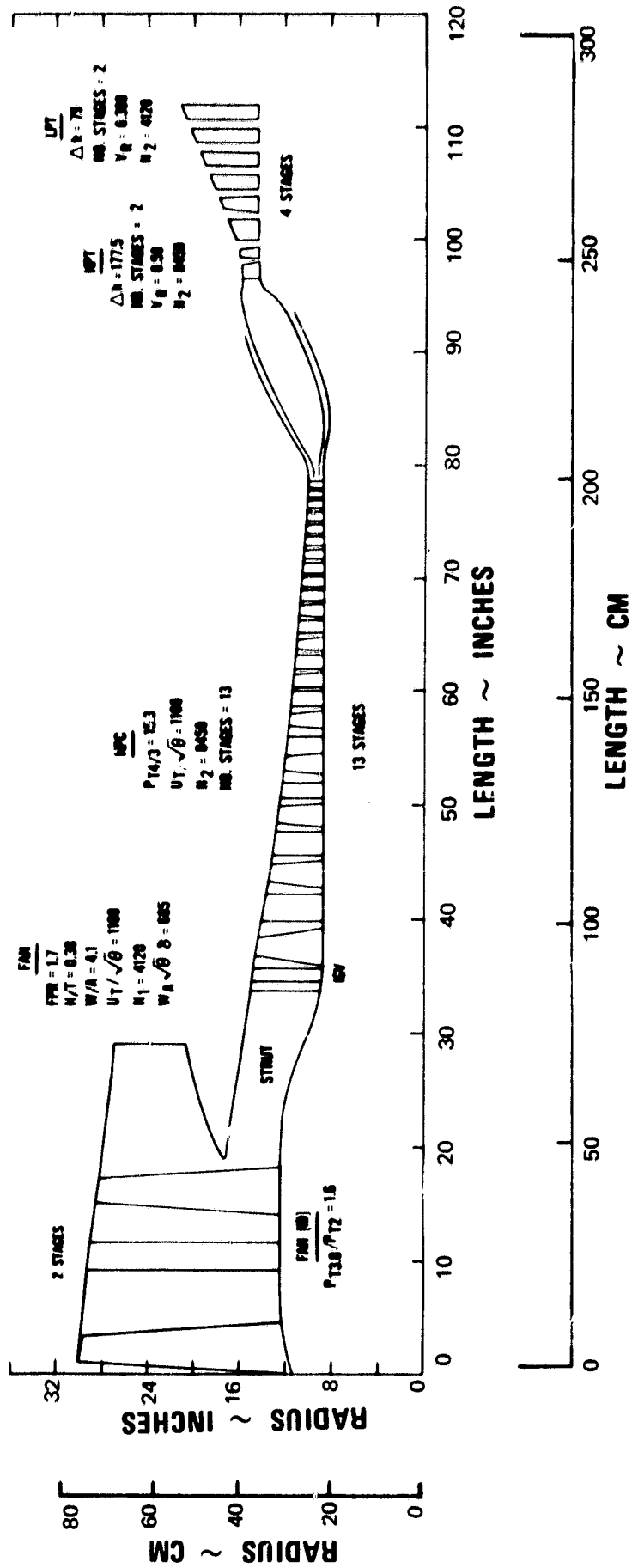

M-51016

Figure 5 QA-2 Preliminary Working Flowpath

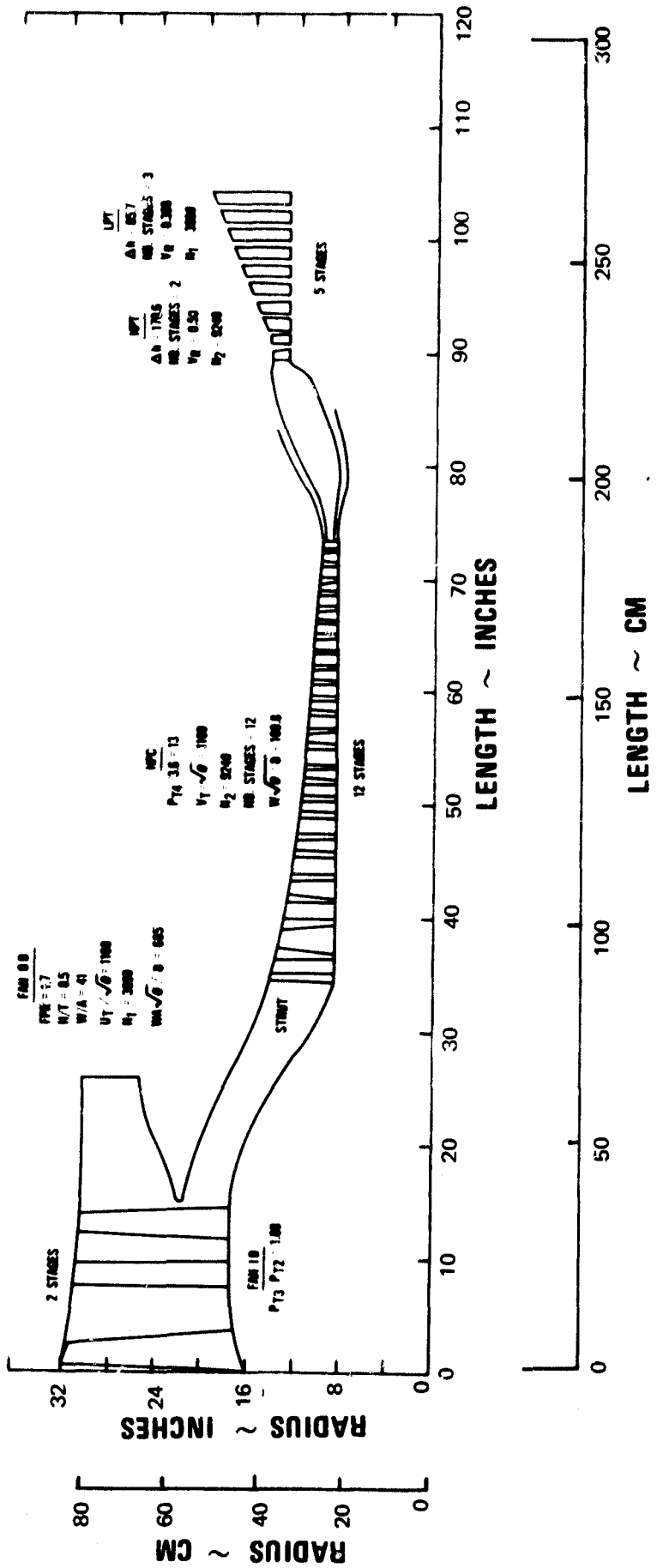

M-51011

Figure 6 QA-3 Preliminary Working Flowpath

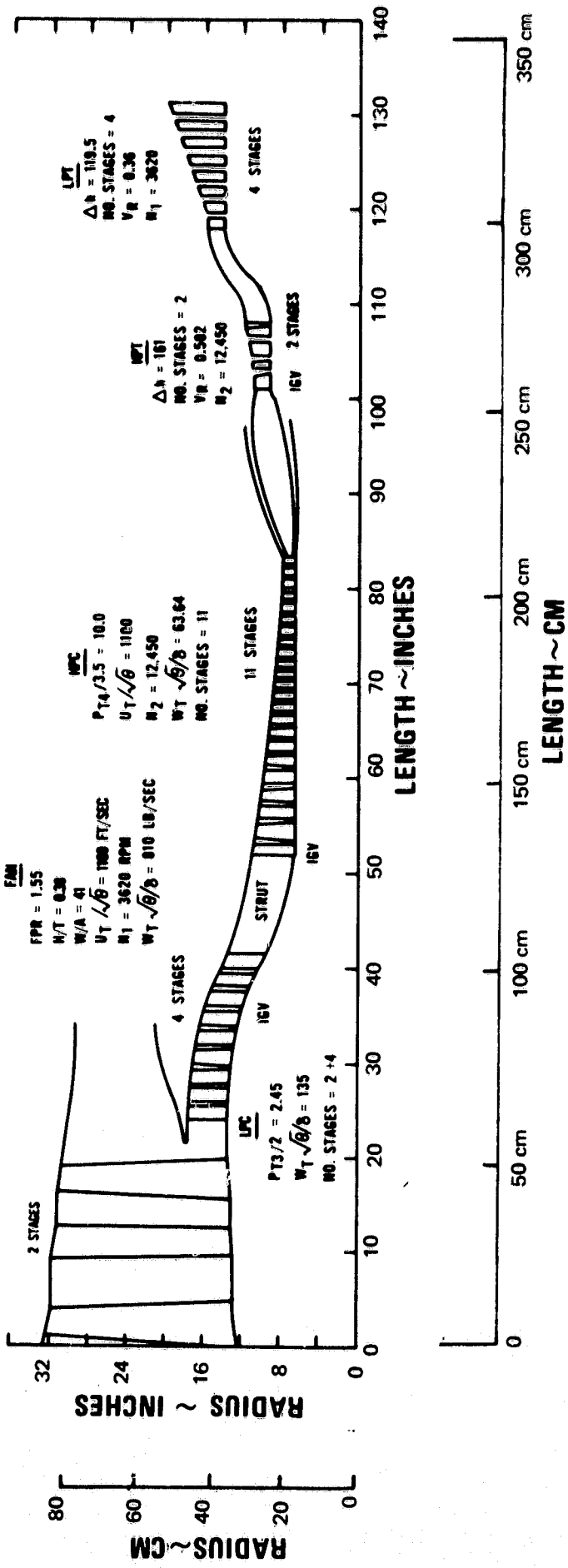

Figure 7 QB-1 Preliminary Working Flowpath

M-51019

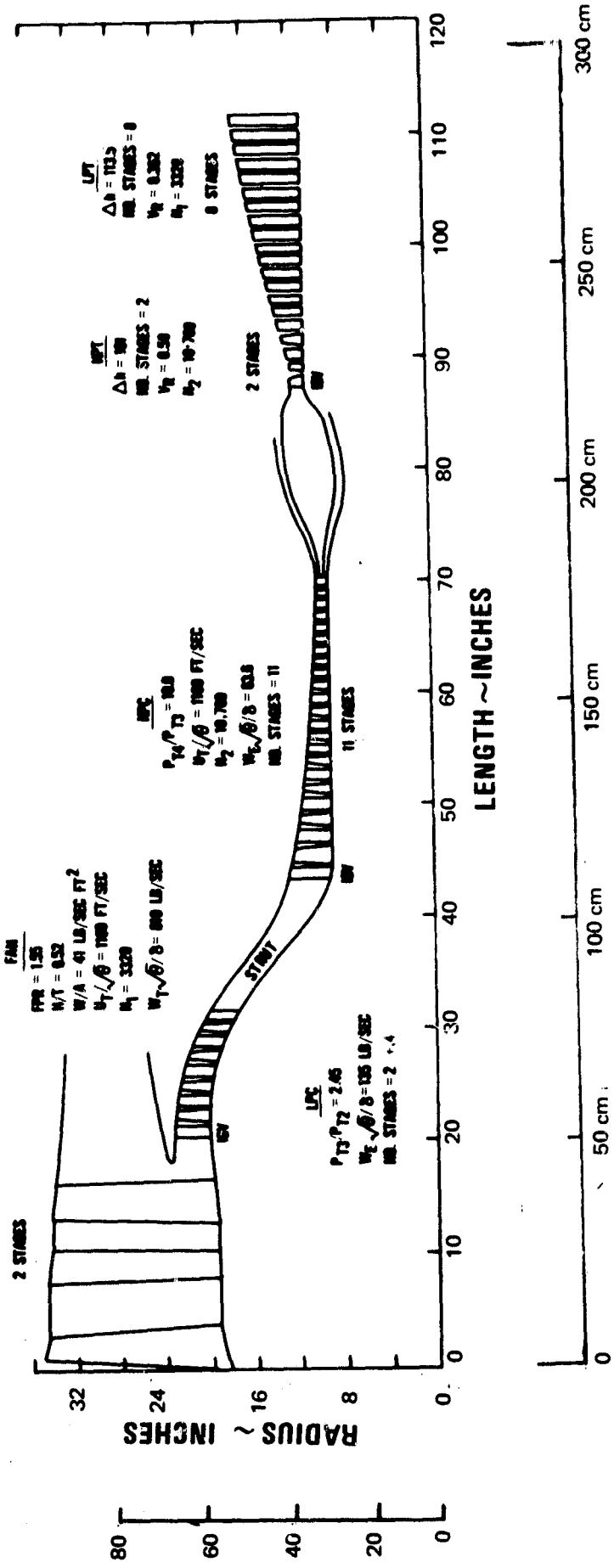

M-51018

Figure 8 QB-2 Preliminary Working Flowpath

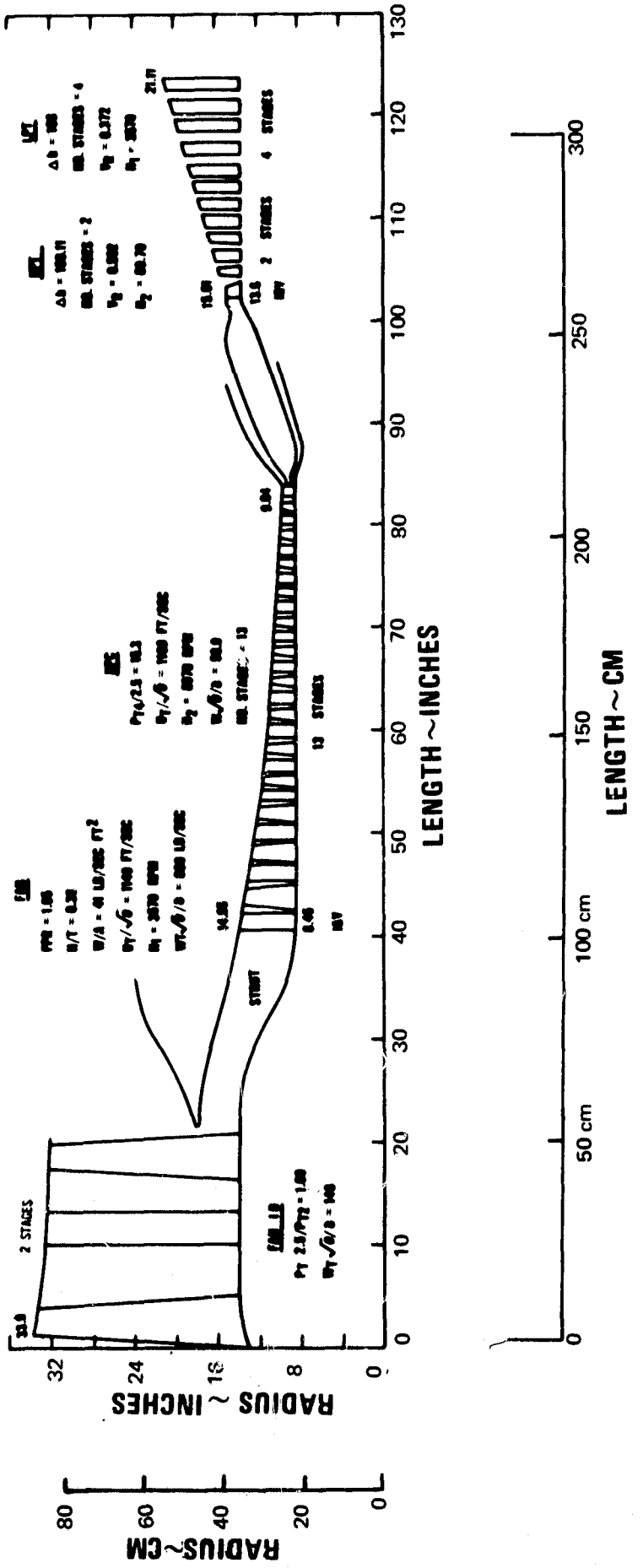

M-51010

Figure 9 QB-3 Preliminary Working Flowpath

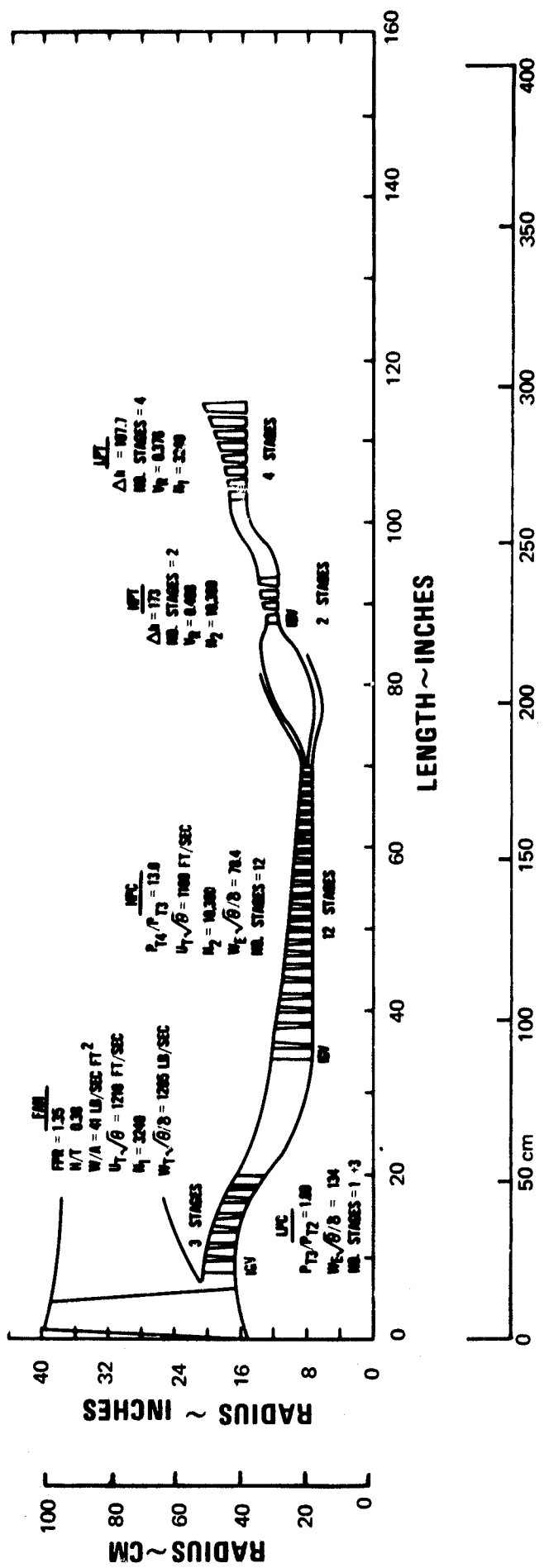

Figure 10 QC-1 Preliminary Working Flowpath

M-51020

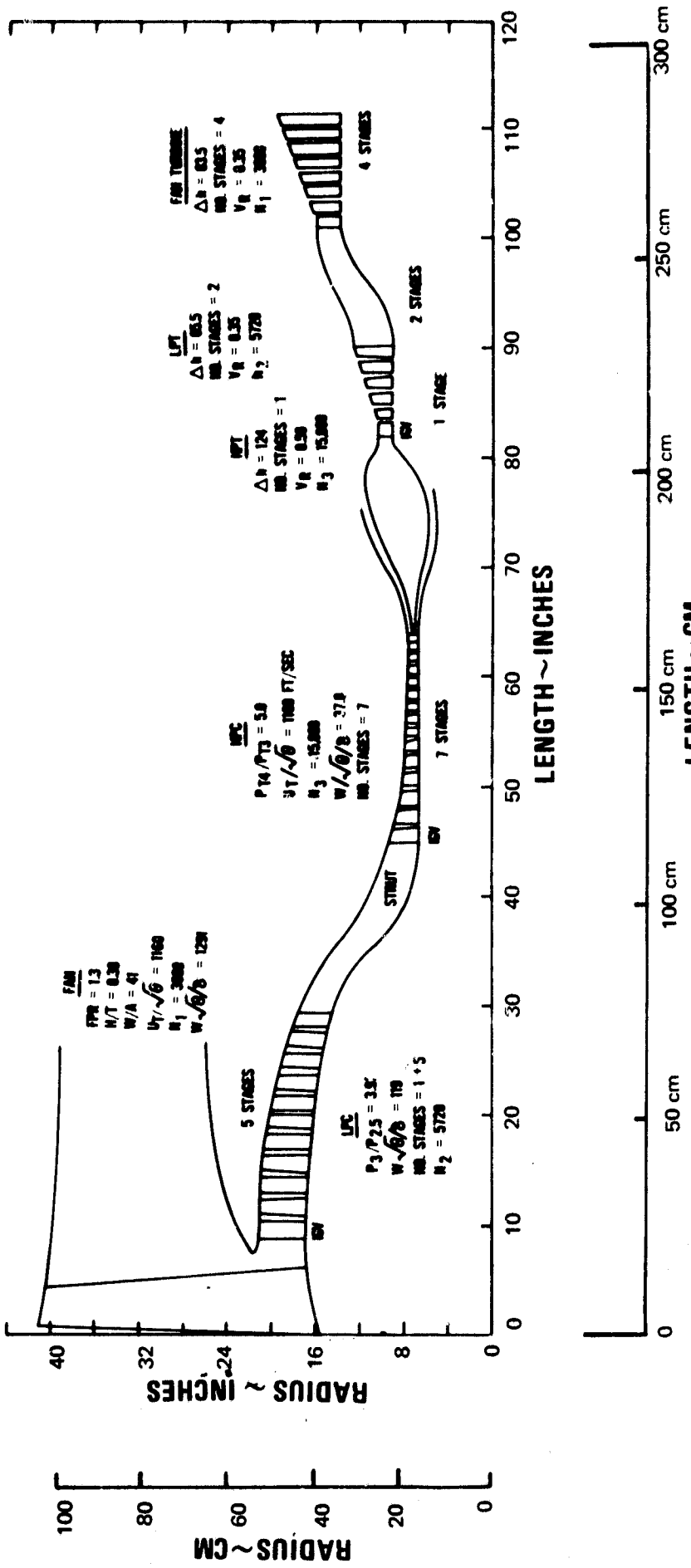

Figure 11 QC-2 Preliminary Working Flowpath M-51009

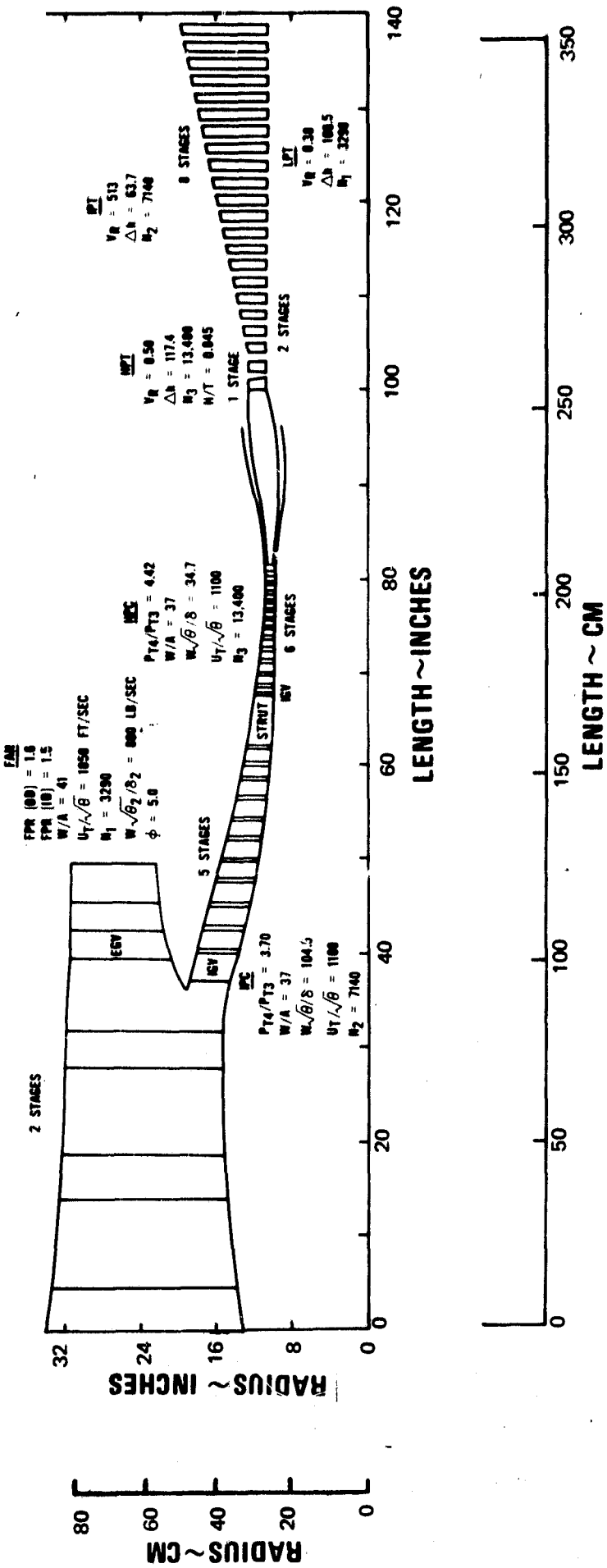

Figure 12 QD-1 Preliminary Working Flowpath

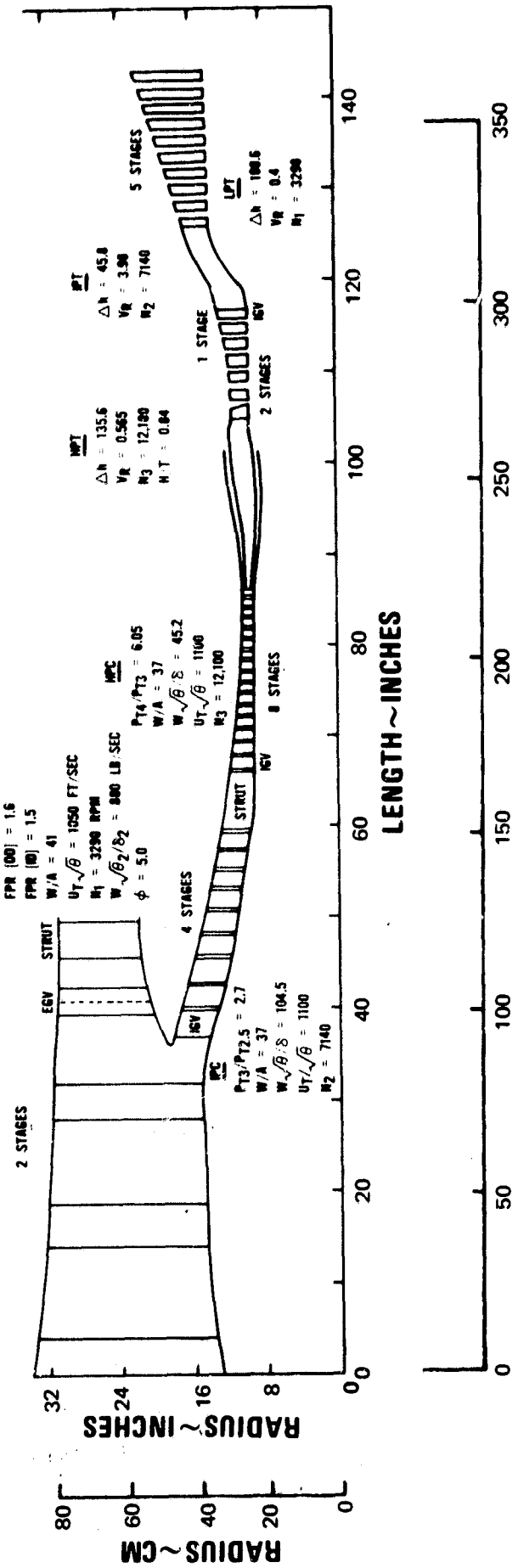

Figure 13 QD-2 Preliminary Working Flowpath

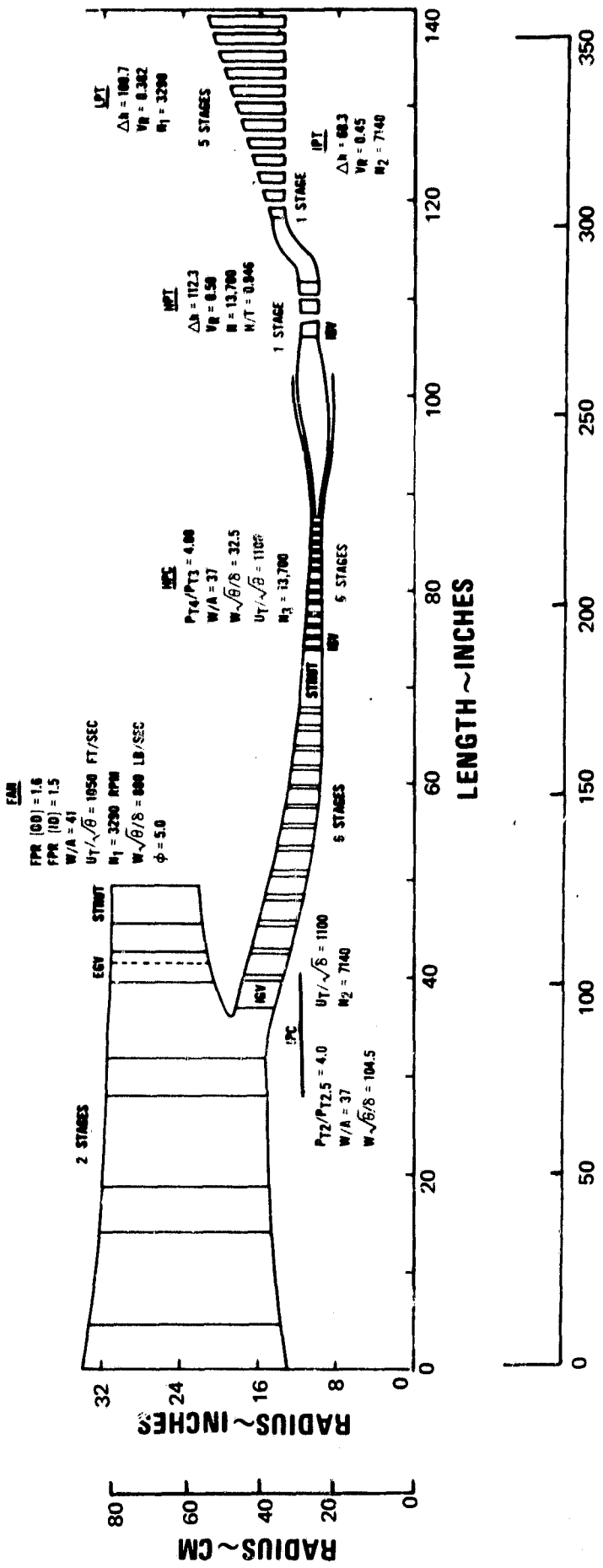

Figure 14 QD-3 Preliminary Working Flowpath

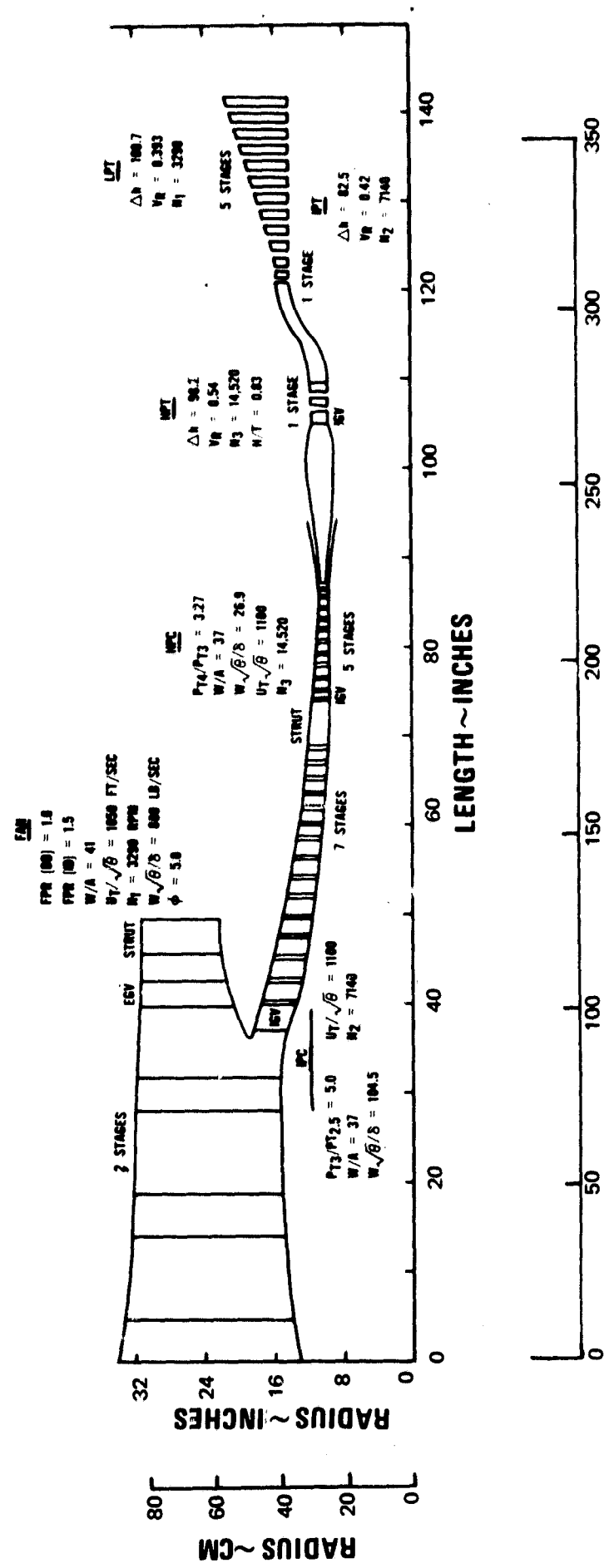

Figure 15 QD-4 Preliminary Working Flowpath

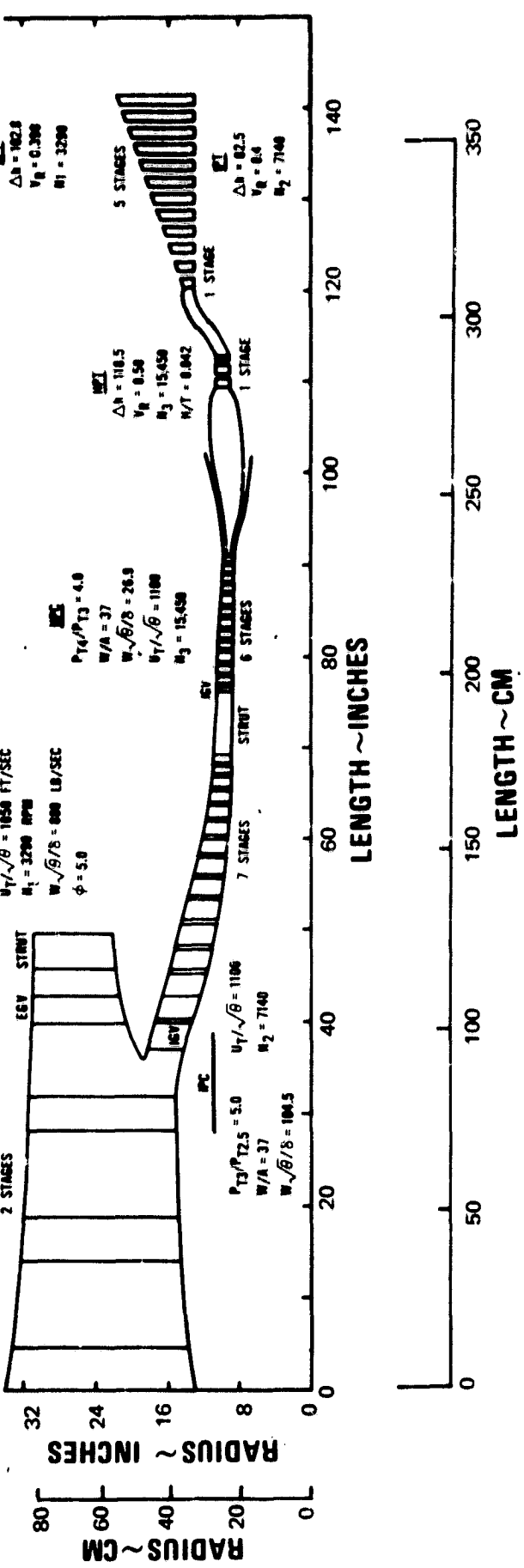

Figure 16 QD-5 Preliminary Working Flowpath

TABLE V

COMPONENT DESIGN ASSUMPTIONS FOR CANDIDATE CONFIGURATIONS

Fan	
Corrected flow/annulus area (lb/sec-ft^2)	41
Corrected flow/annulus area (kg/sec-m^2)	200
Minimum hub-to-tip ratio	0.378
Corrected tip speed at take-off (ft/sec)	maximum - 1100 preferred - 1000
Corrected tip speed at take-off (m/sec)	maximum - 336 preferred - 305
Fan rotor-stator spacing, in blade-tip chord lengths	preferred - 2.0 minimum - 1.5
Aspect ratio	4.35
Low-Pressure Compressor	
Inlet corrected flow/annulus area (lb/sec-ft^2)	37
Inlet corrected flow/annulus area (kg/sec-m^2)	181
Aspect ratio	2.0
Intermediate-Pressure Compressor	
Inlet corrected flow/annulus area (lb/sec-ft^2)	37
Inlet corrected flow/annulus area (kg/sec-m^2)	181
Maximum inlet corrected tip speed (ft/sec)	1100
Maximum inlet corrected tip speed m/sec)	336
Aspect ratio	2.0
High-Pressure Compressor	
Inlet corrected flow/annulus area (lb/sec-ft^2)	37
Inlet corrected flow/annulus area (kg/sec-m^2)	181
Maximum inlet corrected tip speed (ft/sec)	1100
Maximum inlet corrected tip speed (m/sec)	336
Maximum exit hub-to-tip ratio	0.90
Exit annulus Mach number	0.25
Aspect ratio	2.0
Burner	
Approximate burner length (in)	18.5
Approximate burner length (cm)	47.0
High-Pressure Turbine	
Minimum velocity ratio	0.5
Inlet anulus flow parameter* (lbm- $\sqrt{°R}$/lbf-sec)	0.158
Inlet anulus flow parameter (kg- $\sqrt{°K}$/n-sec)	0.00123

* $\frac{W\sqrt{T_t}}{A\ P_t}$

TABLE V (Cont'd)

Intermediate-Pressure Turbine	
Minimum velocity ratio	0.4
Inlet annulus flow parameter (lbm- $\sqrt{°R}$/lbf-sec)	0.37
Inlet annulus flow parameter (kg- $\sqrt{°K}$/n-sec)	0.00282
Low-Pressure Turbine	
Minimum velocity ratio	0.38
Exit annulus flow parameter (lbm- $\sqrt{°R}$/lbf-sec)	0.324
Exit annulus flow parameter (kg- $\sqrt{°K}$/n-sec)	0.00247

2. Results

The key features, advantages, and disadvantages of the preliminary flow path configurations are summarized in Tables VI, VII, and VIII. The items listed on these tables illustrate the sort of factors that were considered in selecting the best configuration for preliminary components design and preliminary mechanical design.

TABLE VI

SUMMARY OF THE QA CYCLE

Bypass Ratio of 3.0

	QA-1 (Figure 4)	QA-2 (Figure 5)	QA-3 (Figure 6)
Distinguishing Characteristics	Low-pressure compressor stages on fan spool	All compressor stages on high-pressure spool	High fan hub-to-tip ratio all compressor stages on high-pressure spool
Advantages	Smallest turbine diameter	Fewest turbine stages	Shortest fan fewest compressor stages
Disadvantages	Greatest number of stages	Largest turbine diameter	Large fan hub. Long transition duct between fan and compressor

TABLE VII

SUMMARY OF THE QB CYCLE

Bypass Ratio 5.0

	QB-1 (Figure 7)	QB-2 (Figure 8)	QB-3 (Figure 9)
Distinguishing Characteristics	Low-pressure compressor stages on fan spool. In-line turbine.	Same as QB-1, but with high fan hub-to-tip ratio	All compressor stages on high-pressure spool
Advantages	Smallest turbine diameter		Fewest total number of stages
Disadvantages	Greatest total number of stages. Nine low-pressure turbine stages	Eight low-pressure turbine stages, large fan hub and inter-compressor transition duct	Largest low-pressure turbine diameter

TABLE VIII

SUMMARY OF THE QC CYCLE

Bypass Ratio 8.0

Engine	QC-1 (Figure 10)	QC-2 (Figure 11)
Distinguishing Characteristics	Two spools. Low-pressure compressor stages on fan spool	Three spools
Advantages		Smallest turbine diameter and fewest number of stages.
Disadvantages	Larger turbine diameter. Greatest number of stages.	Lack of test experience with three-spool system.

a. QA Selection

The QA-2 arrangement (Figure 5) was discarded because of installation deficiencies. It has three fewer stages than the QA-1 (Figure 4) but the diameter of the last turbine stage is larger than the fan-flow splitter, requiring a greatly offset fan duct exhaust nozzle with probable penalties in cowl and engine afterbody nacelle drag. The reduction of three stages consists of a one-stage reduction in the compressor and a two-stage reduction in the turbine.

Because of its high fan hub-to-tip ratio, the QA-3 (Figure 6) is able to achieve a relatively high fan-root pressure ratio. This makes it possible to lower the pressure ratio of the high-pressure compressor and to eliminate one stage. However, the additional fan-root work is sufficient to require an additional stage in the low-pressure compressor, resulting in the same total number of stages as the QA-2. One advantage of the high hub-to-tip ratio in the fan is that the blade chords are shorter than they would be with a lower hub-to-tip ratio and the same aspect ratio. As a result, the spacing required to reduce the rotor-stator interaction noise is reduced, giving a shorter fan. This advantage is compromised somewhat by the heavier hub. A disadvantage of the higher hub-to-tip ratio is the weight and pressure loss of the long transition section required to lead the flow down and into the high-pressure compressor.

b. QB Selection

The QB-3 configuration (Figure 9) was chosen primarily because it had fewer stages than any of the other QB designs. In addition, the QB cycle was best suited for the elimination of low-pressure compressor stages on the fan spool. Although the QB-1 (Figure 7) is a more conservative design and has a slightly smaller maximum diameter, it is so similar to the design of the Pratt & Whitney Aircraft JT9D turbofan that subjecting it to a preliminary design study would have been repetitious. Finally, the QB-3 design readily lent itself to the contrarotating fan concept which was selected for study because of its potential noise advantages. Although these advantages have not been demonstrated by actual tests, it was decided to investigate what kind of over-all engine layout would result from the use of a contrarotating fan.

The QB-1 and QB-2 (Figure 8) were rejected because they both have unacceptably large numbers of turbine stages. In addition to a probable weight disadvantage, the lightly loaded rear stages would not be very efficient. The QB-2 was also rejected because its high fan hub-to-tip ratio resulted in a long transition duct between the compressors.

c. QC Selection

The QC-1 configuration (Figure 10) was selected in preference to the QC-2 because the two-spool system was considered to be more mechanically con-

servative than the three-spool system. Although the QC-2 (Figure 11) has fewer stages and a slightly smaller turbine than the QC-1, these advantages do not compensate for the potential design, development, and assembly difficulties associated with the three-spool configuration. In addition, the three-spool configuration encounters a possible weight disadvantage.

d. QD Selection

At the request of the NASA Project Manager, the contractor agreed to investigate a three-spool version of the 5.0-bypass-ratio cycle. Accordingly, five additional gas paths were drawn representing various pressure-ratio splits between the intermediate-pressure and high-pressure compressors. These gas paths are presented in Figures 12 through 16. One of the configurations used a cycle pressure ratio which had been increased from 24.5 to 30.0. All of the QD designs have two-stage fans. Schematic representations of the designs are shown in Figure 17. The three-spool configuration which was selected for preliminary design was evolved from the configurations shown in Figure 17, but does not correspond precisely to any of them.

The final selection, the QD-1A, corresponds more closely to the QD-1 than any of the other four preliminary configurations. The split of pressure ratios between the spools corresponds exactly to that of the QD-1, and was chosen for the QD-1A because it results in the fewest compressor stages. Also, it appeared to be unlikely that either the intermediate-pressure or the high-pressure compressor would require mechanically variable stators in order to achieve acceptable part-speed surge margin and efficiency. An additional advantage of this pressure-ratio split is that it uses the single-stage high-pressure turbine most effectively. The higher the work extracted in the first turbine stage, the lower the blade and vane temperatures will be in the second stage for a given turbine inlet temperature. This reduces the amount of cooling air required. The amount of work that can be used in the single-stage high-pressure turbine is limited by the expansion ratio which can be obtained efficiently. An expansion ratio of 2.75 has been successfully demonstrated in the contractor's rig and engine work and was used to determine the pressure ratio for the high-pressure spool in the QD-1 (and hence the QD-1A).

The eight-stage, in-line low-pressure turbine of the QD-1 was not used in the QD-1A because of the anticipated weight penalty and extremely light stage loading. It was replaced by the five-stage, offset, low-pressure turbine of the other four candidate configurations.

A final departure from the original QD-1 configuration was the reduction in the rotational speed of the high-pressure rotor. This was done in order to maintain an acceptable DN value at the front bearing, while increasing the shaft diameter to accomodate the fan drive shaft. The speed reduction was sufficient to require

an additional efficiently loaded high-pressure compressor stage. Also, because of the lower speed, it was necessary to increase the diameter of the high-pressure turbine in order to maintain a satisfactory level of velocity ratio. In order to keep the flow path of the intermediate-pressure turbine aligned with the flow path of the high-pressure turbine, its diameter was increased, making it possible to reduce the number of stages in the intermediate-pressure turbine from two to one. The change in diameter also meant that the high-pressure and intermediate-pressure turbines became virtually aligned with the low-pressure turbine, eliminating the aerodynamic difficulties and the weight penalty associated with a transition section.

	CONFIGURATION	FEATURES
QD-1	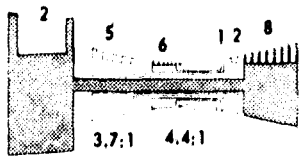	LEAST COMPRESSOR STAGES IN-LINE TURBINES
QD-1A	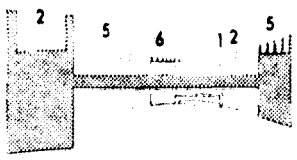	INCREASED DIAMETER FAN TURBINE
QD-1B	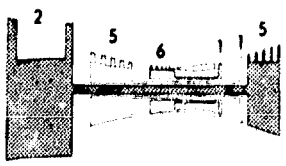	INCREASED DIAMETER FAN AND INTERMEDIATE TURBINES
QD-2	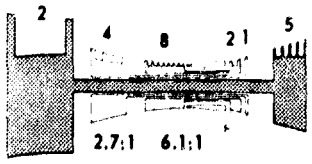	TWO-STAGE HI PRESS TURBINE MOST PRESSURE RATIO ON HIGH SPOOL
QD-3	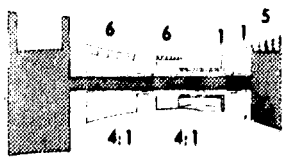	EVEN PRESSURE RATIO SPLIT ON COMPRESSORS
QD-4	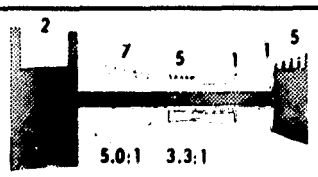	MOST PRESSURE RATIO ON INTERMEDIATE SPOOL
QD-5	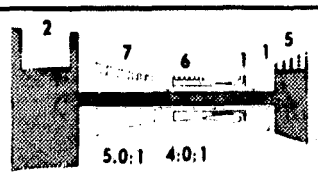	RELAXED OVERALL PRESSURE RATIO CONDITION MAX WORK FROM TURBINE STAGES

Figure 17 Schematics of the QD Engine M-51014

The QD-2 configuration was intended to demonstrate the use of a two-stage high-pressure turbine. Although the arrangement had the lowest high-pressure rotor speed of any of the QD flow path configurations, DN values of the bearings on the high-pressure rotor proved excessive, and the stage loading of the high-pressure compressor was inefficiently low. Finally, a preliminary estimate of the critical speed margin showed that the usual rear bearing arrangement for the high-pressure rotor would be inadequate. Instead of the usual system, where the bearing is located in front of the turbine and supported through the burner-diffuser case, it would be necessary to locate a bearing behind the turbine and to support it with struts between the high-pressure turbine and the intermediate-pressure turbine. This type of support would introduce additional length in the low-pressure and intermediate-pressure spools as well as additional pressure losses in the gas path.

In the QD-3 arrangement, the pressure ratio split between the high-pressure compressor and the intermediate-pressure compressor was made approximately equal. With this arrangement, the low-pressure compressor would ideally require five stages and a fractional stage to do the work efficiently. Thus, while a six-stage low-pressure compressor is aerodynamically efficient, it is underloaded, and would contribute unnecessarily to the weight and length of the engine. In addition, it would probably require variable stator geometry for satisfactory part-speed performance. A similar argument applies to the high-pressure compressor, which would also be underloaded with a pressure ratio of 4.08 in six stages.

A further disadvantage of the QD-3 arrangement is the offset diameter of the intermediate-pressure turbine. The offset is required to maintain an acceptable level of velocity ratio, but it is unsatisfactory because it requires a transition section between the high-pressure turbine and the intermediate-pressure turbine. A transition duct in that location is generally undesirable because it causes extra pressure loss, adds to the length of the intermediate shaft, and is exposed to high gas temperatures, which requires additional cooling air.

The QD-4 arrangement is the converse of the QD-2: it has the greatest pressure ratio in the intermediate-pressure compressor and the least pressure ratio in the high-pressure compressor of any of the configurations under consideration. The QD-4 was considered to be unsatisfactory because it requires variable stators in the intermediate-pressure turbine, has an underloaded high-pressure turbine, and requires a transition section between the intermediate-pressure turbine and the high-pressure turbine. Despite the fact that it has the shortest high-pressure spool of any of the QD configurations, preliminary analysis showed that the QD-4 has an inadequate stiff-bearing critical-speed margin.

The QD-5 arrangement has a cycle pressure ratio of 30 instead of 24.5. This pressure ratio was achieved by combining a scaled fan and intermediate-pressure compressor from the QD-4 with a scaled high-pressure compressor from The QD-3. Because of the higher pressure ratio of the cycle, the thrust-specific fuel consumption was slightly improved, but mechanical difficulties were encountered in the three-spool configuration. A decrease in specific thrust at cruise required that the fan and intermediate-pressure compressor be increased in size, while the high-pressure compressor had to be decreased in size, aggravating the tendency toward unacceptably high DN loadings in the bearings of the high-pressure rotor. Preliminary analysis also indicated that the space required for the fan spool shaft would increase the hub-to-tip ratio of the high-pressure compressor beyond 0.9. To do this would probably lead to a loss in the high-pressure compressor's efficiency, jeopardizing the improvement in thrust-specific fuel consumption brought about by the higher pressure ratio of the cycle.

Other disadvantages of the QD-5 configuration are the probable need for variable stators in the intermediate compressor and the transition section required by the offset intermediate-pressure turbine. This arrangement was evaluated primarily for assurance that the 24.5 over-all pressure-ratio required did not impose an artificial restraint on the optimum arrangement.

The requirement of low fan tip speed in a high-bypass-ratio, concentrically arranged, three-spool, front-fan turbofan leads to high bearing DN values and critical-speed problems in the high-pressure spool. This problem arises because the low-pressure shaft must have a relatively large diameter in order to transmit the high torque resulting from high power transmitted at low rotational speed. As a result, there appears to be a practical upper limit on cycle pressure ratio. As pressure ratio increases, the exit annulus of the high-pressure compressor becomes smaller with respect to the inlet area. Thus, in order to maintain acceptably low hub-to-tip ratios and Mach numbers in the exit of the low-pressure compressor, the core of the high-pressure spool becomes too small to carry a fan shaft which is large enough to transmit the necessary torque. The shafting problem, a key factor in the initial selection of a three-spool arrangement, later proved to be a critical factor in the final portion of the QD engine mechanical design effort.

SECTION IV

PRELIMINARY DESIGN LAYOUTS

The QA-1A Quiet Engine is a twin-spool turbofan engine which consists of the following components: a two-stage fan, a three-stage low-pressure compressor, an eleven-stage high-pressure compressor, an annular combustor, a two-stage high-pressure turbine, and a four-stage low-pressure turbine. Also a twin-spool axial-flow turbofan, the QB-3 consists of a two-stage contrarotating fan, a fourteen-stage high-pressure compressor, an annular combustor, a two-stage high-pressure turbine, and a contrarotating low-pressure turbine. Like the first two designs, the QC-1 is a twin-spool axial-flow turbofan. It consists of a two-stage fan and three-stage low-pressure compressor, an eleven-stage high-pressure compressor, an annular combustor, a two-stage high-pressure turbine, and a four-stage low-pressure turbine. Figures 18, 19, and 20 illustrate the mechanical arrangements of these three designs and show bearing locations and main structural cases.

With noise-reduction features dominating their designs, the QA-1A, QB-3, and QC-1 engines are distinguished by low-tip-speed fans (corrected fan tip speeds are approximately 1090 ft/sec or 332 m/sec) with the first-stage rotor overhung from a support integral with its stator. Aerodynamic integrity has not been compromised in the stator by thickened struts to accomodate oil lines servicing the bearing compartment. However, the rotors are spaced two chord widths from the stators to avoid noise produced by blade-vane wake interactions.

Three additional stages mounted on a single conical hub make up the low-pressure compressor of the QA-1A and the QC-1. The QB-3 has no low-pressure compressor. A variable inlet guide vane to the low-pressure compressor is used in QA-1A and QC-1 to guard against stalling.

The intermediate case is a main structural element of the engine, and like the JT9D, this case contains the main thrust bearings for both shafts. Many engine services, including the accessory drive shaft, pass through the struts of this case.

The high-pressure compressor, which is similar to the JT9D design, has four stages of variable geometry and a constant inner diameter flowpath. Air for various engine and airframe functions is extracted along the outer casing of the high-pressure compressor.

The short annular combustor section consists of an integrated diffuser and burner with film-cooled louvered liners. A structural case in the region of the diffuser section is used to support the Number 4 bearing.

Portions of the fan duct within the envelope usually supplied by the engine manufacturer are lined with sound-absorbent material for additional sound suppression. The fan duct and engine splitter are designed to permit the incorporation of an inside-mounted accessory gear box. The accessories are mounted directly around the high-pressure compressor region, close to the gas generator. The mounts are located in the planes of the intermediate case and the turbine exhaust case.

The QD-1A Quiet Engine is a three-spool axial-flow turbofan engine. It uses a two-stage fan, a six-stage intermediate-pressure compressor, a seven-stage high-pressure compressor, an annular combustor, a single-stage high-pressure turbine, a single-stage intermediate turbine, and a five-stage low-pressure turbine. The mechanical design is shown in Figure 21.

The engine is designed to provide the maximum noise reduction attainable with high efficiency through the use of appropriate axial spacing between the fan stages and selection of the proper blade-to-vane design relationships.

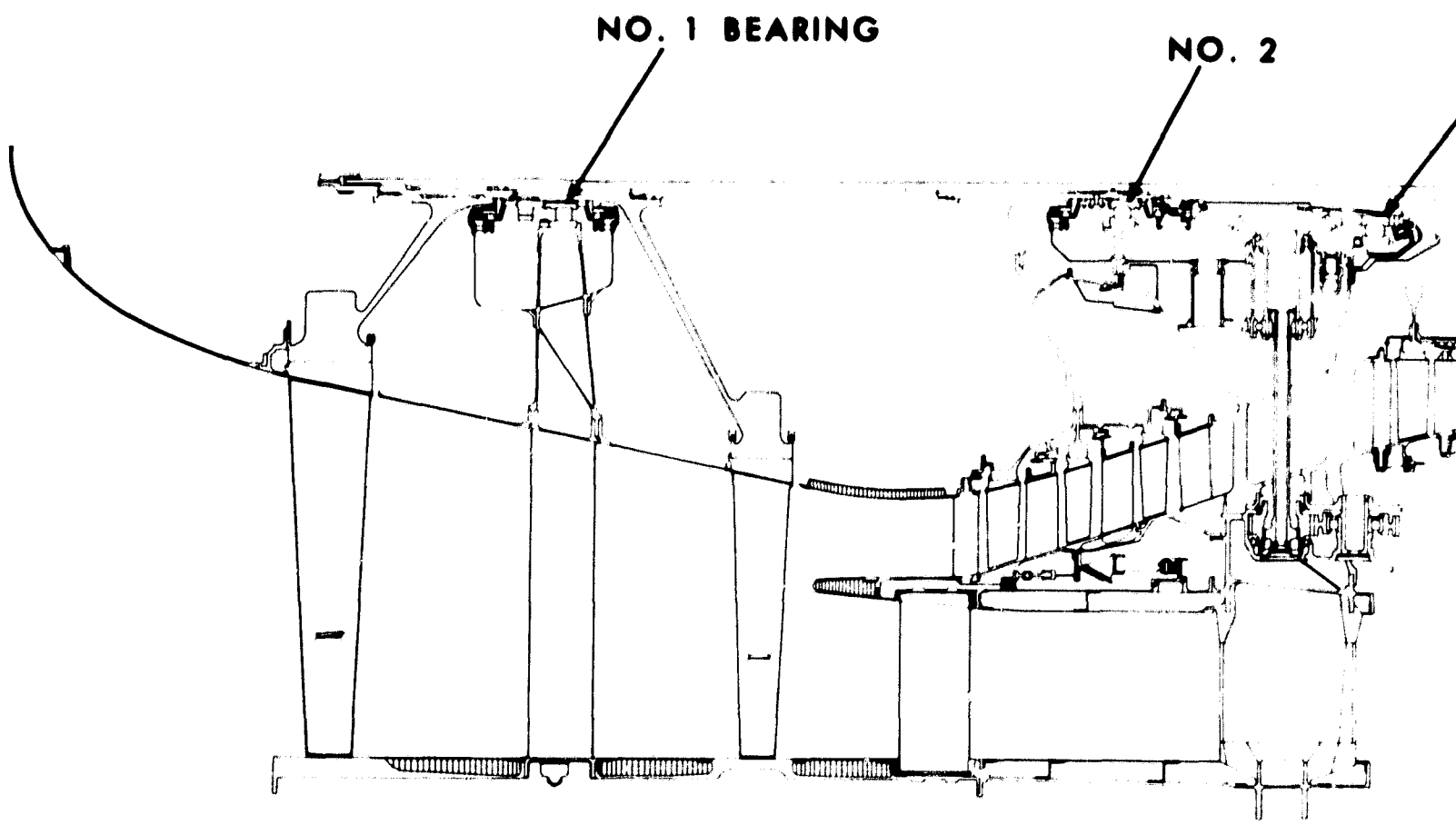
NO. 1 BEARING
NO. 2

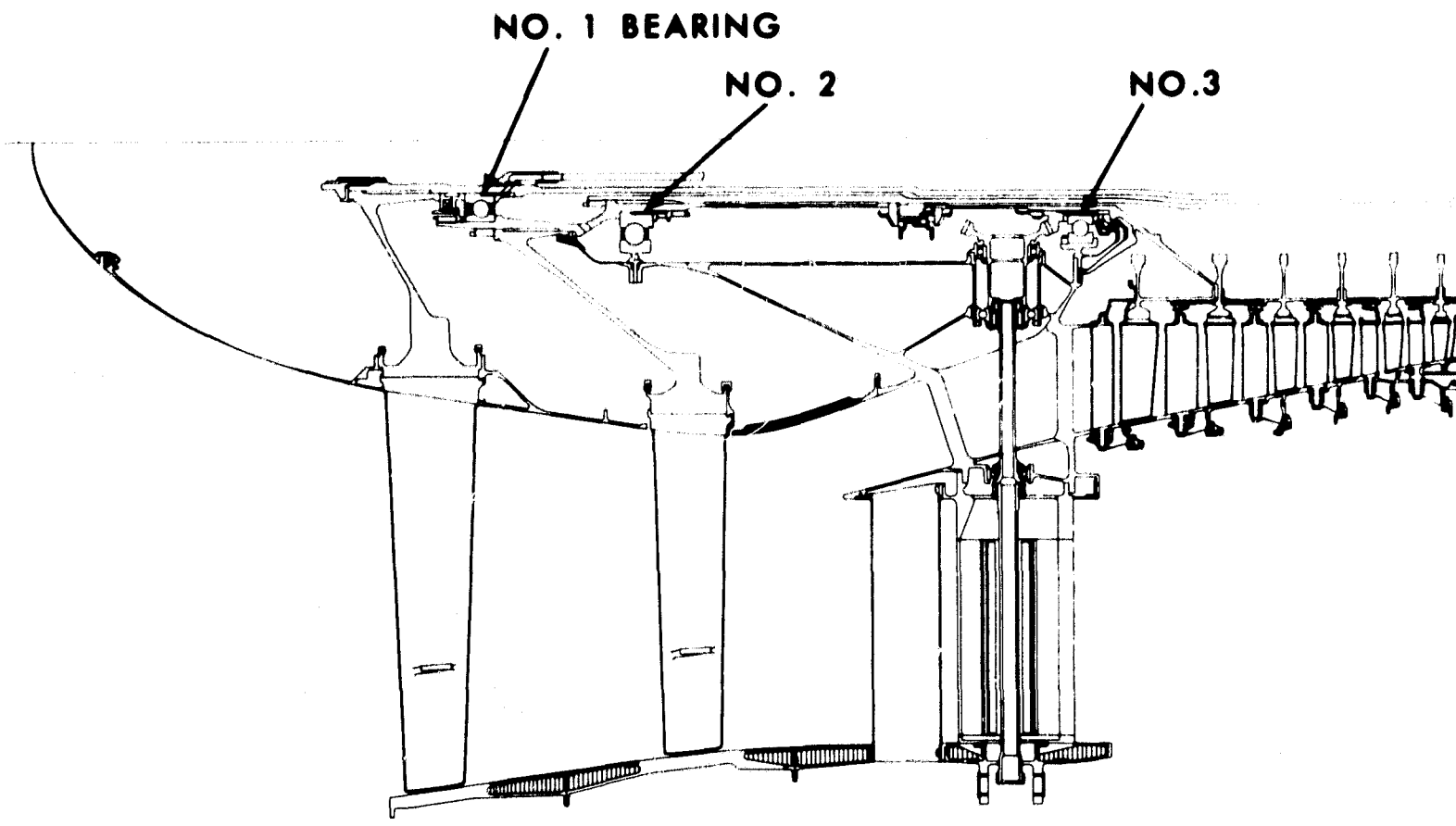
NO. 1 BEARING
NO. 2
NO.3

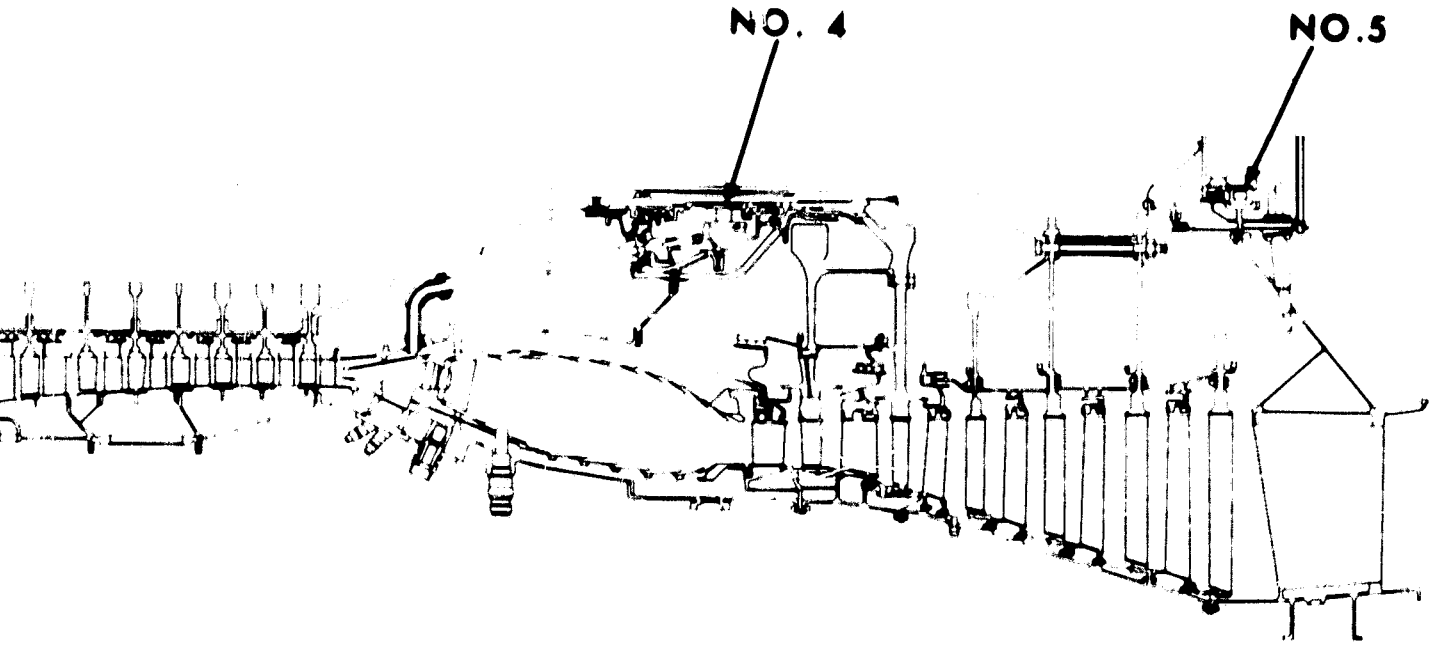

Figure 18 QA-1 Layout

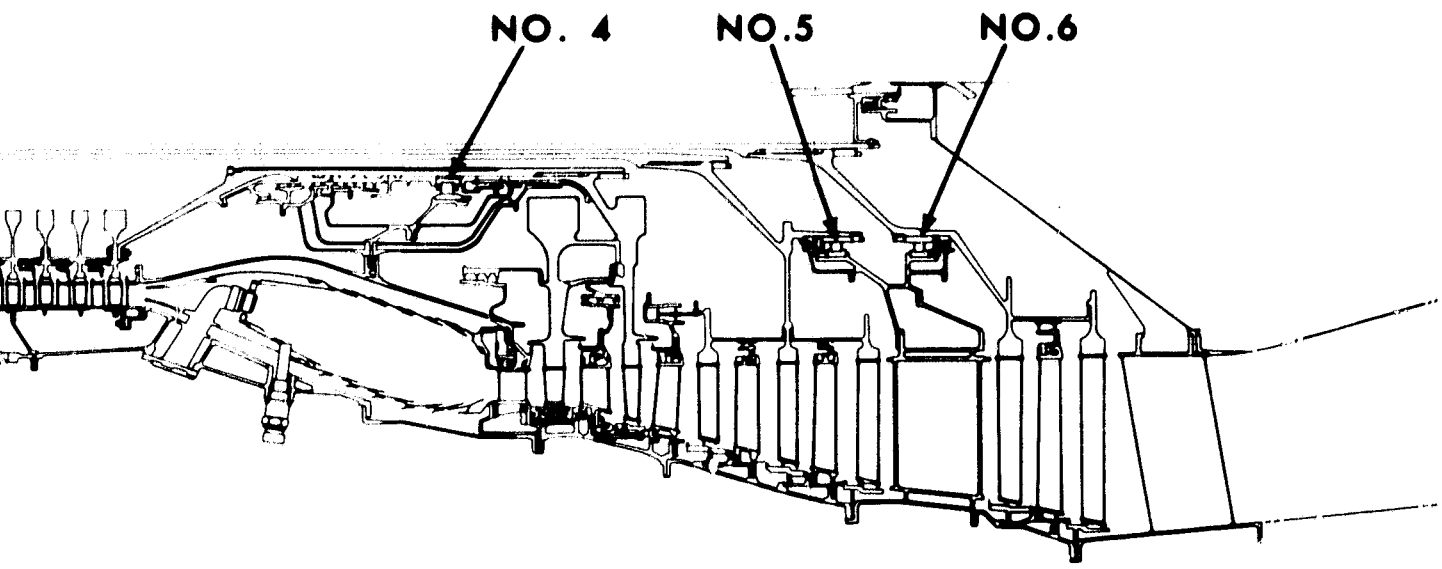

FOLDOUT FRAME 2

Figure 19 QB-3 Layout

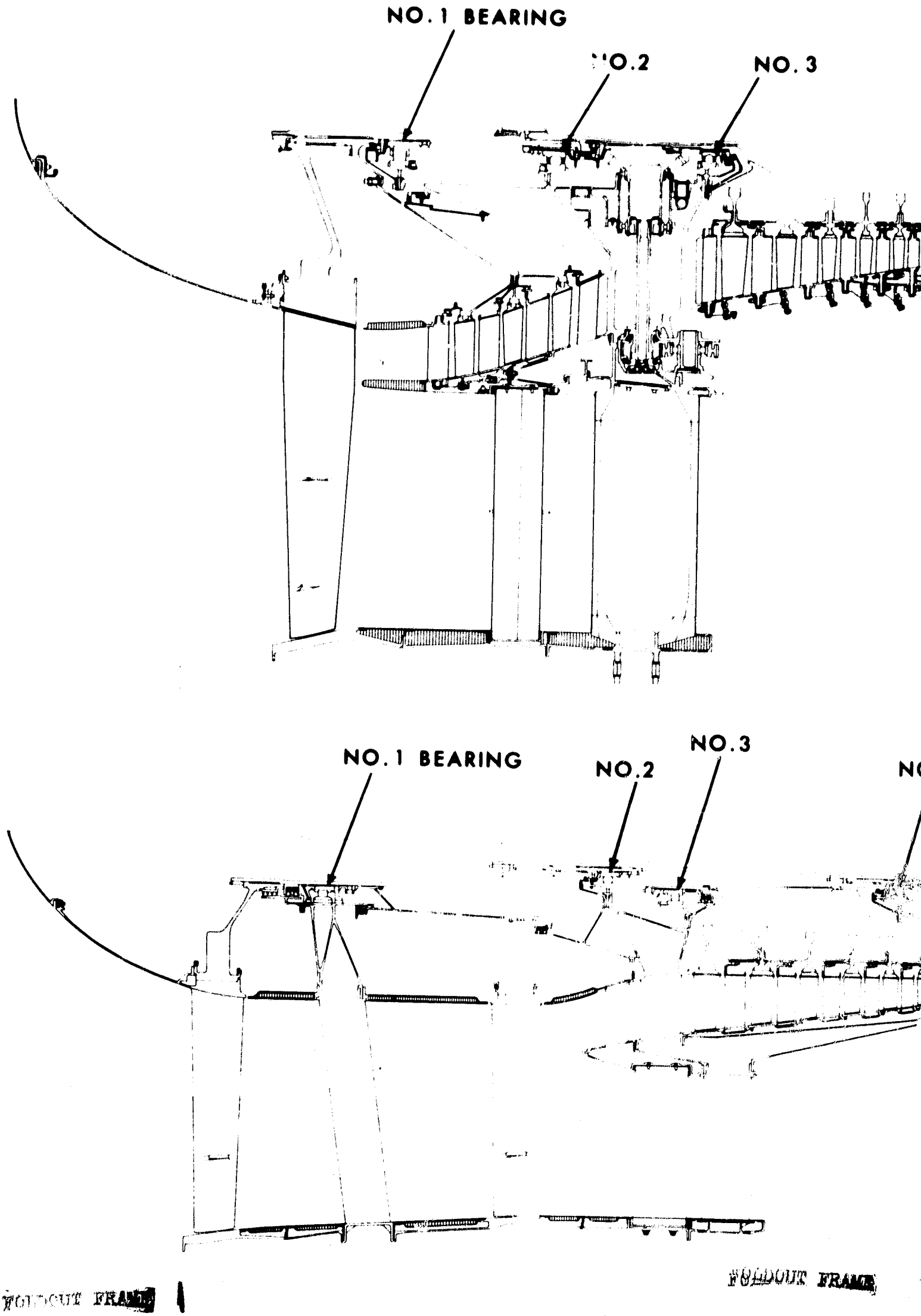

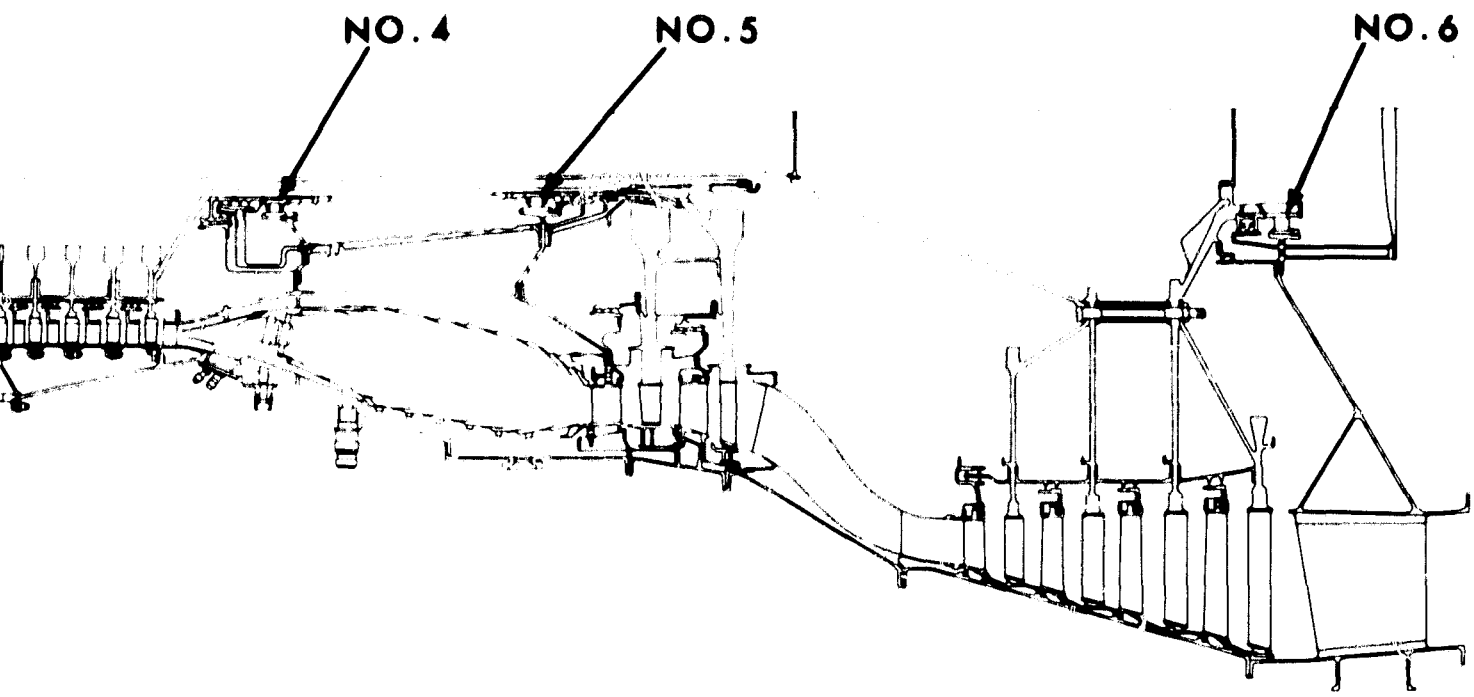

Figure 20 QC-1 Layout

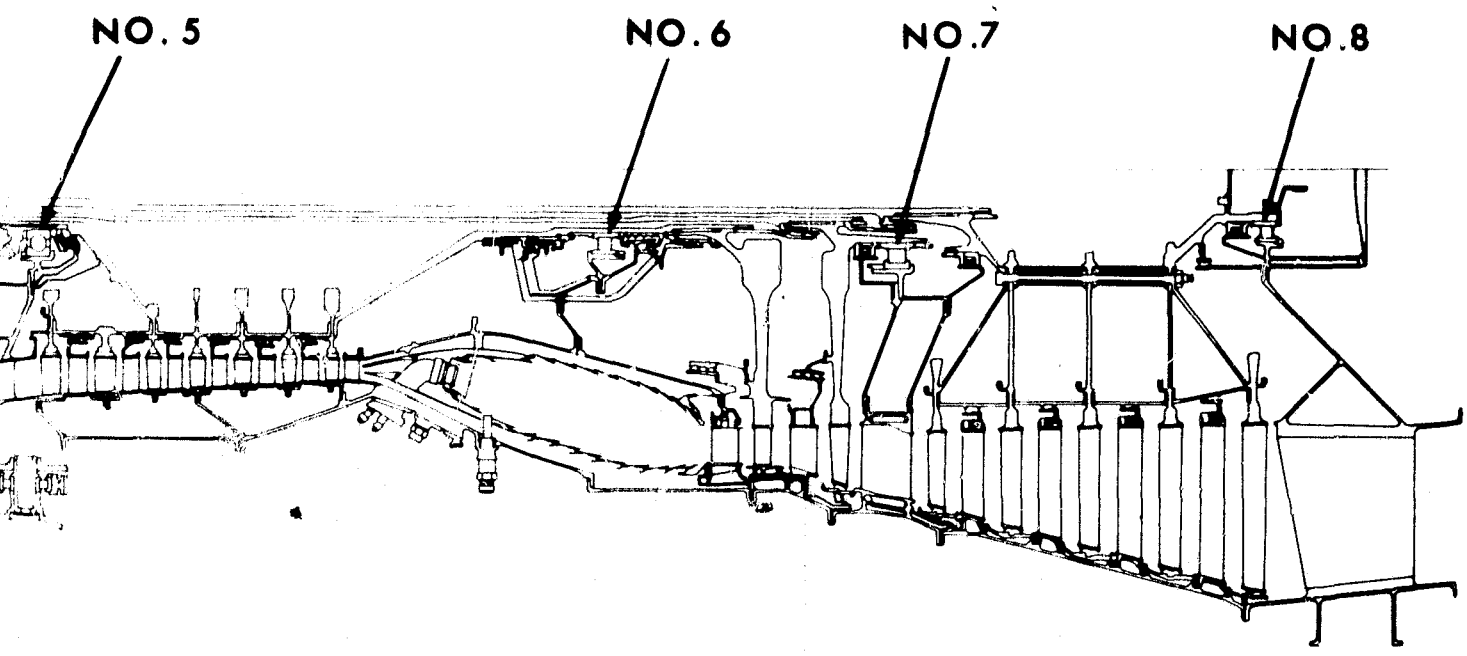

Figure 21 QD-1A Layout

FOLDOUT FRAME 2

1. Mechanical Design

In general, the mechanical design of the Quiet Engines has followed current design practice for advanced commercial engines. The engines are designed for a rear mount located in the turbine exhaust frame, and the main structural strength of the engines comes from the engine cases over the high-pressure compressor, the burner, and the turbine sections. For improved noise characteristics, the aerodynamic features of the fan stators have been preserved without the use of several thickened stators to manage services, as in more conventional designs. Bearing speeds have been kept within the limits of those used and proven in current designs, with the exception of the Number 5 and 6 bearings in the QD-1. These bearings support the high-pressure compressor, and operate at a DN value of 1.76×10^6 mm-rev/min (1.85×10^5 mm - rad/sec). These bearings have been extensively analyzed, and the results of the analysis indicate that they can be used successfully.

Several areas of the four designs having a particular bearing on the mechanical feasibility of the designs have been investigated analytically. These items include bearings, critical speeds, static structure, and blade and disk vibration. A brief description of these items is given below.

a. Bearings

The fan rotor bearing of the QA-1 is supported by the fan stator and inner diaphragm, which are reinforced by a conical member to prevent excessive axial deflection. This support is loaded by the radial bearing loads and axial aerodynamic forces acting on the stator vanes. The radial load is assumed to be the load equivalent to a 10-percent blade loss in the first-stage fan, estimated at 85,000 pounds (378,000 newtons). Blade-loss load stresses are approximately 15 percent of the ultimate strength in the vanes and 60 percent of the ultimate strength in diaphragm areas. The diaphragms are stiffened by means of a conical web resulting in acceptable deflections of about 0.015 inch (0.0387 cm). Thus, this bearing is seen to present no serious difficulties and can safely withstand a 10-percent blade-loss loading.

The bearing support for the overhung fans in the QB-3 consists of a stiffened conical shell structure cantilevered from the inner ring portion of the intermediate case. Here again, the most significant loading is the radial load produced by the 10-percent blade-loss criterion for any rotor stage (about 110,000 pounds or 489,000 newtons for the first-stage fan). Maximum stresses in the inner structure will be less than 20 percent of the ultimate for this titanium alloy structure. The spring rate of this structure was also evaluated to determine that acceptable spring rates could in fact be reasonably attained. The more sensitive portion, the inner cone structure, was found to have a spring rate of 1.7×10^6 lb/in (2.98×10^6 N/cm). This, in combination with the struts

and outer casing will result in an overall spring rate for this structure of not less than 1.0×10^6 lb/in (1.75×10^6 N/cm), based on experience with similar systems. The bearing support system can thus adequately withstand the blade loss loading and is sufficiently stiff not to adversely affect the rotor system's natural frequencies.

In order to meet the torque requirements for the high-speed shaft of the QD-1 design, the minimum shaft diameter was set at 160 mm. This results in a bearing DN value of 1.76×10^6 mm-rpm (1.84×10^5 mm-rad/sec) at the aerodynamic design point and a maximum DN value of 1.93×10^6 mm-rpm (2.02×10^5 mm-rad/sec) at sea-level take-off on a hot day. This DN number exceeds the maximum DN value considered well established by Pratt & Whitney Aircraft. However, careful review of the QD-1 bearing design in more detail than just the DN criteria established that its mechanical integrity can be expected to be adequate.

b. Shaft Critical Speeds

The stiff-bearing critical-speed analysis for the QA-1A design showed that the low-speed rotor has a critical-speed margin of 91 percent, while the high-speed rotor has a margin of 49 percent. These margins are based on a reference speed equal to 1.10 times the design speed. A margin of 20 to 25 percent is generally acceptable in modern jet engines.

A stiff-bearing critical-speed analysis for the QB-3 showed that the low-speed rotor had a 28-percent critical-speed margin, the intermediate rotor had an 83-percent margin, and the high-speed rotor had a 62-percent margin. For the QC-1 design, the low-speed rotor had a critical-speed margin of 78 percent, while the high-speed rotor had a margin of 58 percent.

For the QD-1A design, the margins were found to be 86 percent for the low-speed rotor, 64 percent for the intermediate rotor, and 50 percent for the high-speed rotor. With this relatively comfortable critical-speed margin and the high torque requirements resulting from its low speed, the low-speed shaft presented an unusual design limitation. The shaft thickness and diameter were determined solely by the torque-carrying requirement, unlike the thickness and diameter of most turbofan engine shafts. If the diameter of the shaft in the QD-1A were decreased, the shaft thickness would increase rapidly to the point where the shaft would become solid. That is, the shaft is essentially at its smallest outer diameter. On the other hand, an increase in the diameter of the high-speed shaft would be necessary to accomodate a low-speed shaft with a larger diameter. This would result in an excessive DN value for the high-speed rotor bearings. As discussed above, the DN value for these bearings has already been set at the maximum value consistent with the current state of the art. It has been estimated that, as currently designed, the low-speed shaft would shear if the rotor speed were reduced by more than about 10 percent without a commensurate reduction in transmitted power.

c. Blade and Disk Vibrations

A computer analysis of blade and disk vibrations was made for all applicable stages in the compressor and turbine sections of each design. The analysis showed that the aerodynamic design of the blade elements provides sufficient chord lengths to ensure stage vibration integrity, which means that no unforeseen component lengthening is anticipated on account of vibration.

2. Weight Analysis

During Task II of the program, the four configurations were evaluated to predict noise, performance, and weight data. The weight analysis technique was an extension of that used in past Pratt & Whitney Aircraft programs, and has been verified by checking predictions against the actual weights of manufactured engines.

As a first step in the weight analysis, preliminary layouts defining the over-all mechanical arrangements were obtained. A Bill of Material was then established for the layout to ensure that all major items were considered. An effort was made to have consistency between the four designs insofar as material selections and structural integrity were concerned.

Weights of rotating parts were obtained from a computer program. This program is a tried and proven tool for predicting disk weights with a minimum of input data. An essential part of the program is an accurate estimate of rotor polar moments of inertia. Both rotor weights and polar moments of inertia were used for the critical-speed analysis of the shaft. The results of the critical-speed determination were used to determine shaft and bearing geometry, and are reflected in the preliminary layouts and weights.

The latest commercial design practice is accounted for in the weight analysis, which includes provisions for fan blade containment, blade loss, and increased structural integrity in rotor and disk design. In addition, all weight estimates account for sound suppression materials incorporated in the fan section.

The accessories listed below are consistent with those being supplied with current large commercial turbofans. They are lumped together under the term "accessories" in Table IX, which is a summary of the established component weights in each configuration.

- Full-duty gearbox
- Fuel control
- Ignition system
- Pressurizing and dump valve
- Oil tank
- Fuel-oil cooler
- Fuel heater
- Instrumentation
- Fuel pump and filter
- Fuel, air, and oil lines
- Variable-geometry actuators

TABLE IX

WEIGHT SUMMARY

	QA-1A (lb)	QA-1A (kg)	QB-3 (lb)	QB-3 (kg)	QC-1 (lb)	QC-1 (kg)	QD-1 (lb)	QD-1 (kg)
Fan rotors and stators	1050	476	1005	456	1055	479	1225	556
Support structure	-	-	-	-	-	-	335	152
Low-pressure compressor rotors and stators	320	145	-	-	330	150	-	-
Support structure	465	211	410	186	600	272	-	-
Intermediate compressor rotors, stators, and case	-	-	-	-	-	-	350	159
Support structure	-	-	-	-	-	-	130	72
High-pressure compressor rotor and stators	635	288	680	308	650	295	305	138
Diffuser and burner	490	222	490	222	500	227	495	224
High-pressure turbine rotor and stators	480	218	545	247	430	195	390	177
Intermediate turbine rotor, stators, and case	-	-	-	-	-	-	220	100
Transition section	-	-	-	-	-	-	165	75
Low-pressure turbine rotor, stators, and exhaust	850	386	1250	568	1195	543	855	388
Rear support structure	-	-	-	-	-	-	210	95
Shafting	265	120	495	225	305	138	365	166
Accessories	525	232	545	247	545	247	525	232
Total Estimated Weight	5080	2298	5420	2459	5610	2550	5570	2534

3. Maintainability

Each of the Quiet Engine designs was reviewed by the contractor to ensure that all phases of maintenance were given careful consideration during the design. Special attention was given to inspection provisions, rotor balancing techniques, and parts replacement procedures to ensure that the maintenance capabilities of these engines were consistent with current trends in commercial airline practice.

Inspection of the inlet areas was improved by the elimination of the inlet case structure, thus allowing visual inspection of the first- and second-stage fan blades. The fan assemblies were designed so that the first-stage disks and blades could be replaced as balanced units. The use of moment-weighted blades in these units also allows blades to be replaced in moment-weighted pairs without rebalancing the units.

Parts in the front ends of the engines can be removed without disturbing the aft units. This maintainability feature is permitted by the modular design used for each of the engines. Figures 22 and 23 illustrate the removal of modules in the teardown of the QB-3, which is typical of all the designs. The modular construction will decrease engine turn-around time in the shop, thereby increasing availability. This feature also presents possibilities for the incorporation of new support concepts such as modular replacement at dock facilities and component overhaul. In addition, it permits accomplishment of more unscheduled maintenance with the engine installed in the aircraft.

4. Reliability

In establishing the various mechanical arrangements for the engine cycles that have been studied, reliability was one of the major design considerations. Maximum inherent reliability, consistent with the required performance, has been achieved by advances in the state of the art of gas turbine technology and by the knowledge gained from extensive past experience on commercial and military engine programs. These two factors have had an effect on the mechanical design of these engines by reducing the complexity of the functional components and by incorporating specific design features which yield high reliability.

The following is a list of significant design concepts that have been incorporated into the design of each of the engines.

- The incorporation of an overhung fan rotor has eliminated the need for an inlet case and associated inlet guide vane anti-icing requirements.
- The use of an annular combustor in place of the can-annular configuration simplifies the combustor design and eliminates requirements for transition ducts, clamps, and crossover tubes.
- Single rather than duplex thrust bearings are used at mainshaft locations.

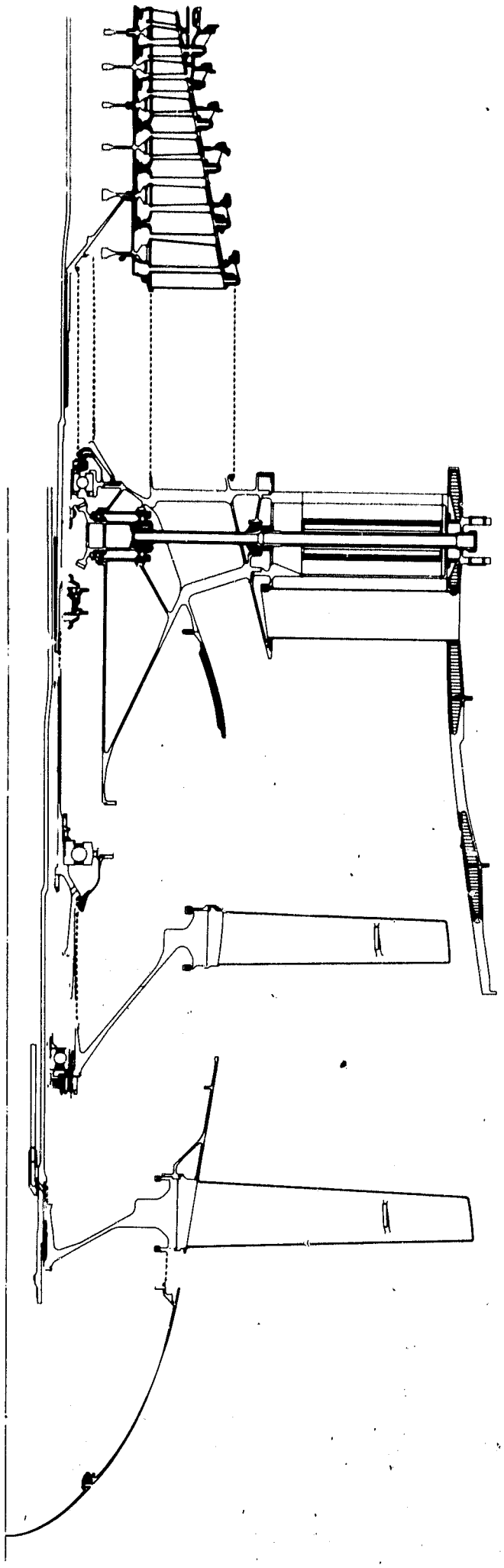

Figure 22 QB-3 Engine Front End Construction Modules

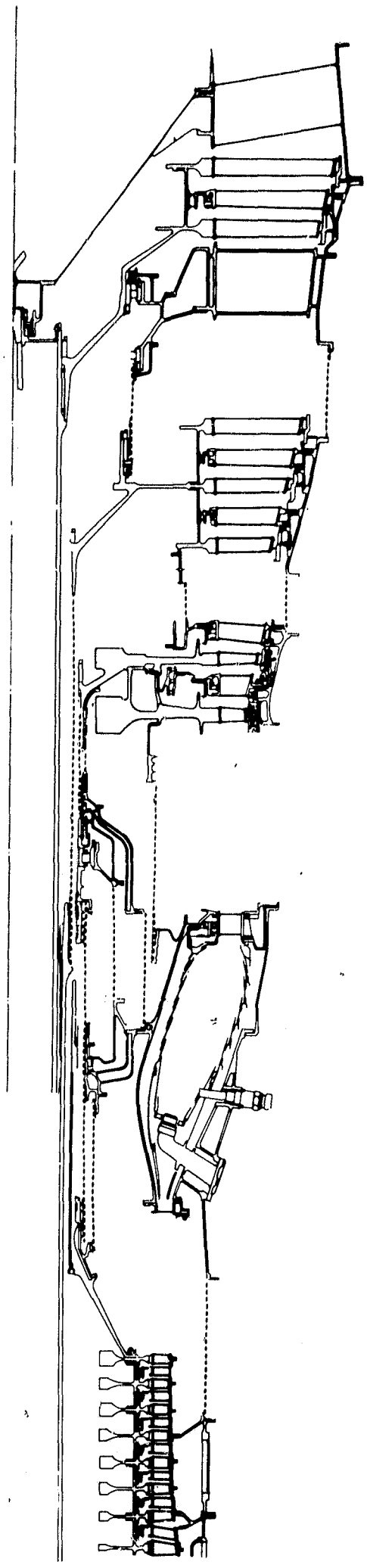

Figure 23 QB-3 Engine Aft End Construction Modules

With the experience gained from over 122 million hours accumulated by Pratt & Whitney Aircraft commercial and military gas turbine engines, many design improvements have evolved specifically directed at increasing engine reliability and durability. Some of the more general features incorporated into the four Quiet Engine designs are discussed below.

The design of static structures has been improved to reduce the amount of welding required in the fabrication of the cases. This is accomplished primarily by extensive utilization of forgings with integrally machined stand-up strut sections that are joined together with butt welds at locations that are removed from points of load introduction or high stress concentration.

Vibration and balance characteristics are enhanced by unit construction features. Compressor and turbine rotor and stator assemblies are to be built up and balanced as separate units, reducing the possibility of rotor imbalance and assembly error. Previously, balancing and assembly procedures entailed assembly, balance, disassembly, and reassembly. As an additional feature to reduce a source of rotor vibration and imbalance, disks and spacers were designed as integral parts, reducing the number of mechanical joints between supporting bearings.

Fan compressor blades were designed to be retained in their disks by either shear devices or trapped flanges on the blade root. Such devices are stronger than the sheetmetal tablocks used in the past and provide more positive blade retention.

Mainshaft bearings were designed for under-race oil cooling, providing a more even temperature gradient across the race. Mainshaft thrust bearings are located in the cool section of the engine.

The fuel manifold was designed to be mounted outside of the engine case to keep it at a lower temperature.

SECTION V

SUPPLEMENTARY STUDIES

In keeping with the spirit of the Quiet Engine Definition Program to "select the desirable characteristics for quiet high-bypass-ratio turbofans", a few supplementary design studies were conducted during Task II. Essentially, these studies involved design variations from the basic QA and QB candidate engines to investigate special aspects of the configuration arrangements originally selected. In each instance, the aspect investigated involved the fan, which is the critical source of engine noise. Variations were made to the basic fan design to either improve the mechanical arrangement for a given level of fan noise or to improve noise at the possible expense of the mechanical configuration or aerodynamics. The following discussion summarizes the basis for each alternate configuration and design, evaluates the results, and presents an interpretation of the results as they pertain to the over-all goals of the program.

A. QA-2 ENGINE

1. Discussion

The QA-2 arrangement was aimed toward evaluation of alternate approaches to the problem of blade-vane interaction noise effects intrinsic in two-stage fans. One of the desirable features of the single-stage fan without inlet guide vanes is that it contains no mechanism for producing the discrete-frequency whine normally associated with two-stage fans. It is now a well-established acoustical theory that the source of discrete-tone fan and compressor noise is the interaction between the stationary pressure field (generated by the stators) and the rotating pressure field (generated by the rotor blades). It is also well established that this noise will decay if the number of rotor blades is less than half the number of stator blades. In the case of the QA-1 and QB-3 designs this procedure was not deemed practical, therefore large axial spacings were used between the stators and the rotor to allow the wakes produced by the rotor blades to dissipate.

The QA-2 engine design was made in an attempt to circumvent the problems associated with large axial spacings evident in the QA-1 fan. The increased spacing in the fan requires additional bearings and support structure as well as a lengthened case. Both the added support structure and the lengthened case contribute to added engine weight and complexity. On the other hand, the use of many stator vanes to reduce interaction noise results in compromising the aerodynamics or the structural integrity of the fan. If vane row solidity is held constant, large numbers of stators have excessively thin chord widths for the loads to which they are subjected: if the chords are held fixed, the solidity becomes excessive.

The QA-2 design represents one compromise solution to this dilemma which still meets the requirement that the number of stator vanes be greater than twice the number of rotor blades. The aspect ratios of the rotors are decreased below levels that would be aerodynamically sufficient. This means that for fixed solidities, the number of rotor blades is reduced, allowing the number of stator vanes to be only slightly larger than that of the QA-1.

2. Results

The two resulting configurations are compared in Figure 24. To achieve the same acoustic effect of the QA-1's axial spacing, the fan geometry in the QA-2 was altered as follows:

Fan Geometry	QA-1	QA-2
First rotor aspect ratio	4.5	3.0
Number of first rotor blades	46	36
Stator aspect ratio	4.5	6.0
Number of stator vanes	66	86
Second rotor aspect ratio	4.5	3.0
Number of second rotor blades	76	48

As a result of this design approach, the estimated weight of the QA-2 is 50 pounds (22.7 kg) less than that of the QA-1.

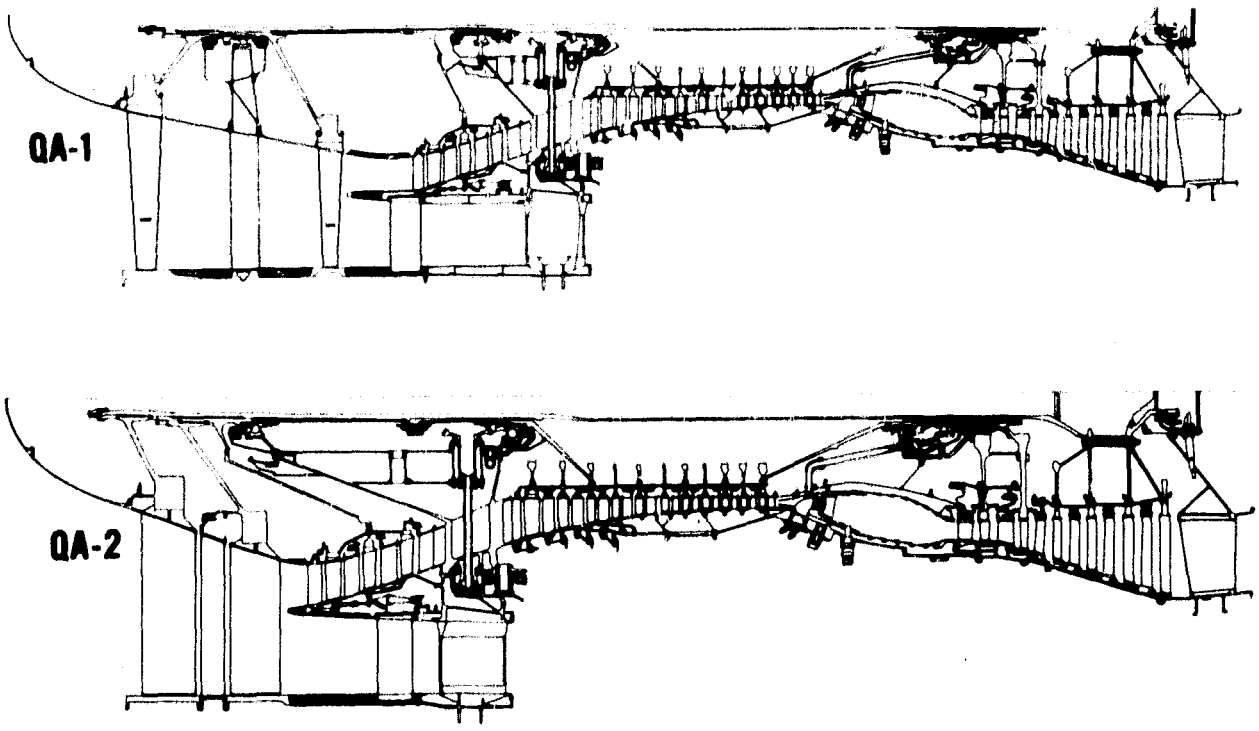

Figure 24 QA-1 Vs. QA-2 (M-51026)

3. Interpretation of Results

Acoustically, the phenomenon of blade-vane wake interaction is well understood. However, in actual practice, the resulting discrete-tone production is difficult to predict with any degree of certainty. Even the effects of axial spacing, based on considerable experimental evidence, tend to show only approximate trends. Nevertheless, the experience gained through experimentally varying axial spacing between the rotors and stator has confirmed the efficiency of this method.

The increased-chord low-aspect-ratio fan blades in the QA-2 design are largely outside the realm of experience, from both the aerodynamic and acoustic aspects. For example, it could be possible that the wider QA-2 blades create greater broadband noise than their QA-1 counterparts. Such uncertainty does not appear to justify the nominal weight savings gained by the reduced-spacing QA-2 configuration.

B. QB-4 ENGINE

1. Discussion

The QB-3 engine has a contratotating two-stage fan. This approach was selected as a means of avoiding the mechanical design and acoustics problems associated with the intervening stator in the conventional two-stage fan. Not only does the stator present an additional source of discrete-tone noise (although the two adjacent rotors in the contrarotating design can also produce discrete-tone noise), but also the extra axial spacing plus the actual presence of the stator row add to engine complexity, cost, and weight. Such considerations led to the selection of the QB-3 as a basic design. However, it was felt that with such an unconventional arrangement, further justification was necessary. As a result, the QB-4 conventional two-stage arrangement was evaluated for direct comparison.

2. Results

Layouts for the QB-3 and QB-4 designs are compared in Figure 25. Based on these layouts, weights were estimated for both desings, and it was determined that they have virtually identical weights.

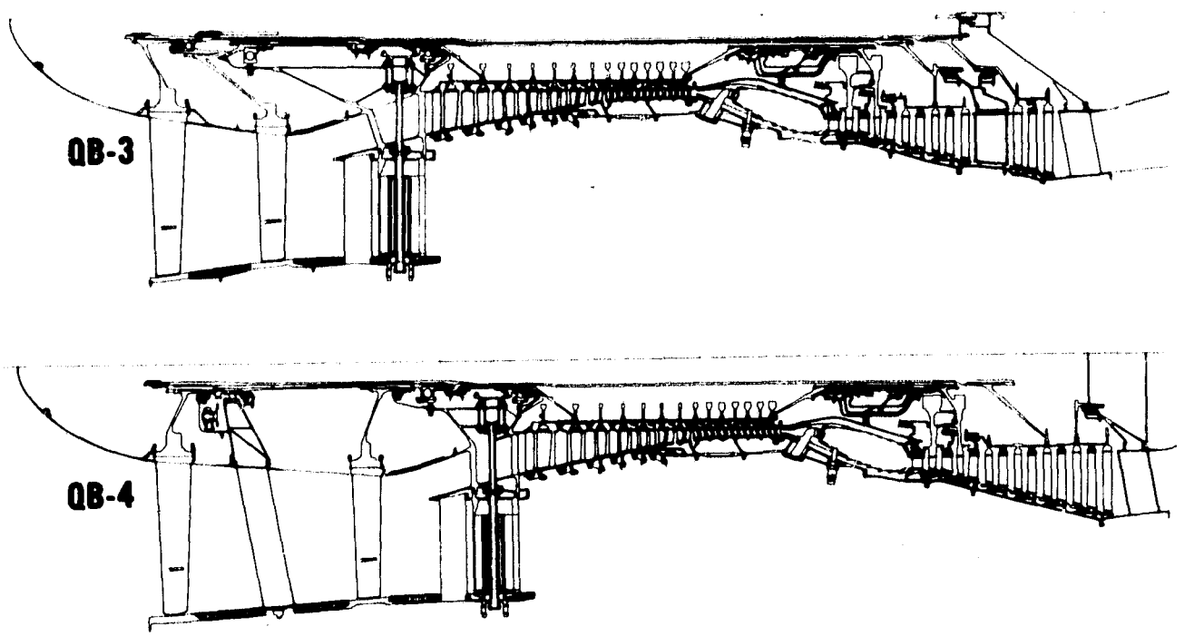

Figure 25 QB-3 Bs. QB-4 (M-51029)

3. Interpretation of Results

There are virtually no external differences between the QB-3 and QB-4 engines. Performance and weights are essentially the same, and while the QB-3 is slightly shorter, over-all length is not a significant factor. The choice between the two engines must depend on internal and somewhat intangible factors. While the presence of the stator in the QB-4 fan could produce additional noise if its axial spacing proves to be insufficient, the QB-3 has the contrarotating fan, whose acoustic performance is largely unknown. While the QB-4 mechanical arrangement is more complex as a result of the awkward location of the front bearing under the fan stator, the QB-3 front fan stage is supported by an intershaft bearing between contrarotating shafts, which is not in the realm of well established bearing technology. With such uncertainties, the detailed analysis necessary to make the choice is beyond the scope of Task II.

C. QB-5 ENGINE

1. Discussion

The QB-5 engine was investigated in order to take advantage of the two-stage contrarotating fan's aerodynamic capability to produce the required fan pressure ratio at lower fan speeds.

2. Results

The QB-5 arrangement is compared to the QB-3 in Figure 26. The QB-5 fan design represents the least tip speed required to develop a pressure ratio of 1.6 in the contrarotating two-stage fan. The following is a comparison of QB-5 and QB-3 take-off tip speeds.

	QB-3	QB-5
First rotor take-off tip speed (ft/sec)	990	795
First rotor take-off tip speed (m/sec)	302	242
Second rotor take-off tip speed (ft. sec)	765	480
Second rotor take-off tip speed (m/sec)	233	146

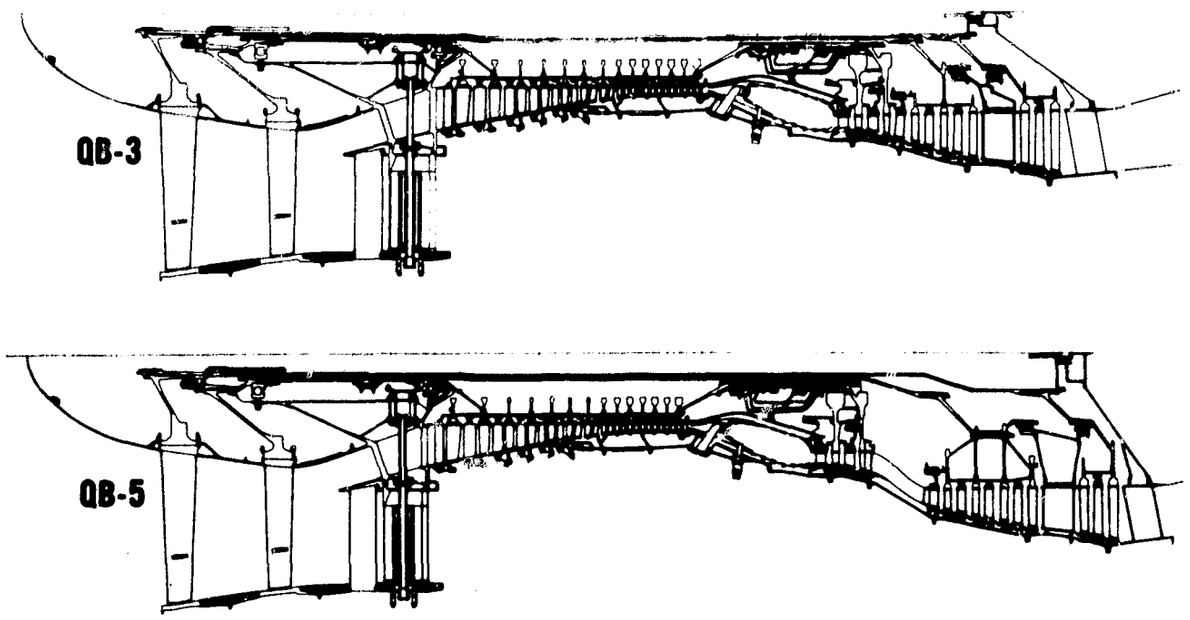

Figure 26 QB-3 Vs. QB-5 (M-51027)

The drive turbine's capability to produce work was reduced in direct proportion to the reduction in the tip speed of the fan. Accordingly, the QB-5 turbine design involved both the addition of a stage and an increase in average diameter to compensate. As evidenced in Figure 26, this added length to the extent of 12 inches (30.3 cm) and weight to the extent of 860 pounds (390 kg) relative to the QB-3.

3. Interpretation of Results

As uncertain as the noise characteristics of the QB-3 are, the QB-5 noise characteristics are even more uncertain. For the purpose and scope of Task II it is not evident whether the added weight and length of the QB-5 is worth its potential noise advantages. Certainly, the QB-5 concept merits further evaluation, but this depends on further experimental research on its acoustic and aerodynamic characteristics.

D. QB-6 ENGINE

1. Discussion

The QB-3 arrangement with its high-pressure-ratio, single-spool inner compressor offers a certain degree of flexibility in adapting various fan configurations. As a brief check on its design flexibility, the QB-3 high-pressure spool was fitted with a single-stage, highly loaded research fan. The resulting engine design, designated QB-6, has a low-aspect-ratio, single-stage fan which is considered suitable for developing a high tip pressure ratio with low tip speeds.

2. Results

As is evident in Figure 27, the QB-6 design results in an appreciable simplification of the mechanical arrangement as compared to the QB-4. However, as a result of the exceptionally wide chord of its fan blades, the expected large weight savings was not realized. The QB-6 is estimated to weigh only 20 pounds (9.07 kg) less than the QB-3.

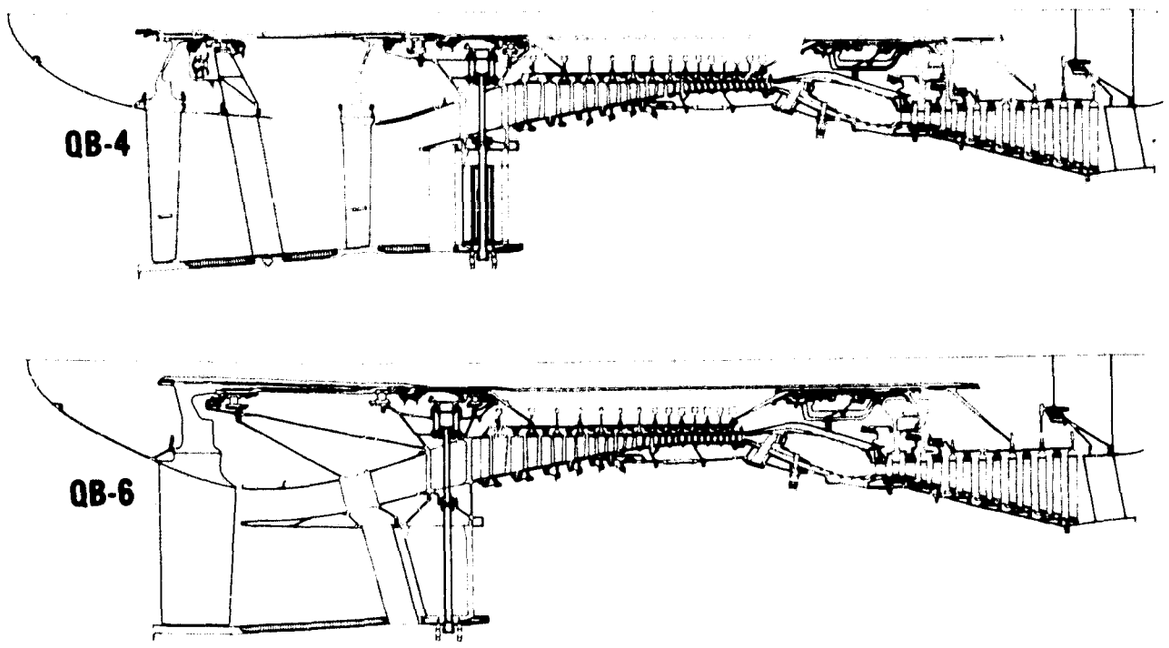

Figure 27 QB-4 Vs. QB-6 (M-51028)

3. Interpretation of Results

The QB spool is well-suited to a single-stage fan arrangement, and the resulting configuration is mechanically much simpler than its two-stage fan counterparts (both QB-3 and QB-4). However, to effect a weight saving, the QB-6 must have blading with a higher aspect ratio. It is estimated that a single-stage fan with an aspect ratio comparable to that of the QB-3 (current JT9D technology) would be about 500 pounds (226 kg) lighter in total weight than the QB-3 and QB-4 designs.

SECTION VI

NOISE

Task II acoustics work covered two areas: computing uninstalled engine noise and advising in engine design. Uninstalled engine noise was presented in terms of outlines of airport neighborhood areas subjected to 90, 95, and 100 PNdb during take-off and landing for the conditions of bare engine, unmixed jet noise alone, and jet noise with completely mixed exhaust. In engine design, particular emphasis was placed on adequate axial spacing of rotors and stators in the fan and on using acoustically desirable numbers of blades and vanes in the fan.

To provide a method for predicting noise levels for the various engine designs considered in Task II, a more inclusive prediction procedure was developed. This procedure was based on empirical relationships developed from noise measurements on the JT3C, JT3D, JTF14, and JT9D engines. It is intended to reduce the uncertainties inherent in predicting noise levels for the untested fan designs studied in Task II. The contrarotating fan and two-stage low-tip-speed fans without inlet guide vanes lack direct previous experience upon which noise predictions can be based. However, acoustical data from existing engines having two-stage fans with inlet guide vanes and single-stage fans without inlet guide vanes have been used indirectly to provide a procedure for predicting engine noise levels in Task II.

This section describes the new noise prediction procedure and presents the background leading to its development. This follows a brief discussion of engine noise-reduction design techniques. Some of the significant assumptions are then interpreted in terms of the final results. The predicted noise contours are presented at the end of this section.

A. ENGINE DESIGN CONSIDERATIONS

Discrete frequency blade passing noise levels can be minimized by providing adequate axial spacing between adjacent blades and vanes and by providing acoustically desirable numbers of adjacent blades and vanes. With the exception of the QA-2 design, axial spacing of at least two chord lengths between rotors and stators have been included in all fan designs. Past experience has shown that axial spacing of approximately two chord lengths is optimum, since greater spacing procedures negligible benefits in noise reduction. A typical curve showing the effect of axial spacing on noise level is shown in Figure 28.

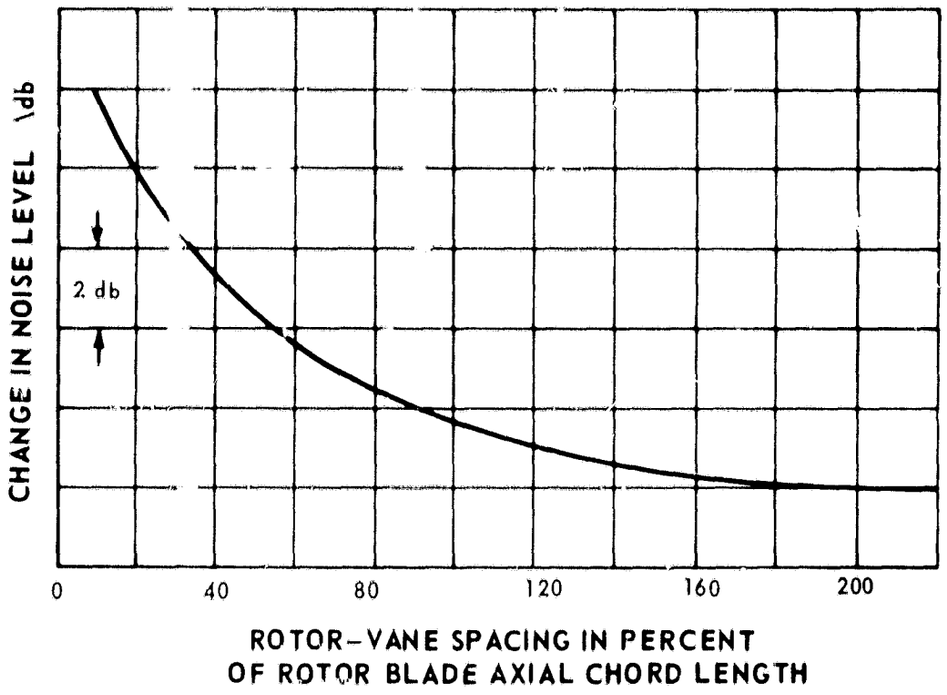

Figure 28 Effect of Fan Exit Guide Vane Spacing on Fan Discrete Noise

Desirable combinations of blade and vane numbers were selected within mechanical and aerodynamic restraints. The theoretically optimum number of vanes for noise reduction is equal to more than twice the number of blades. In some engines, this large number of vanes results in excessive solidity. The use of fewer rotor blades reduces the number of stator vanes required, but if stage performance is fixed, decreases in the number of rotor blades require corresponding increases in blade aspect ratio. In consequence, increased blade chord and additional spacing is required to maintain a spacing of two axial chord lengths. Excessive increases in engine length and weight can result from including both axial spacing and acoustically optimum combinations of blades and vanes. Past experience has shown that axial spacing is the more dependable and predictable of the two alternatives. Therefore, with the exception of the QA-2 engine (where optimum blade and vane numbers were deliverately chosen to evaluate the resulting design) adequate spacing was incorporated in all Task II fan designs in preference to optimum combinations of blade and vane numbers. However, it should not be inferred that blade and vane numbers were neglected. For each engine, the numbers were slected to be as near optimum as possible within reasonable design restraints.

A summary tabulation of predicted peak perceived noise levels from study engines QA, QB/QD and QC is given in Figure 29, which also includes predicted noise levels from JT3D and scaled JT9D engines for use as references. Total noise

levels and unmixed and completely mixed jet exhaust noise levels are presented for maximum take-off at 180 knots (92.4 m/sec) and 4800 pounds (21,550 newtons) net thrust, and approach conditions at 130 knots (66.4 m/sec). The data represent the peak noise levels along a line 200 feet (61 meters) from and parallel to the engine centerline.

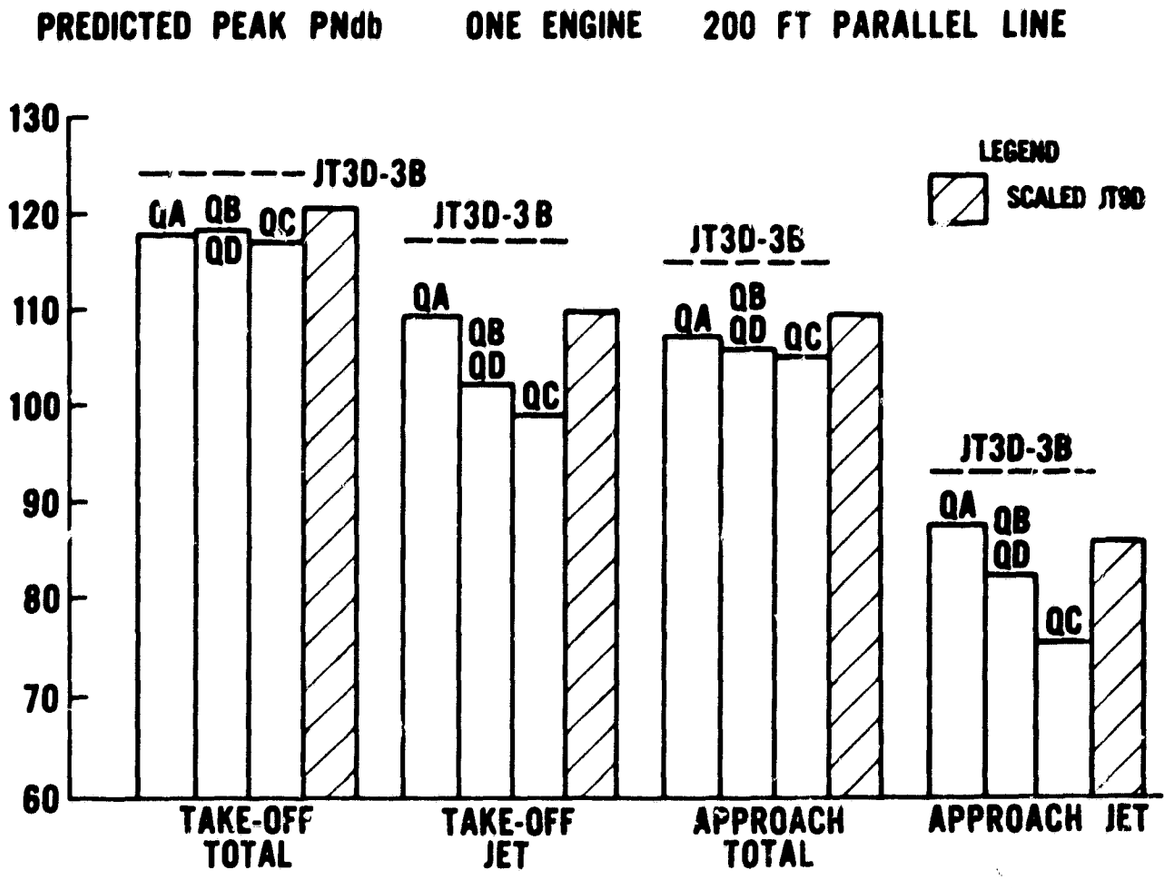

Figure 29 Summary of Noise Results (M-50991)

Take-off and landing flight profiles were assumed for a 325,000-pound (147,500-kg) gross weight Boeing 707 or DC8 type of aircraft equipped with the QA, QB/QD, QC, JT3D, and scaled JT9D engines. Using these flight paths and predicted noise levels, contours showing airport neighborhoods exposed to 90, 95, and 100 PNdb were computed for total noise, unmixed jet noise, and completely mixed jet noise. These contours are presented at the end of this section.

B. NOISE PREDICTION PROCEDURES

A more inclusive prediction procedure than that of Task I was developed for Task II to provide the best method available for coping with the new engine design concepts studied in this task. This procedure had the added benefit that field noise measurements from JT9D engines could be used. In the Task II prediction system, noise levels for each of the significant noise components were computed separately and then combined. Components included were jet exhaust noise, discrete fan noise, broadband fan noise, and combination tone fan noise.

Jet exhaust noise prediction procedures used in Task II were similar to those used in Task I. The best method available for predicting fan noise is to extrapolate from measured data. All engine designs considered in Task I had single-stage fans with no inlet guide vanes, a design for which measured data were available. Engine designs considered in Task II included new concepts for which measured data were not available to use as a basis for prediction. To overcome this lack of data, the Task II prediction procedure was based on data from conventional two-stage fans with inlet guide vanes and single-stage fans without inlet guide vanes. Each fan noise component was related empirically to relative blade tip Mach number and these relationships were extended in Task II to predict noise levels of contrarotating two-stage fans, corotating two-stage fans without inlet guide vanes, and highly loaded single-stage fans.

The sequence of operation in the noise prediction system is summarized in Figure 30. Space average sound pressure levels on a 150-foot (45.7 meter) radius around the engine were predicted for each of the noise components. Empirically determined directivity indices were then applied to provide octave band sound pressure levels for each component at three angles on the arc. These angles were 50°, 110°, and 135° (0.897, 1.97 and 2.42 radians), where peak flyover noise levels were expected from the inlet, fan discharge, and jet exhaust, respectively. Octave bend sound pressure levels from each of the noise components were combined at each of the angles and the combined octave band levels and the jet noise levels alone were extrapolated to required altitudes to calculate perceived noise levels.

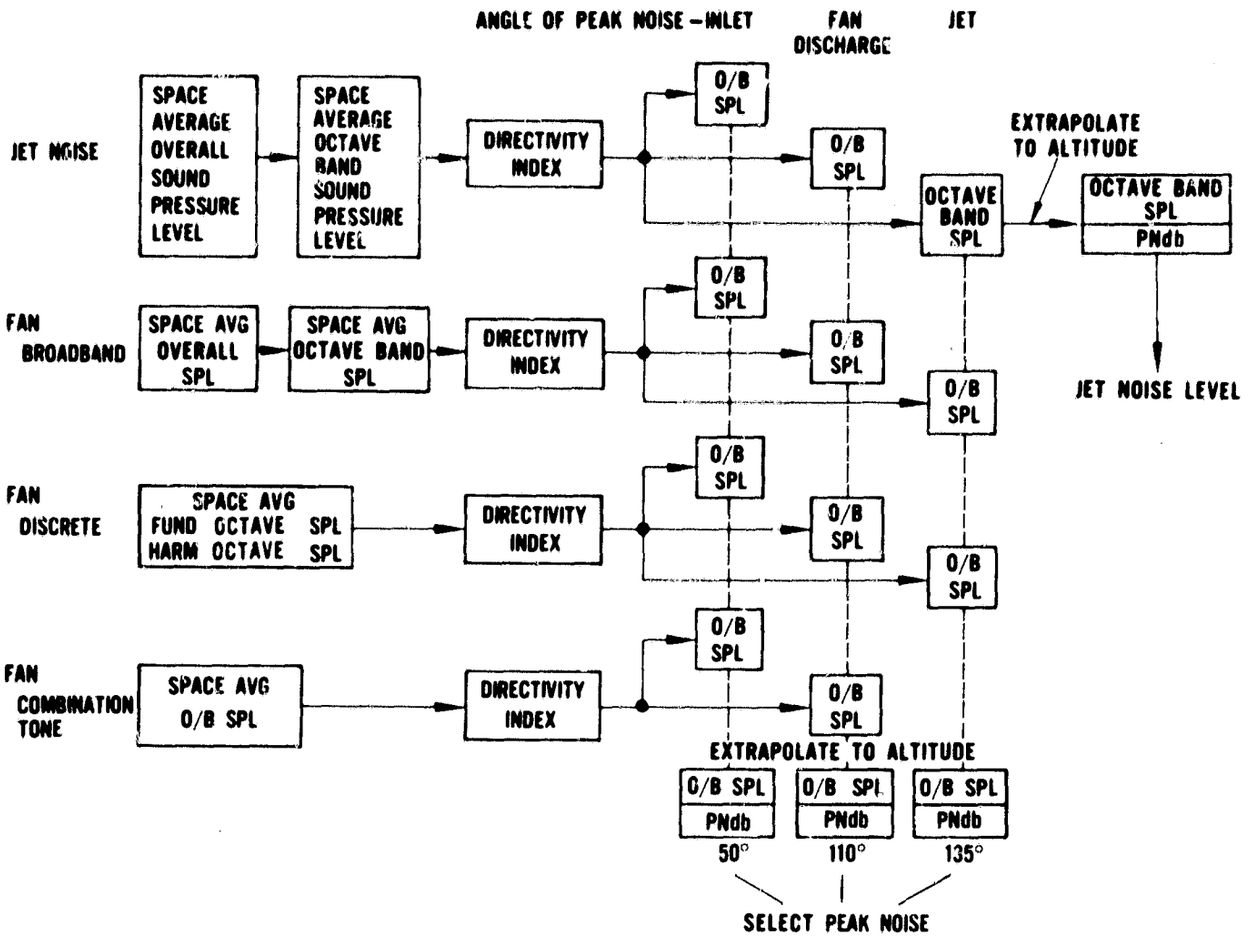

Figure 30 Noise Prediction Sequence (M-51248)

1. Jet Noise Predictions

a. Prediction Procedures

Jet noise prediction procedures were similar to those used in Task I and are basically the procedures described in SAE document AIR876 "Jet Noise Predictions". The SAE procedure has been expanded to include relationships between noise level and jet velocity at velocities less than 1000 ft/sec (305 m/sec), as shown in Figure 31. It also includes directivity indices to allow the prediction of jet noise levels at other than the peak angle.

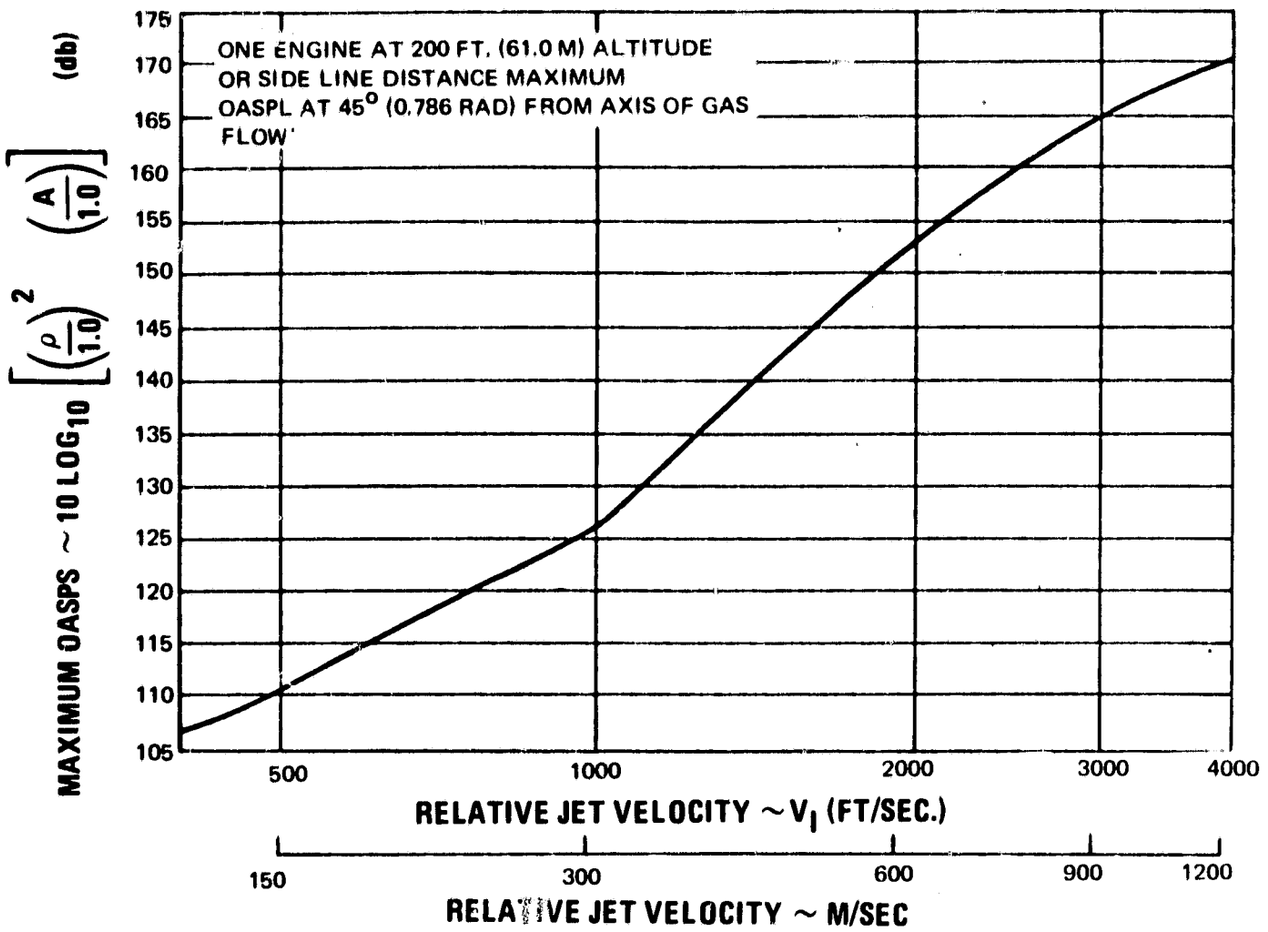

Figure 31 Maximum Over-all Sound Pressure Level as a Function of Relative Jet Velocity

b. Assumptions

The jet noise prediction procedure reported in the SAE document is for a conventional conical primary exhaust nozzle. It has been observed that both noise level and directivity can be affected by nozzle shape variations and the location of the fan nozzle relative to the primary nozzle. However, no procedures exist to predict these effects, so that jet noise was predicted on a straight forward basis using flow performance data and assuming conical-nozzle characteristics.

Jet noise levels were predicted for complete mixing of the fan and primary streams. It should be noted that in practice, complete mixing is very difficult to achieve, and best attempts to encourage mixing generally result only in partial mixing.

It is assumed that relationships developed empirically to relate jet noise to jet velocity at low velocities are acceptably accurate. Relative jet velocities from

high-bypass-ratio engines fall below 1000 ft/sec (305 m/sec), and the SAE procedure is limited to jet velocities between 1000 and 2000 ft/sec (305 and 610 m/sec). No procedures were available for predicting jet noise at these low velocities, so empirical relationships were developed from noise measurements from existing engines during operation at low jet velocities. This data indicated that the relationship between noise and velocity was different at velocities below 1000 ft/sec (305 m/sec) as shown in Figure 31.

2. Fan and Turbine Noise Predictions

a. Broadband Noise

Empirical relationships were developed from JT3D and JT9D measured data to formulate a procedure for predicting fan broadband noise. Over-all broadband noise levels were related to blade tip relative Mach numbers after normalizing JT3D and JT9D data to a constant diameter. It was then observed that the normalized broadband noise level from the two-stage JT3D was about 3 db higher than that from the single-stage JT9D, so the data were further normalized to inslge-stage noise assuming an increase in noise of 3 db per added fan stage.

The frequency distribution of the broadband noise was obtained by empirically relating the measured data to the parameter fc/m, where f is frequency, c is blade chord, and m is the blade tip relative Mach number. This relationship is shown in Figure 32. Tip Mach number was used in the correlating parameter, rather than tip belocity. Although the use of velocity would have resulted in a nondimensional parameter, the use of Mach number was more consistent with other correlations.

Directivity indices were developed from the measured data to apply to the space average spectrum to obtain octave band sound pressure levels at inlet, fan discharge, and exhaust angles. Variations in inlet and fan discharge over-all noise levels with blade tip relative Mach numbers are shown in Figure 33.

The procedure for predicting fan broadband noise thus consisted of the following consecutive steps:

1. Using blade tip relative Mach number, determine space average over-all sound pressure level and add diameter correction.

2. Using the parameter fc/m, determine an octave band sound pressure level frequency distribution.

3. Apply directivity indices to obtain octave band sound pressure levels for inlet, fan discharge, and exhaust noise.

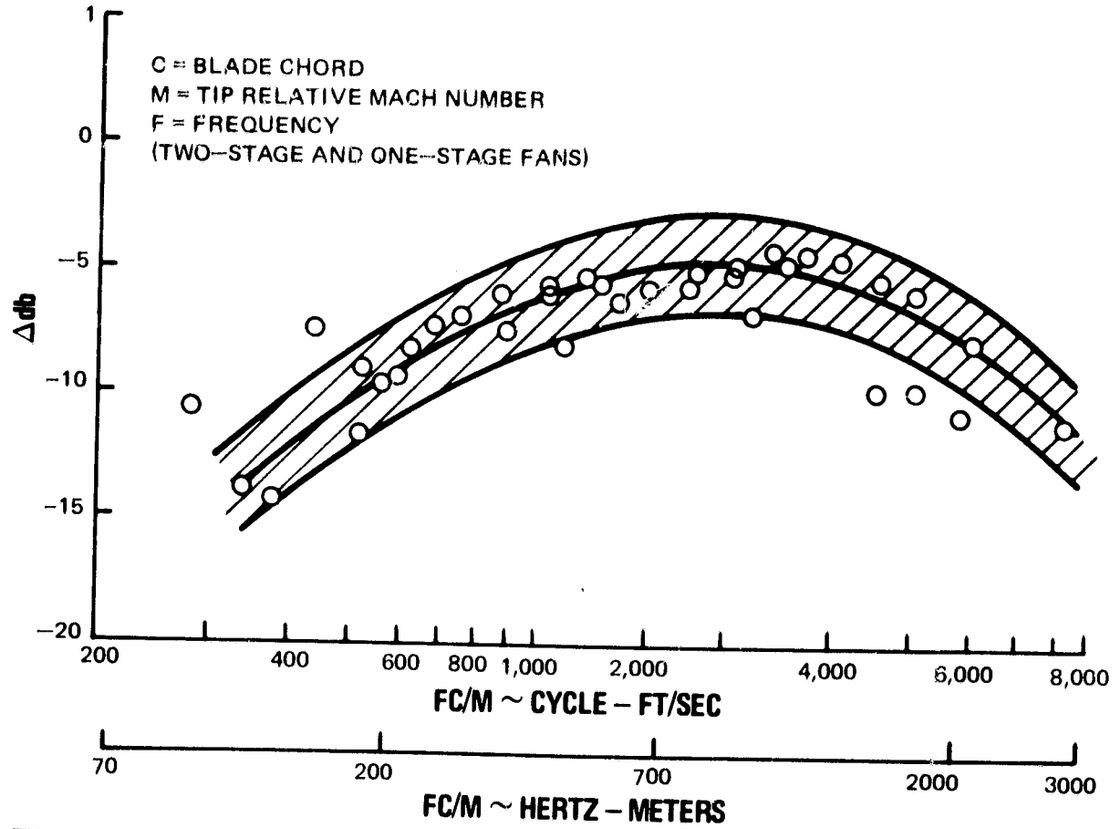

Figure 32 Broadband Noise Frequency Distribution (M-51188)

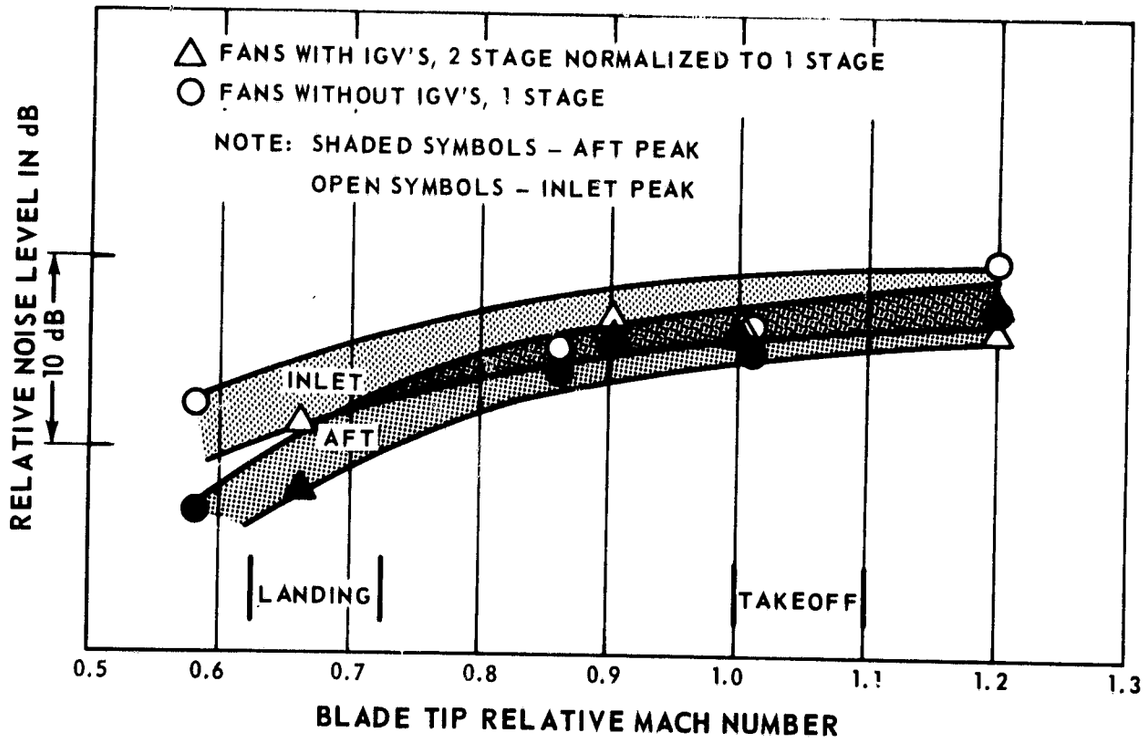

Figure 33 Broadband Noise Levels

b. Fan Discrete Noise

Relationships were developed from JT3D and JT9D data to relate fan discrete noise to blade tip relative Mach number. The data were normalized to a constant diameter and separate curves were drawn for first- and second-stage noise from the JT3D and the first stage of the JT9D. These curves are shown in Figures 34 and 35.

The procedure for predicting fan discrete noise consisted of using blade tip relative Mach number to determine the discrete frequency level at each angle and adding a diameter correction. The curves were interpreted as follows:

1. For single-stage fans with no inlet guide vanes, the single-stage no-inlet-guide-vane curve was used.

2. For two-stage fans without inlet guide vanes, it was assumed that the first-stage noise would follow the curve for single-stage fans without inlet guide vanes. The noise from the second stage was assumed to fall midway between the curve for a single stage with no inlet guide vanes and the curve for the second stage with vanes. This assumption was based on the increased spacing between the first stator and the second rotor of the Quiet Engine designs.

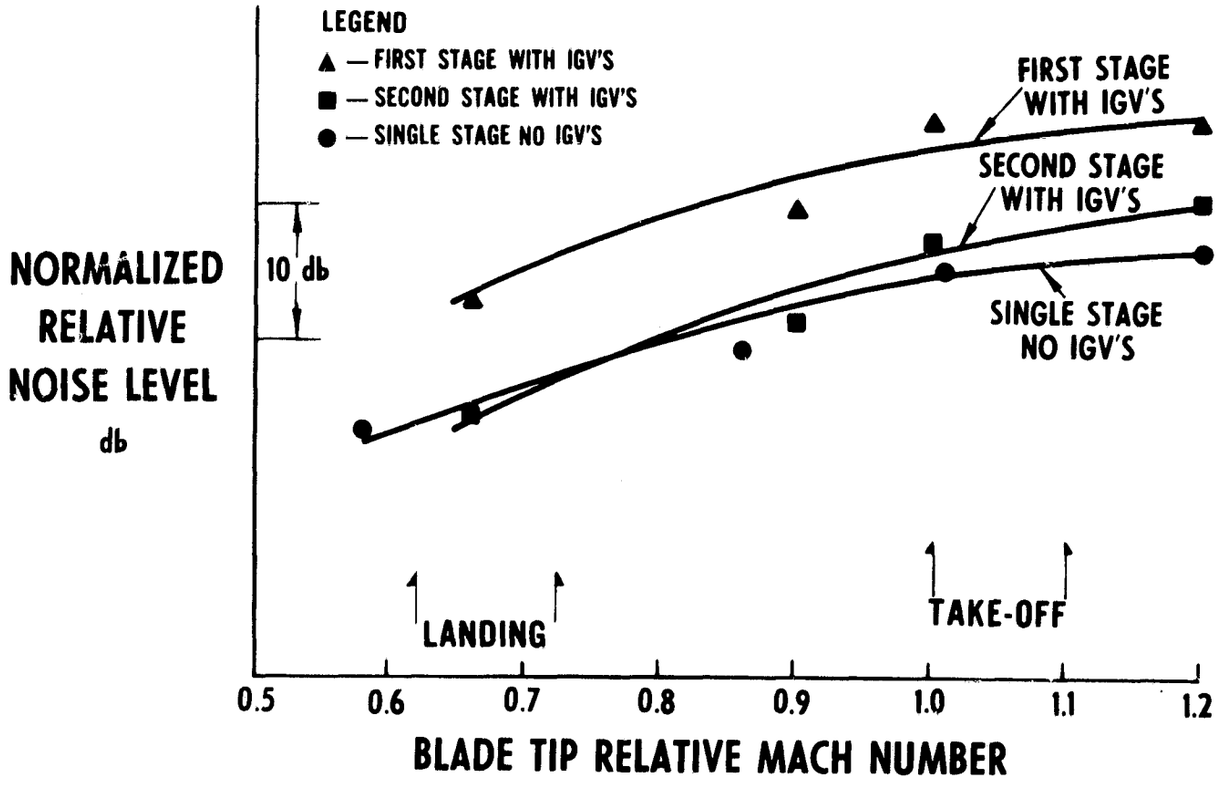

Figure 34 Inlet Peak Discrete Noise Levels (M-51193)

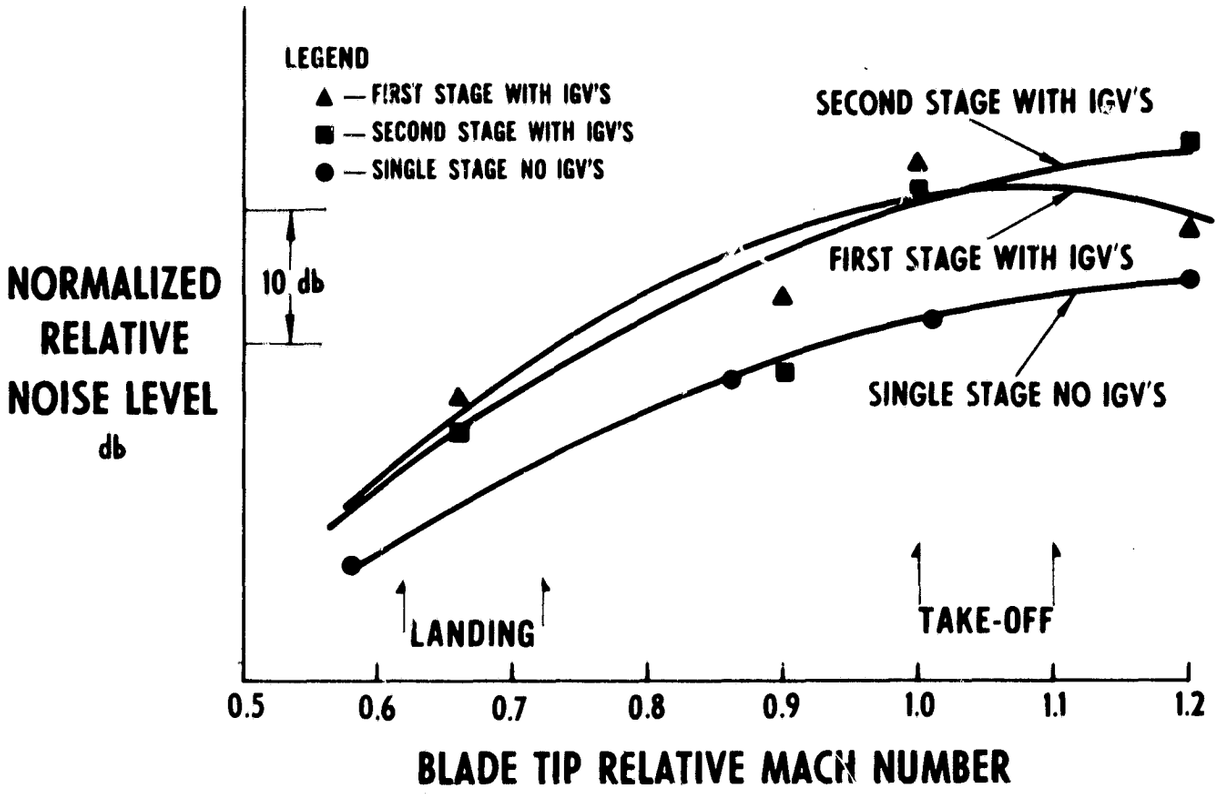

Figure 35 Aft Peak Discrete Noise Levels (M-51192)

c. Combination Tone Noise

JT3D and JT9D data were used to develop empirical relationships relating combination tone noise levels to blade tip relative Mach number. This noise does not become significant until the blade tip relative speed is transonic and shock waves are formed. The shock waves decay into a system of unequally spaced Mach waves which propagate forward out the inlet. Figure 36 shows the relationship between the level of combination tone noise normalized to a constant diameter, and blade tip relative Mach number for the angle of peak inlet noise.

The prediction procedure consisted of entering the curve shown in Figure 36 at the proper Mach number to obtain the level of combination tone noise, which was then corrected for blade tip diameter. Although the level of combination tone noise radiated aft was relatively insignificant, directivity indices were used to determine the level at aft angles. Octave band spectra were determined from JT3D and JT9D data which provided curves of normalized relative noise level as a function of octabe band, as shown in Figure 37.

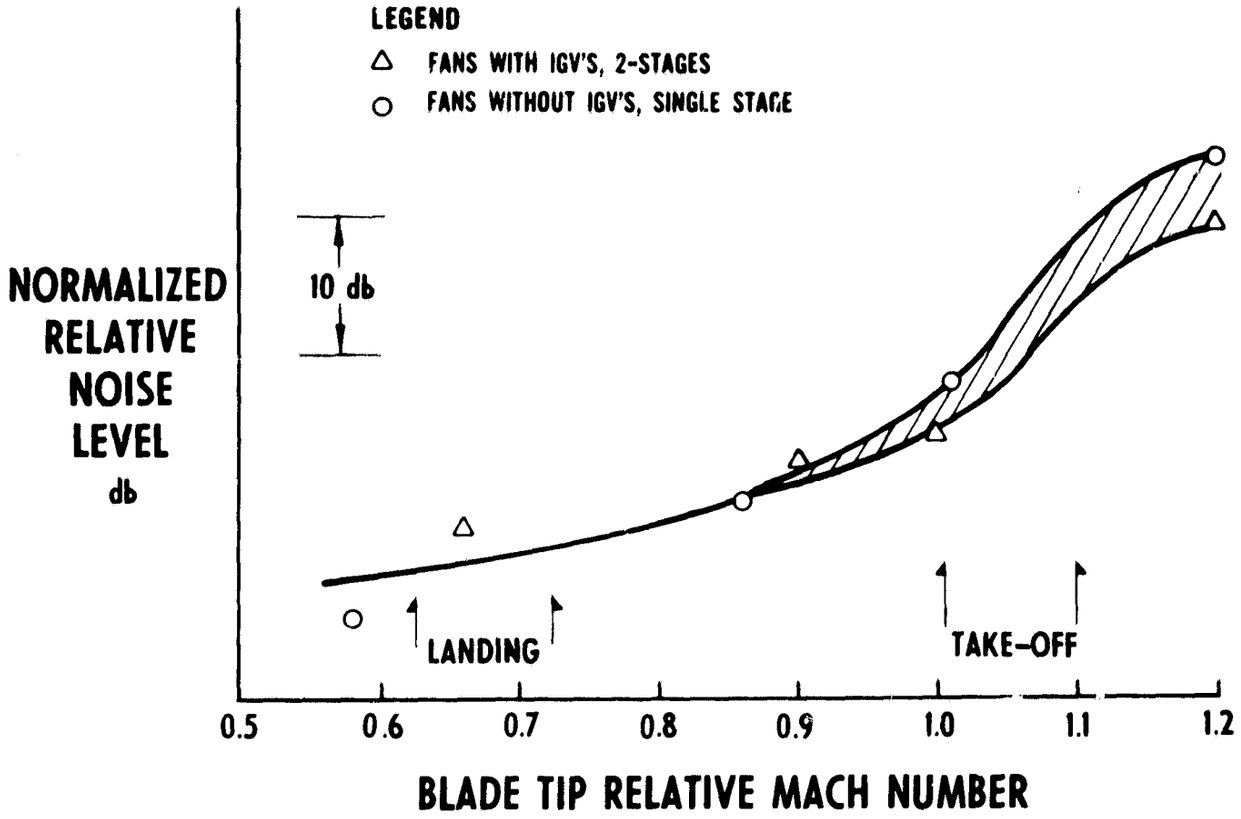

Figure 36 Peak Inlet Combination Tone Noise Levels (M-51191)

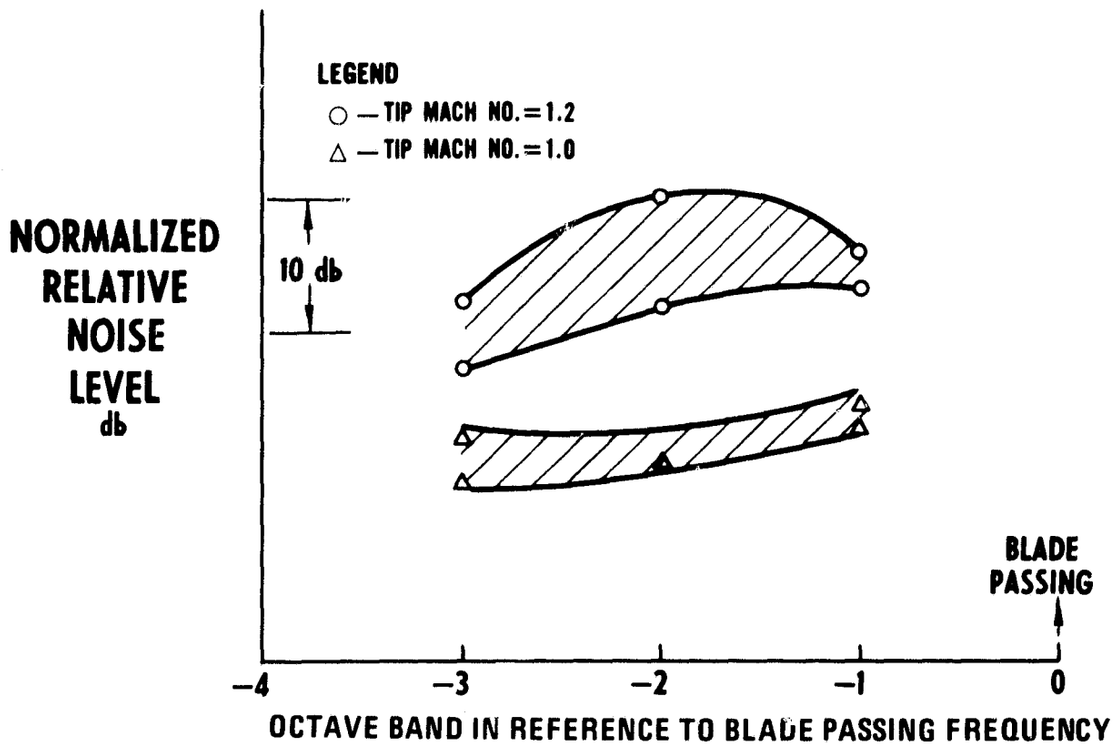

Figure 37 Typical Combination Tone Noise Spectra (M-51190)

d. Turbine Noise

Turbine noise has been identified in noise measurements from some current low-bypass turbofan engines with two-stage fans, and from high-bypass engines with single-stage fans. In no instance has turbine noise been the dominant noise source. It can be identified only at very low power settings in low-bypass turbofans, and is masked by jet exhaust noise at power settings within the normal operating range of the engine. Turbine noise levels measured from high-bypass engines are more significant, but appear only at lower powers. They are masked in these engines at higher powers. With the lower jet noise levels of the Quiet Engines, turbine noise may surface and become dominant if fan noise is sufficiently suppressed. No procedures currently exist for predicting turbine noise and an empirical relationship cannot be developed from the limited data available in which turbine noise can be identified.

e. Assumptions and Accuracy

In developing empirical relationships for the Task II fan and turbine noise prediction procedure, the following assumptions were made:

1. Relative blade tip Mach number was assumed to be the major correlation parameter. Noise data from existing engines indicated that basic relationships exist between noise level and relative blade tip Mach number. However, there is the possibility that other parameters such as stage pressure rise may be quite significant in establishing the fan noise level at a given blade tip Mach number. Adequate data from a variety of fan designs to resolve this effect is not available.

2. It was assumed that many design features and performance parameters can be neglected. These parameters include stage pressure rise, rotor and stator aspect ratio, stage efficiency, airfoil camber, airfoil section shape, fan duct length, and fan duct geometry. These parameters were neglected not because their relationship with fan noise is necessarily unimportant, but because their relationship has not been defined. Only a limited variation in these parameters exists in current engines which have been tested. Varying one parameter without affecting the others to determine noise effects requires extensive tests of a variety of fan designs.

3. It was assumed that empirical relationships established from available test data applies to the untested designs of the duct engines including two-stage fans without inlet guide vanes and the contrarotating QB-3 engine designs.

It is felt that the prediction procedures used in Task II are the best available having the benefit of empirical relationships based on extensive measurements from low-bypass-ratio two-stage fan JT3D and JT8D engines with inlet guide vanes and high-bypass-ratio single-stage fan JT9D and JTF14 engines without inlet guide vanes. Empirical relationships are used in making predictions rather than an analytical approach, since the detailed generating mechanisms of fan or compressor noise are not completely understood.

3. Noise Contour Calculations

In computing airport neighborhood noise contours from the basic predicted engine noise levels for Task II, the same approximate aircraft flight path calculation procedure and aerodynamic assumptions were employed as in Task I. Noise contours for the QA, QB/QD, JT3D, and scaled JT9D engines are presented in Figures 38 through 45. Some of the more significant in-flight noise calculation procedures are discussed below.

a. Aircraft Flight Paths

No installation penalties were accounted for. In more accurate calculations such factors as nacelle drag, inlet pressure recovery, bleed and power extraction, and nozzle performance would influence aircraft flight paths.

b. Installation Effects on Noise

It was assumed that noise levels generated by the engine were not increased by nacelle features. For example, inlet guide vanes were eliminated from the study engine designs to reduce noise and the incorporation of structures in the inlet such as struts may tend to negate this benefit. Similar effects may be noted from inlet blow-in doors or any device which may distort flow into the inlet.

It was assumed that no noise suppression features were included in the nacelle. Thus, noise predictions are based on bare engine noise levels without acoustical treatment in inlet or fan ducts, choked inlet, or any other external noise-suppression device.

It was assumed that forward airplane velocity does not affect noise generation. Considerable disagreement exists in the industry on the difference between measured aircraft flyover noise levels and flyover noise levels predicted from engine static data. No standard procedure exists for extrapolating ground data to flight data. The procedure used in Task II was to estimate engine noise levels on the basis of inflight performance with inflight fan noise levels related to static data at the same relative jet velocity. Although ground-to-flight prediction procedures may be improved by further tests planned by the industry, a consistent procedure was used for all engines studied in Task II to insure that proper relative noise levels of the different engines have been calculated.

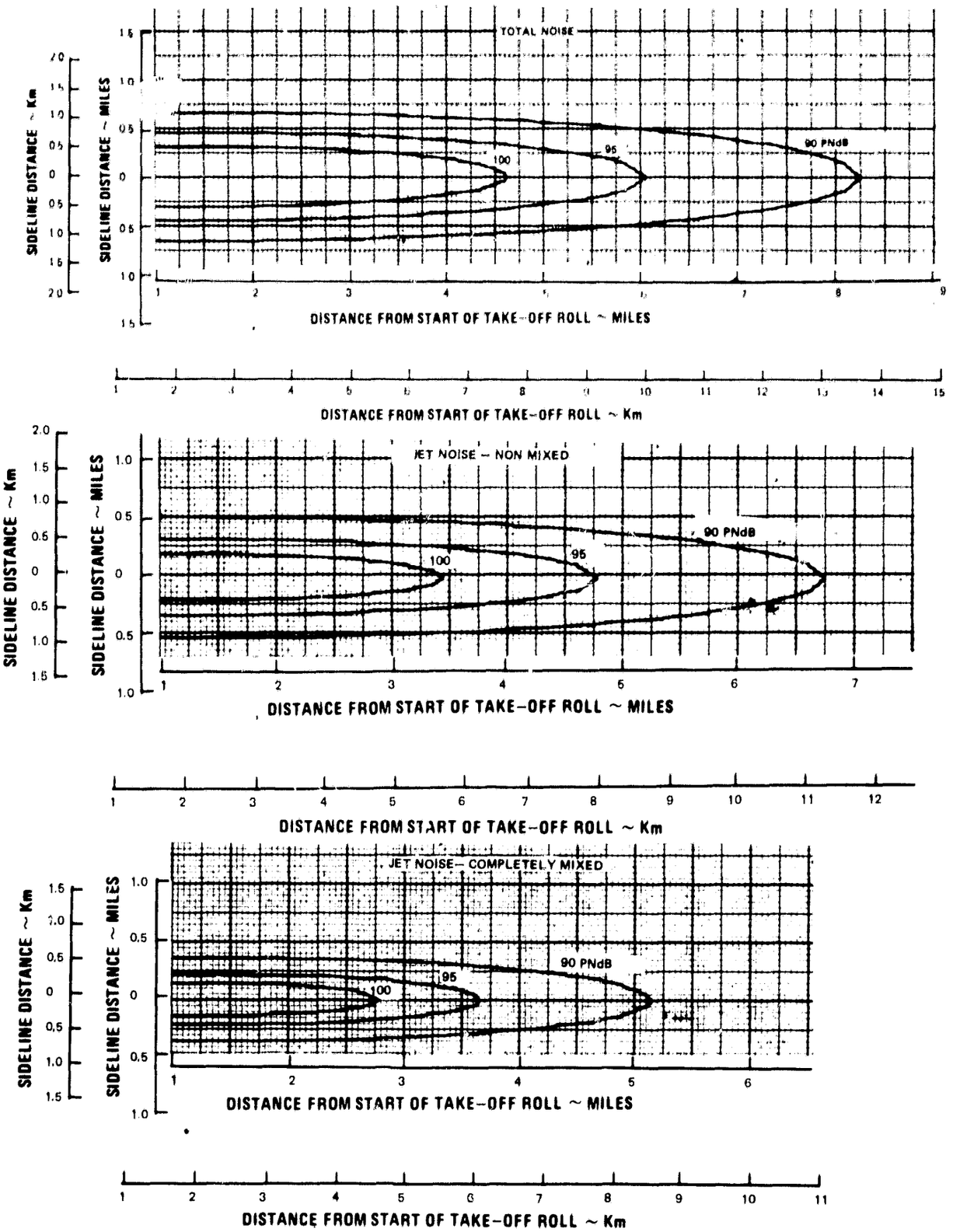

Figure 38 Takeoff Noise Contours for 4 QA Engines, 325,000 Pounds (147,000 kg) Gross Aircraft Weight

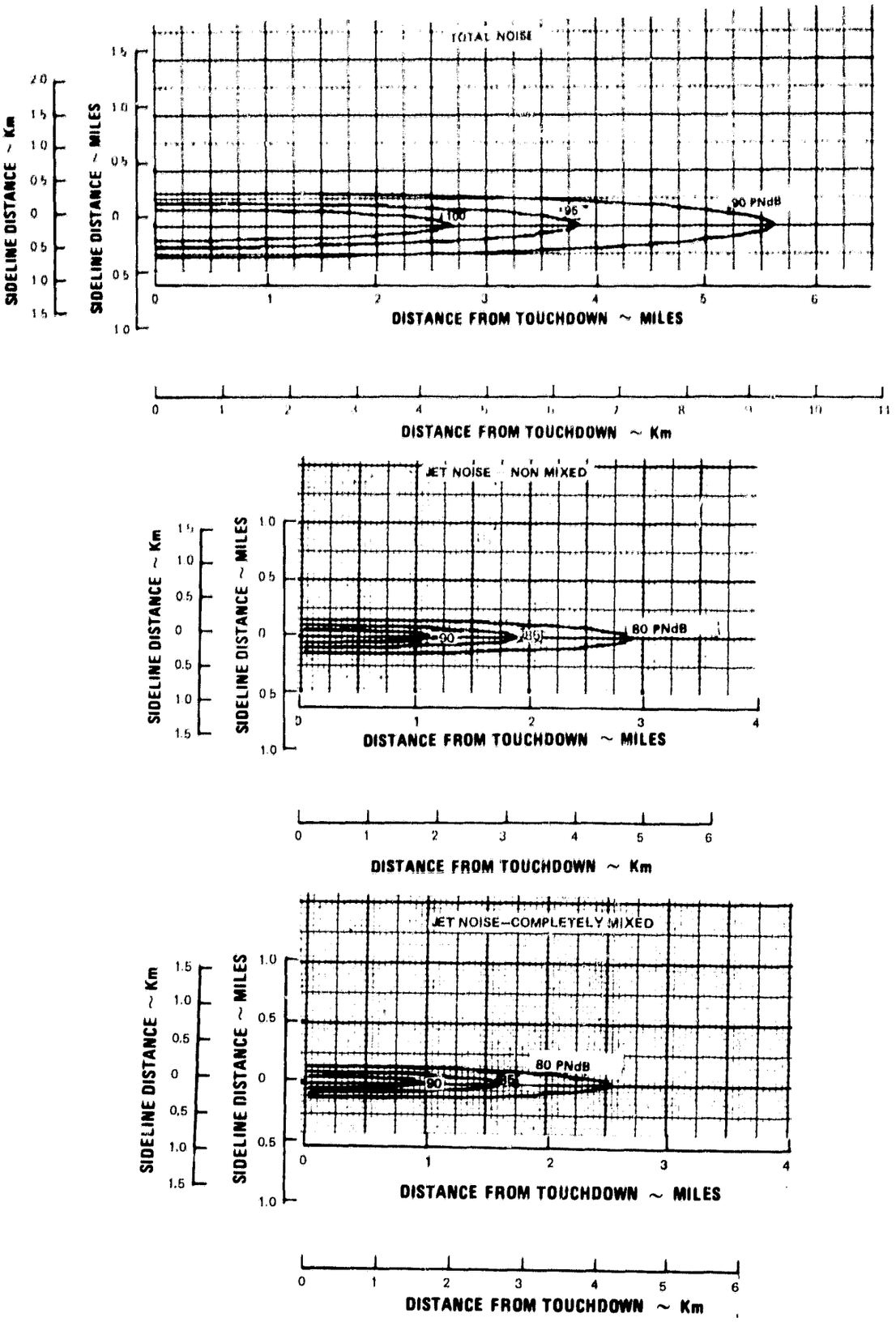

Figure 39 Landing Noise Contours for 4 QA Engines, 4800 Pounds/ Engine Thrust (21,400 Newtons)

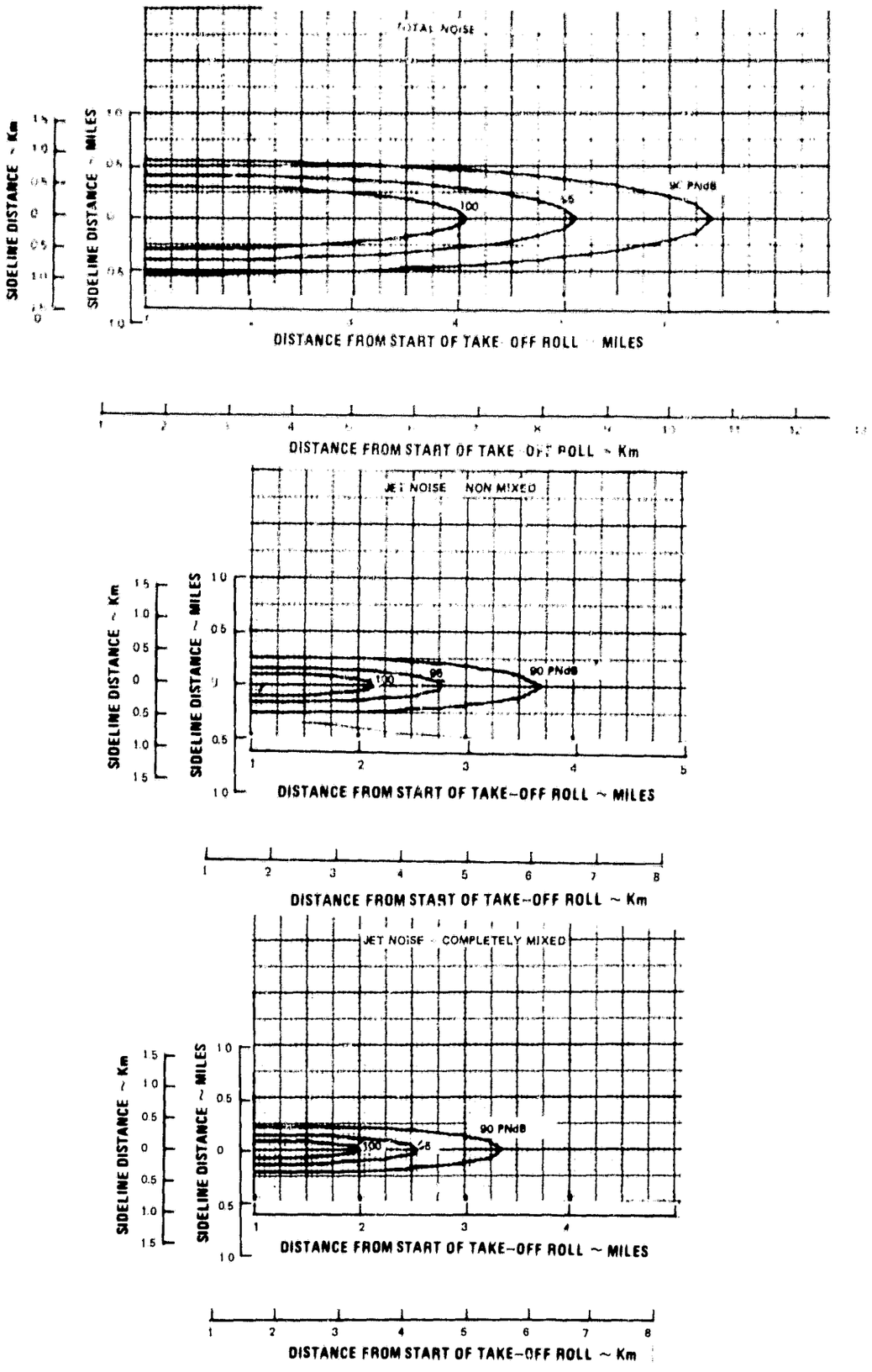

Figure 40 Takeoff Noise Contours for 4 QB/QD Engines, 325,000 Pounds (147,000 kg) Gross Aircraft Weight

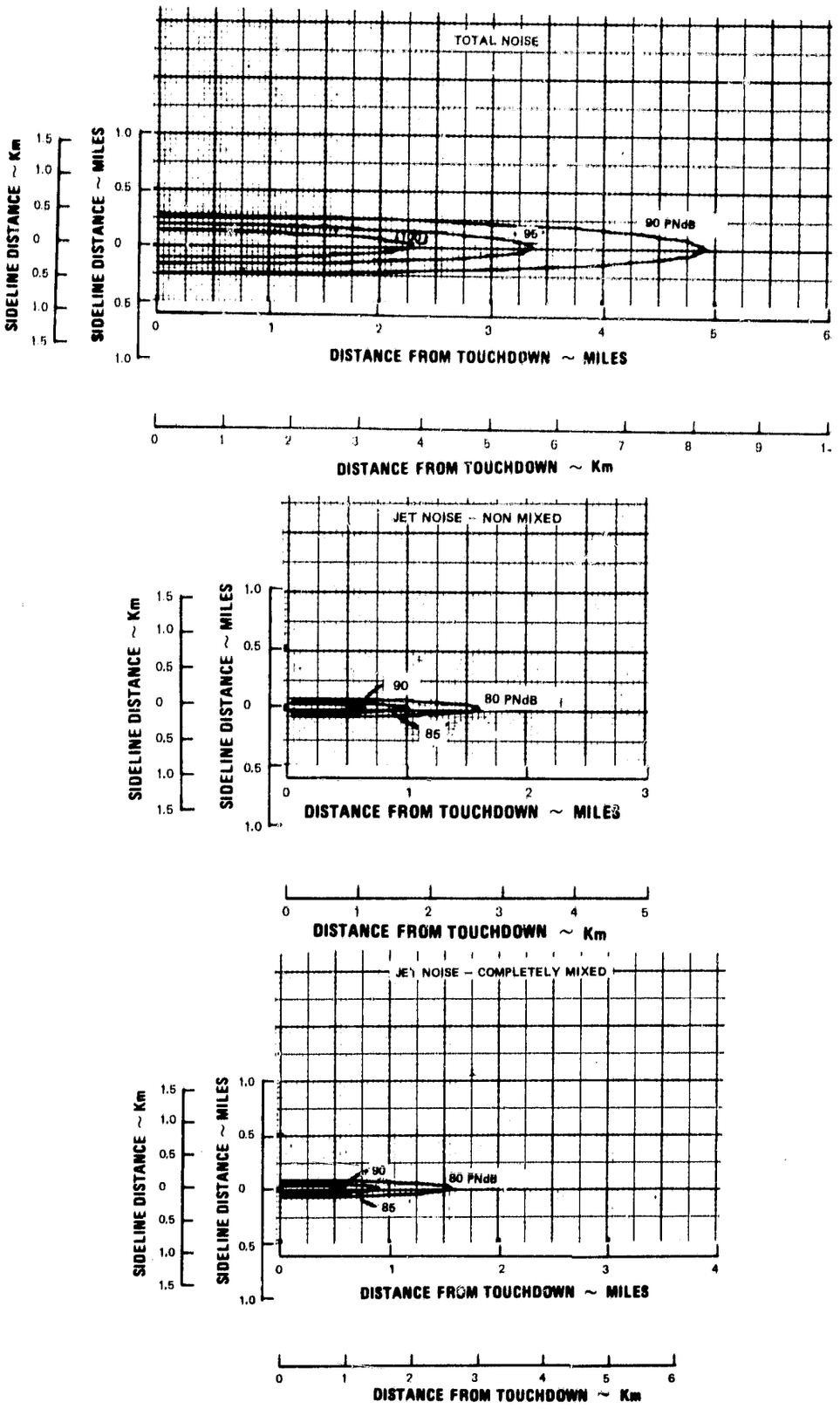

Figure 41 Landing Noise Contours for 4 QB/QD Engines, 4800 Pounds/ Engine Thrust (21,400 Newtons)

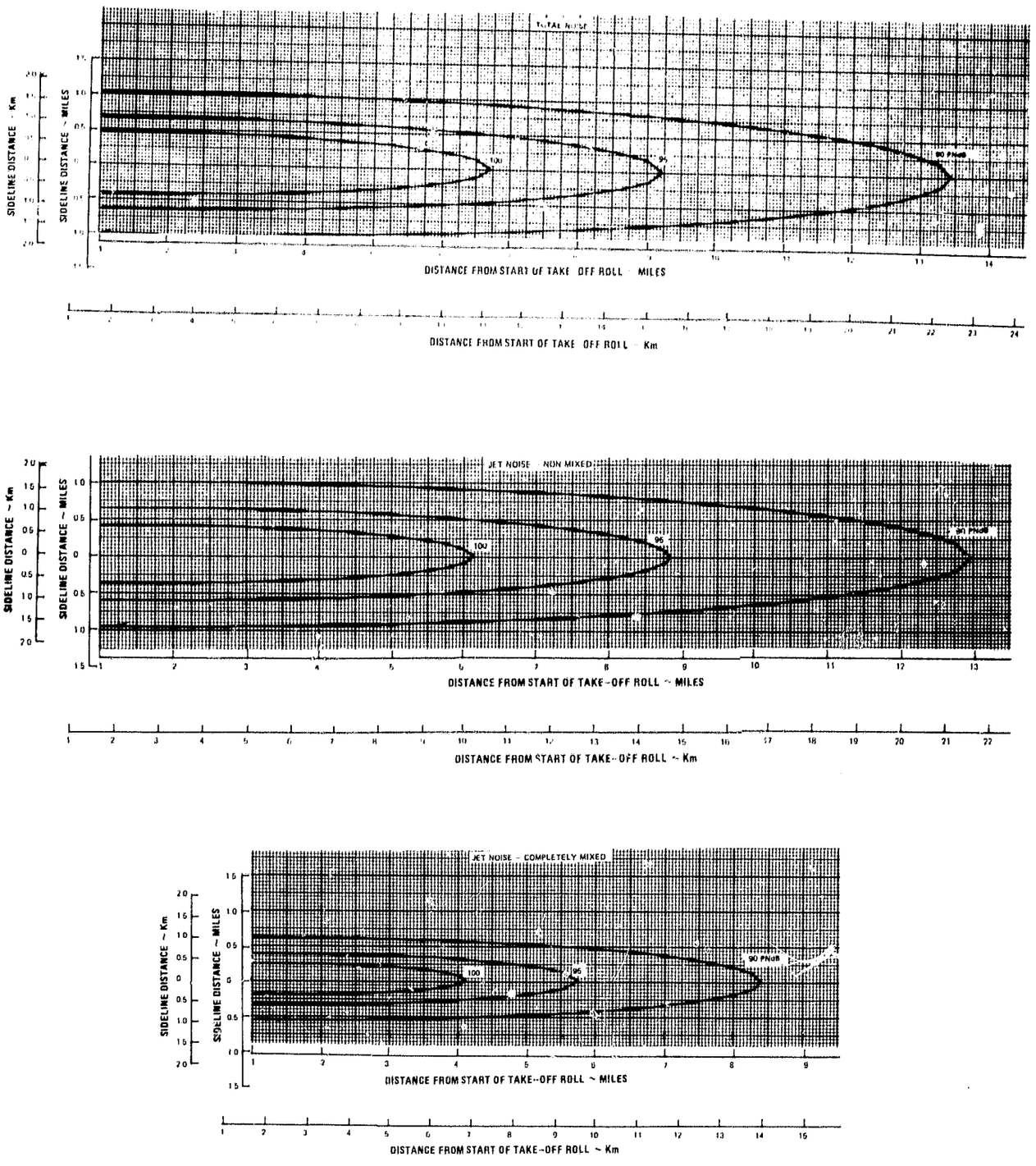

Figure 42 Takeoff Noise Contours for 4 JT3D Engines, 325,000 Pounds (147,000 kg) Gross Aircraft Weight

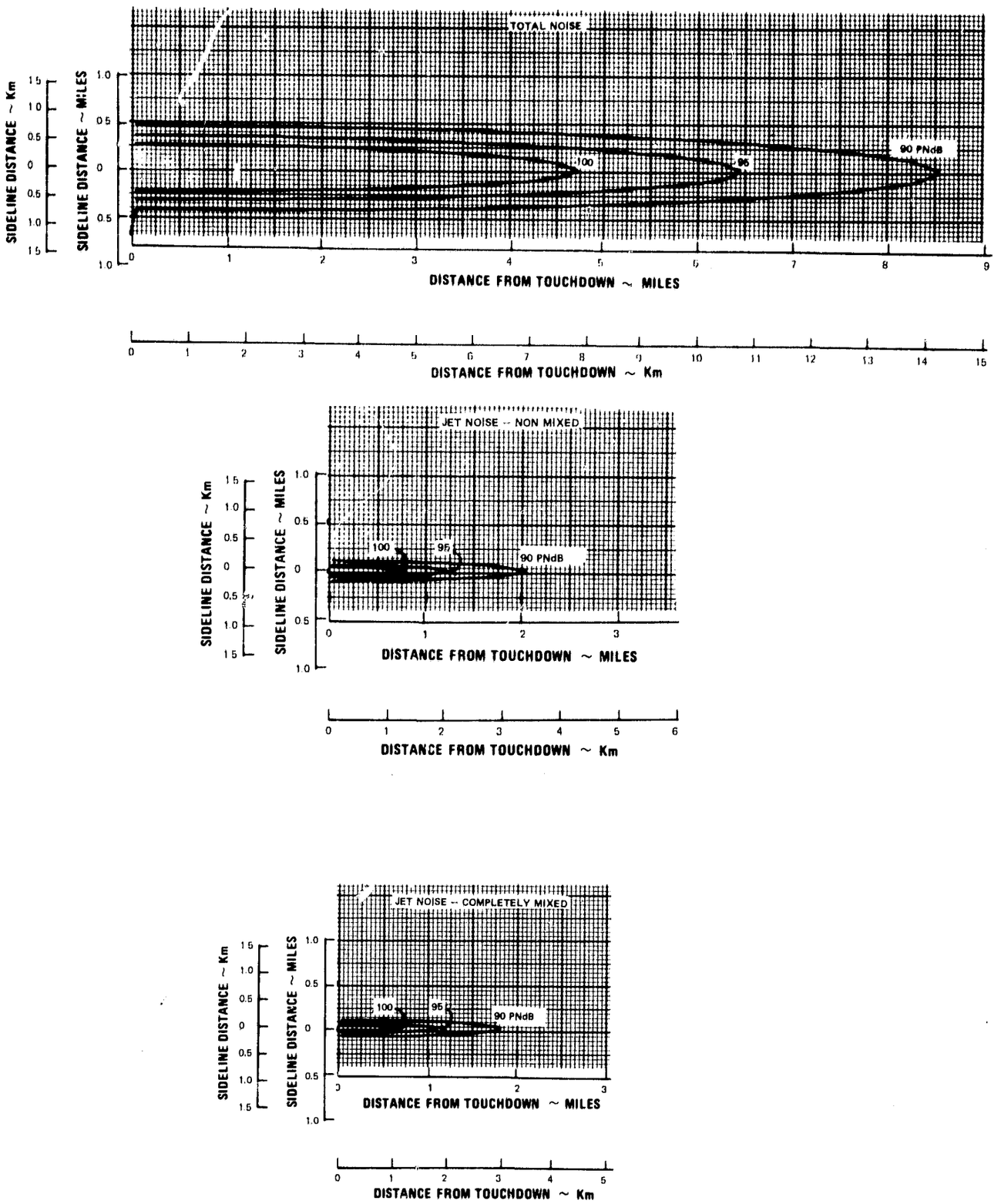

Figure 43 Landing Noise Contours for 4 JT3D Engines, 4800 Pounds/ Engine Thrust (21,400 Newtons)

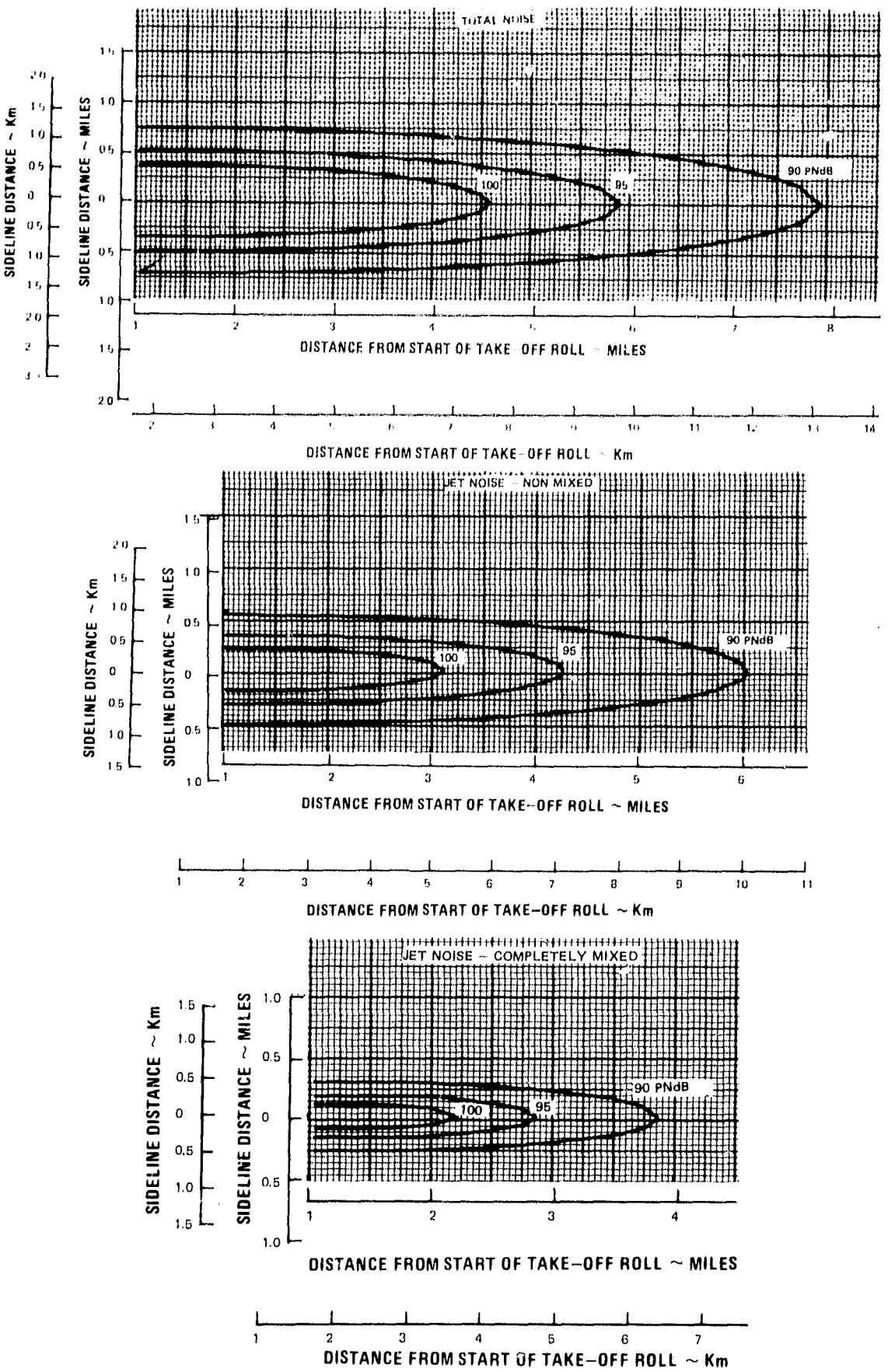

Figure 44 Takeoff Noise Contours for 4 Scaled JT9D Engines, 325,000 Pounds (147,000 kg) Gross Aircraft Weight

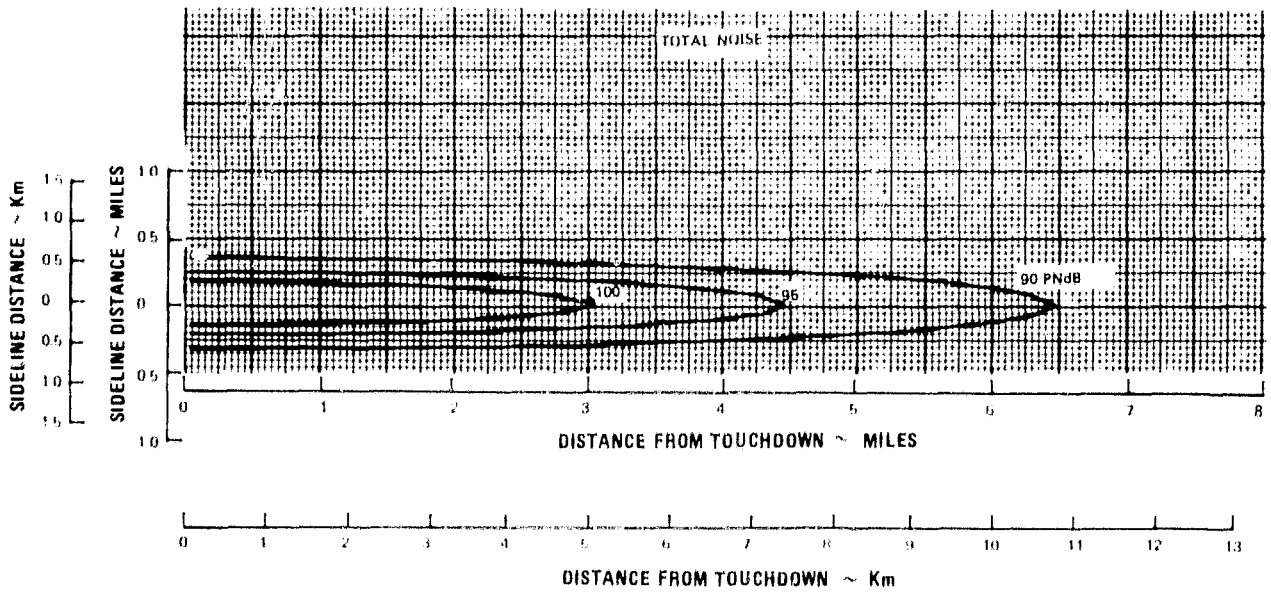

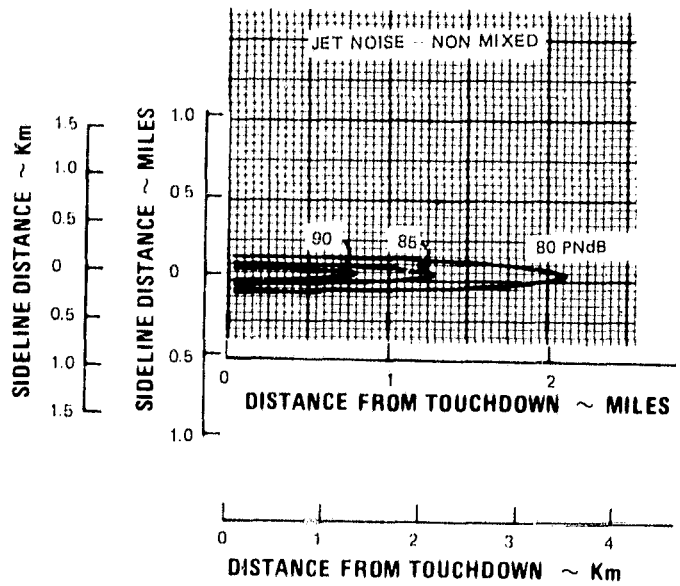

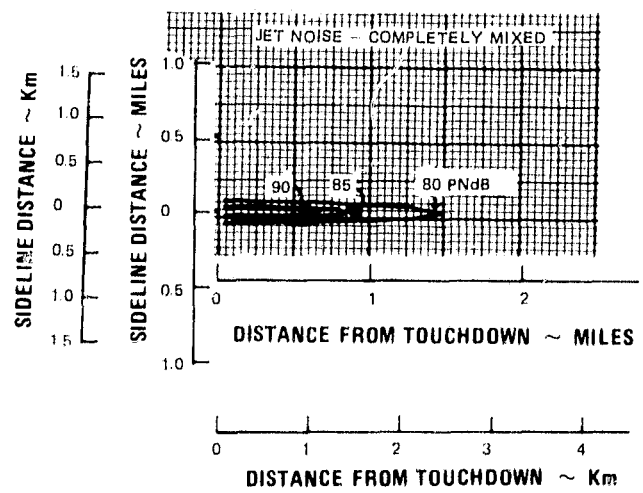

Figure 45 Landing Noise Contours for 4 Scaled JT9D Engines, 4800 Pounds/Engine Thrust (21,400 Newtons)

Differences between predicted and measured flyover noise levels using this system are shown in Figure 46.

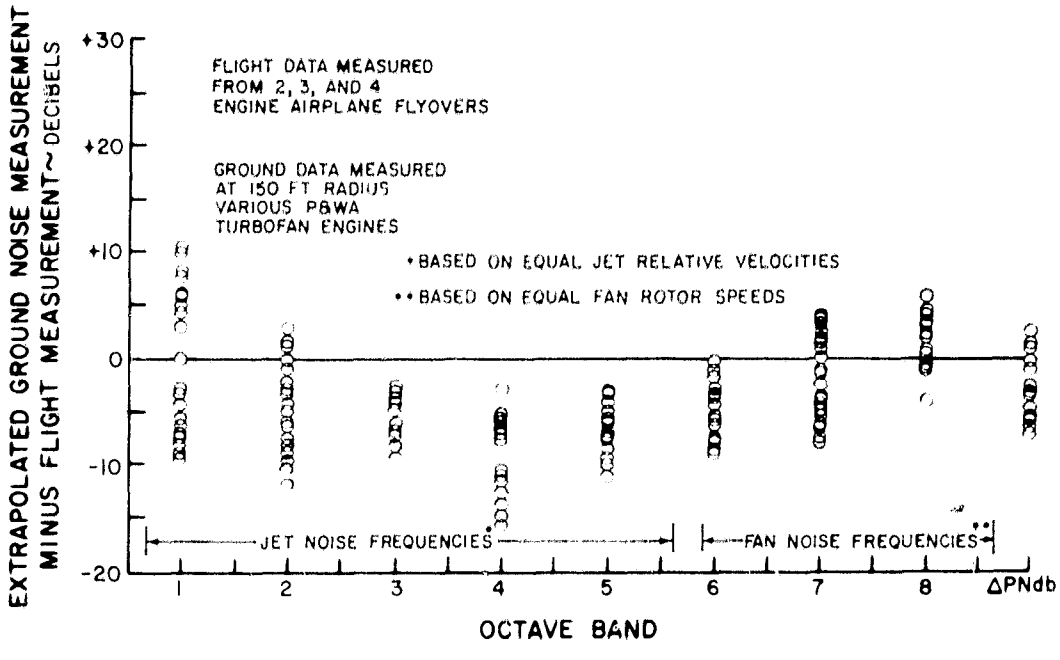

Figure 46 Predicted Perceived Noise Levels

c. Noise Propagation

Spherical divergence and standard-day extra air attenuation values as given in SAE document ARP866, "Standard Values of Atmospheric Absorption as a Function of Temperature and Humidity for Use in Evaluating Aircraft Flyover Noise", were used to extrapolate noise levels from the aircraft to the receiver on the ground. Atmosphere attenuation rates vary considerably from day to day compared to the rates which were used. Indeed, temperature and humidity vary with altitude. Although extrapolations of noise have been made over great distances in this study, attenuation rates were consistent with each engine and although absolute noise levels may be inaccurate on account of the large extrapolation, relative noise levels from each engine will remain unaffected.

The Doppler shift was neglected. Changes in frequency as a result of Doppler shift were not expected to have a significant effect on noise level.

Extra ground attenuation and shielding of engines by the fuselage were not considered. When the aircraft is at a large distance from the observer, and, therefore, at a shallow angle with respect to the ground, both of these effects may help to reduce the observed noise level. As no firm data exists to permit calculation of these effects, the effects were not included.

SECTION VII

ENGINE PERFORMANCE PREDICTIONS

A. PERFORMANCE DATA

Predictions of uninstalled thrust and specific fuel consumption were prepared covering a range of flight altitudes from sea level to 45,000 ft (13,716 meters) and Mach numbers from 0 to 0.9. In addition, nozzle areas and over-all dimensions for the four engine designs were established. Each of the engine performance summaries presented below assumes an ICAO model atmosphere, a lower fuel heating value of 18,400 Btu/lb (43.2 x 10^6 J/kg), a ram recovery of 100 percent, no external bleed or power extraction, short ducts and a converging nozzle in the bypass stream, and a conical converging nozzle in the gas generator exhaust. Weight and area of the engines may be assumed to scale proportionally with nominal thrust in the 20,000 to 26,000-pound (89,000 to 116,000-newton thrust range. In the same thrust range, diameter and length may be assumed to scale proportionally with the square root of nominal thrust.

1. QA-1 Performance

The QA-1 engine weighs 5080 pounds (2730 kg), is 131.20 inches (334 cm) long, has a maximum diameter of 63.25 inches (160 cm), has a gas-generator exhaust nozzle area of 3.42 ft^2 (0.318 m^2), and a bypass duct exhaust nozzle area of 6.89 ft^2 (0.641 m^2). The quoted weight includes fuel pumps, controls, fuel heater, fuel-oil cooler, oil tank, gearbox, ignition system, fuel supply lines and manifolds, and oil supply lines and instrumentation. A performance summary for the engine is shown in Table X.

2. QB-3 Performance

The QB-3 engine weighs 5420 pounds (2460 kg), is 125.75 inches (318 cm) long, has a maximum diameter of 70.0 inches (178 cm), has a gas-generator exhaust nozzle area of 4.00 ft^2 (0.377 m^2), and a bypass duct exhaust nozzle area of 10.35 ft^2 (0.975 m^2). The quoted weight includes fuel pumps, controls, fuel heater, fuel-oil cooler, oil tank, gearbox, ignition system, fuel supply lines and manifolds, and oil supply lines and instrumentation. A performance summary for the engine is shown in Table XI.

TABLE X

QA-1 PERFORMANCE SUMMARY

Altitude (ft)	Altitude (m)	Mach No	Power Setting	Thrust (lb)	Thrust (N)	TSFC (lb/hr-lb)	TSFC (mg/sec-N)	Total Airflow (lb/sec)	Total Airflow (kg/sec)
0	0	0	Take-off	20,666	92,000	0.385	10.9	629	288
0	0	0	Max cont	18,604	82,800	0.378	10.7	597	271
0	0	0	Max cr	17,115	76,200	0.374	10.6	574	261
0	0	0.45	Take-off	14,066	62,800	0.573	16.2	619	281
0	0	0.45	Max cont	12,252	54,100	0.578	16.3	592	268
0	0	0.45	Max cr	11,029	49,000	0.583	16.5	572	260
10,000	3,048	0	Take-off	16,282	72,400	0.371	10.5	670	304
10,000	3,048	0	Max cont	15,152	67,400	0.363	10.3	648	294
10,000	3,048	0	Max cr	14,191	63,100	0.358	10.1	628	285
10,000	3,048	0.90	Max cont	8,340	37,100	0.776	22.0	589	267
10,000	3,048	0.90	Max cr	7,477	33,300	0.789	22.3	574	260
20,000	6,096	0.60	Max cont	8,049	35,800	0.594	16.8	670	304
20,000	6,096	0.60	Max cr	7,452	33,200	0.593	16.7	654	297
20,000	6,096	0.90	Max cont	7,293	32,400	0.721	20.4	630	286
20,000	6,096	0.90	Max cr	6,576	29,300	0.729	20.6	613	278
30,000	9,144	0.60	Max cont	6,127	27,300	0.581	16.5	703	319
30,000	9,144	0.60	Max cr	5,808	25,900	0.575	16.3	692	314
30,000	9,144	0.90	Max cont	5,979	26,600	0.686	19.4	673	305
30,000	9,144	0.90	Max cr	5,529	24,600	0.685	19.3	658	298
35,000	10,669	0.82	Max cont	5,195	23,100	0.649	18.4	700	318
35,000	10,669	0.82	Max cr	4,903	21,800	0.643	18.2	688	312
40,000	12,192	0.60	Max cont	4,102	18,200	0.581	16.5	715	324
40,000	12,192	0.60	Max cr	3,916	17,400	0.574	16.3	706	320
40,000	12,192	0.90	Max cont	4,142	18,400	0.676	19.2	692	314
40,000	12,192	0.90	Max cr	3,881	17,300	0.672	19.0	679	308
45,000	13,716	0.60	Max cont	3,184	14,200	0.584	16.5	711	323
45,000	13,716	0.60	Max cr	3,033	13,500	0.577	16.4	702	318
45,000	13,716	0.90	Max cont	3,205	14,300	0.680	19.3	687	312
45,000	13,716	0.90	Max cr	2,990	13,300	0.677	19.2	674	306

TABLE XI

QB-3 PERFORMANCE SUMMARY

Altitude (ft)	Altitude (m)	Mach No	Power Setting	Thrust (lb)	Thrust (N)	TSFC (lb/hr-lb)	TSFC (mg/sec-N)	Total Airflow (lb/sec)	Total Airflow (kg/sec)
0	0	0	Take-off	22,749	101,000	0.341	9.66	791	359
0	0	0	Max cont	19,869	88,400	0.334	9.45	741	336
0	0	0	Max cr	18,418	82,000	0.331	9.36	713	323
0	0	0.45	Take-off	14,681	65,330	0.538	15.2	796	361
0	0	0.45	Max cont	12,265	54,600	0.547	15.4	751	341
0	0	0.45	Max cr	11,121	49,500	0.555	15.7	728	331
10,000	3,048	0	Take-off	17,970	80,000	0.328	9.28	846	384
10,000	3,048	0	Max cont	16,237	72,400	0.320	9.06	806	361
10,000	3,048	0	Max cr	15,258	67,900	0.316	8.94	782	355
10,000	3,048	0.90	Max cont	8,110	36,100	0.766	21.6	772	350
10,000	3,048	0.90	Max cr	7,313	32,500	0.783	22.1	756	343
20,000	6,096	0.60	Max cont	8,026	35,700	0.561	15.8	858	389
20,000	6,096	0.60	Max cr	7,436	33,700	0.563	15.9	839	381
20,000	6,096	0.90	Max cont	7,109	32,200	0.701	19.8	820	372
20,000	6,096	0.90	Max cr	6,467	28,800	0.710	20.1	803	365
30,000	9,144	0.60	Max cont	6,221	27,700	0.544	15.4	903	410
30,000	9,144	0.60	Max cr	5,883	26,200	0.540	15.3	889	404
30,000	9,144	0.90	Max cont	5,884	26,200	0.658	18.6	870	395
30,000	9,144	0.90	Max cr	5,444	24,100	0.660	18.7	853	387
35,000	10,669	0.82	Max cont	5,200	23,100	0.616	17.5	903	410
35,000	10,669	0.82	Max cr	4,902	21,800	0.613	17.4	889	403
40,000	12,192	0.60	Max cont	4,217	18,800	0.542	15.3	922	418
40,000	12,192	0.60	Max cr	4,002	17,800	0.537	15.9	909	413
40,000	12,192	0.90	Max cont	4,112	18,300	0.644	18.2	893	405
40,000	12,192	0.90	Max cr	3,856	17,200	0.643	18.1	879	349
45,000	13,716	0.60	Max cont	3,254	14,480	0.545	15.4	916	416
45,000	13,716	0.60	Max cr	3,084	13,700	0.540	15.3	902	409
45,000	13,716	0.90	Max cont	3,170	14,100	0.649	18.4	887	403
45,000	13,716	0.90	Max cr	2,959	13,200	0.648	18.3	872	396

3. QC-3 Performance

The QC-3 engine weighs 5610 pounds (2550 kg), is 125.5 inches (318 cm) long, has a maximum diameter of 84.3 inches (214 cm), has a gas-generator exhaust nozzle area of 4.06 ft^2 (0.382 m^2), and a two-position bypass exhaust nozzle. From Mach 0 to Mach 0.25, the nozzle area is 20.6 ft^2 (1.94 m^2), and above Mach 0.25 the area is 18.7 ft^2 (1.76 m^2). The quoted weight includes fuel pumps, controls, fuel heater, fuel-oil cooler, oil tank, gearbox, ignition system, fuel supply lines and manifolds, and oil supply lines and instrumentation. A performance summary for the engine is shown in Table XII.

4. QD-1 Performance

The QD-1 engine weighs 5570 pounds (2520 kg), is 146.8 inches (372 cm) long, has a maximum diameter of 70.6 inches (179 cm), has a gas-generator exhaust nozzle area of 4.13 ft^2 (0.384 m^2), and a bypass duct exhaust nozzle area of 10.50 ft^2 (0.977 m^2). The quoted weight includes fuel pumps, controls, fuel heater fuel-oil cooler, oil tank, gearbox, ignition system, fuel supply lines and manifolds, and oil supply lines and instrumentation. A performance summary for the engine is shown in Table XIII.

TABLE XII

QC-3 PERFORMANCE SUMMARY

Altitude (ft)	Altitude (m)	Mach No	Power Setting	Thrust (lb)	Thrust (N)	TSFC (lb/hr-lb)	TSFC (mg/sec-N)	Total Airflow (lb/sec)	Total Airflow (kg/sec)
0	0	0	Take-off	25,551	113,700	0.286	8.10	1,127	512
0	0	0	Max cont	23,677	105,400	0.280	7.93	1,088	488
0	0	0	Max cr	21,703	96,700	0.276	7.81	1,044	475
0	0	0.45	Take-off	14,941	66,800	0.506	14.3	1,134	514
0	0	0.45	Max cont	13,344	59,200	0.510	14.5	1,098	495
0	0	0.45	Max cr	11,770	52,500	0.519	14.7	1,061	481
10,000	3,048	0	Take-off	19,724	87,700	0.277	7.84	1,189	536
10,000	3,048	0	Max cont	18,689	82,700	0.271	7.67	1,160	527
10,000	3,048	0	Max cr	17,511	77,900	0.266	7.58	1,125	508
10,000	3,048	0.90	Max cont	8,140	36,200	0.780	22.1	1,173	535
10,000	3,048	0.90	Max cr	6,941	30,700	0.822	23.2	1,146	521
20,000	6,096	0.60	Max cont	8,385	37,300	0.541	15.3	1,249	563
20,000	6,096	0.60	Max cr	7,662	24,100	0.541	15.3	1,223	554
20,000	6,096	0.90	Max cont	7,376	32,800	0.695	19.7	1,234	559
20,000	6,096	0.90	Max cr	6,413	28,500	0.717	20.3	1,205	547
30,000	9,144	0.60	Max cont	6,207	27,600	0.534	15.1	1,284	581
30,000	9,144	0.60	Max cr	5,905	26,300	0.524	14.9	1,272	576
30,000	9,144	0.90	Max cont	6,096	27,100	0.648	18.4	1,289	586
35,000	10,669	0.82	Max cont	5,192	23,100	0.612	17.3	1,308	594
35,000	10,669	0.82	Max cr	5,901	21,800	0.605	17.2	1,297	589
40,000	12,192	0.60	Max cont	4,071	18,200	0.537	15.2	1,292	586
40,000	12,192	0.60	Max cr	3,911	17,700	0.526	14.9	1,284	581
40,000	12,192	0.90	Max cont	4,154	18,600	0.640	18.1	1,306	543
40,000	12,192	0.90	Max cr	3,886	19,200	0.635	18.0	1,292	586
45,000	13,716	0.60	Max cont	3,173	14,100	0.539	15.3	1,289	585
45,000	13,716	0.60	Max cr	3,043	13,600	0.527	14.9	1,281	580
45,000	13,716	0.90	Max cont	3,224	14,300	0.644	18.2	1,302	592
45,000	13,716	0.90	Max cr	2,997	13,600	0.639	17.1	1,286	584

TABLE XIII

QD-1 PERFORMANCE SUMMARY

Altitude (ft)	Altitude (m)	Mach No	Power Setting	Thrust (lb)	Thrust (N)	TSFC (lb/hr-lb)	TSFC (mg/sec-N)	Total Airflow (lb/sec)	Total Airflow (kg/sec)
0	0	0	Take-off	23,318	104,000	0.340	9.65	828	373
0	0	0	Max cont	20,524	91,200	0.330	9.34	781	354
0	0	0	Max cr	19,207	85,700	0.326	9.25	757	344
0	0	0.45	Take-off	14,930	66,300	0.542	15.3	829	376
0	0	0.45	Max cont	12,577	56,000	0.547	15.5	788	358
0	0	0.45	max cr	11,492	50,700	0.552	15.6	768	349
10,000	3,048	0	Take-off	18,368	81,500	0.328	9.28	881	399
10,000	3,048	0	Max cont	16,498	73,400	0.318	9.00	839	381
10,000	3,048	0	Max cr	15,559	69,200	0.313	8.85	817	371
10,000	3,048	0.90	Max cont	8,375	37,220	0.765	21.6	796	362
10,000	3,048	0.90	Max cr	7,566	33,650	0.780	22.1	780	354
20,000	6,096	0.60	Max cont	8,020	35,600	0.568	16.2	878	399
20,000	6,096	0.60	Max cr	7,441	33,100	0.568	16.2	861	391
20,000	6,096	0.90	Max cont	7,220	32,100	0.707	20.0	839	381
20,000	6,096	0.90	Max cr	6,632	29,500	0.713	22.0	825	374
30,000	9,144	0.60	Max cont	6,247	27,900	0.549	15.6	922	418
30,000	9,144	0.60	Max cr	5,912	26,300	0.546	15.5	909	413
30,000	9,144	0.90	Max cont	5,864	26,100	0.668	18.9	883	402
30,000	9,144	0.90	Max cr	5,440	24,200	0.669	18.9	868	394
35,000	10,668	0.82	Max cont	5,204	23,100	0.623	17.6	917	416
35,000	10,668	0.82	Max cr	4,901	21,800	0.620	17.5	904	410
40,000	12,192	0.60	Max cont	4,210	18,700	0.546	15.4	938	425
40,000	12,192	0.60	Max cr	4,022	17,900	0.540	15.3	929	423
40,000	12,192	0.90	Max cont	4,117	17,800	0.652	18.4	907	412
40,000	12,192	0.90	Max cr	3,853	17,000	0.651	18.4	893	405
45,000	12,192	0.60	Max cont	3,260	14,550	0.548	15.5	934	424
45,000	12,192	0.60	Max cr	3,112	13,800	0.542	15.3	924	419
45,000	12,192	0.90	Max cont	3,179	14,120	0.655	18.5	902	409
45,000	12,192	0.90	Max cr	2,967	13,300	0.655	18.5	887	406

B. BACKGROUND ASSUMPTIONS

In generating the performance data given in the summaries above, standard off-design equilibrium-matching computer programs were used. The component performance levels used in the computations were based on the results of the component analytical design studies performance during Task II. A summary of the component performance values is given in Table XIV.

TABLE XIV

COMPONENT DESIGN-POINT PERFORMANCE LEVELS

	QA-1	QB-3	QC-3	QD-1
Net Adiabatic Efficiencies at the Cycle Design Point				
Fan outer duct	0.892	0.898	0.895	0.898
Fan inner duct and low-pressure compressor	0.883	0.889	0.889	0.900
High-pressure compressor	-	-	-	0.866
Cooled high-pressure turbine	0.908	0.900	0.895	0.895
Cooled low-pressure turbine	0.908	0.904	0.892*	0.905*
Pressure Losses				
Burner	0.047	0.047	0.047	0.047
Turbine exhaust system	0.016	0.016	0.016	0.016
Fan duct and exhaust system	0.01	0.01	0.01	0.01

Computing estimates of engine performance is keyed to selecting a so-called "nominal" design point. For engines primarily intended for application in commercial transports, the design point is usually selected to be the point of expected cruise operation, where fuel consumption is most important. This cruise design point is ordinarily selected at a typical cruise flight condition on a standard day, slightly below the maximum cruise rated thrust. Although in practice the engine never operates at exactly its hypothetical cruise design point, the actual variation is small enough that the initially selected "nominal design point" performance is quite representative. This means that variations from standard day, power setting variations from the cruise rating caused by variations in gross weight, and variations in engine sizing required by minor performance adjustments during design refinements are properly neglected in the selection of the cruise design point.